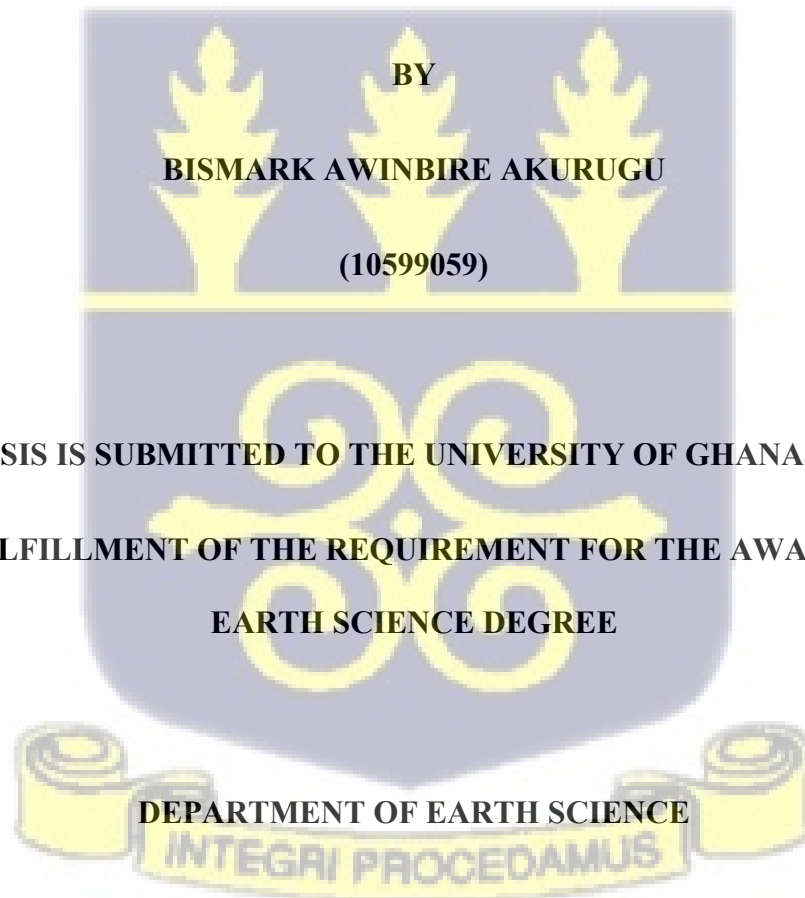


UNIVERSITY OF GHANA

COLLEGE OF BASIC AND APPLIED SCIENCES

**AQUIFER CHARACTERISATION AND NUMERICAL MODELLING FOR
GROUNDWATER RESOURCES ASSESSMENT IN THE DENSU RIVER BASIN**

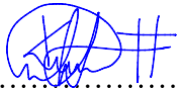


**THIS THESIS IS SUBMITTED TO THE UNIVERSITY OF GHANA, LEGON IN
PARTIAL FULFILLMENT OF THE REQUIREMENT FOR THE AWARD OF PHD IN
EARTH SCIENCE DEGREE**

October, 2025

DECLARATION

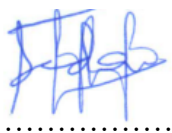
This thesis is the result of research undertaken by Bismark Awinbire Akurugu towards the award of Doctor of Philosophy Degree in Earth Science in the Department of Earth Science, University of Ghana.


.....

Date... 06/10/2025

BISMARK AWINBIRE AKURUGU

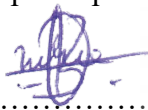
(Student)


.....

Date... October 9, 2025

PROF. SANDOW MARK YIDANA

(Principal Supervisor)


.....

Date... 08/10/2025

DR. EMMANUEL OBUOBIE

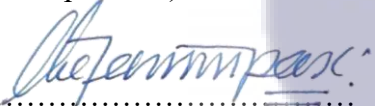
(Co-Supervisor)


.....

Date... 10/10/2025

PROF. SIMON STISEN

(Co-Supervisor)


.....

Date... 06/10/2025

PROF. LARRY PAX CHEGBELEH

(Co-Supervisor)



ABSTRACT

Groundwater plays a crucial role in the delivery of water for domestic, industrial, and agricultural uses for communities in and around the Densu River Basin. A detailed understanding of the hydrogeological properties, hydrochemistry, and groundwater dynamics is crucial for informed and practical sustainable management of the resource. Assessment of essential aquifer parameters, recharge, and hydrochemical data was conducted for a holistic understanding of the hydrogeology of the basin. The study adopted the water table fluctuation (WTF), chloride mass balance (CMB), and baseflow filters (BFF) to estimate groundwater recharge, which is essential for understanding groundwater demand versus availability. Assessment of recharge and essential hydrogeologic parameters provided new insights for the construction of a conceptual and 3D transient groundwater flow model. The model was calibrated using PEST for various parameters and pilot points to represent heterogeneity in the hydraulic conductivities of two hydrostratigraphic units representing the regolith and fractured bedrock, and used to assess the potential impacts of enhanced abstractions and reduced recharge on groundwater resources in the basin. The study revealed groundwater recharge in the basin ranges from 27 - 338 mm/year, representing 4 – 24% of the total annual rainfall, trending north to south in magnitude. The basin averages were estimated at 34, 150, and 80 mm/year, representing 3%, 15%, and 7% for CMB, WTF, and BFF, respectively, with an overall average of ~144 mm/year, representing ~ 15% of the rainfall. The CMB and BFF methods largely agree on basin average recharge, whereas the WTF methods generate much higher average recharge estimates. The CMB method revealed weaknesses in the lower bound estimates (underestimated) compared to the other methods. Although the major rainy season peaks around May/June in the basin, the highest groundwater recharge occurs in the peak

of the minor rainy season in October, which is attributable to the 2.5 months lag time between rainfall and recharge. Within the basin, the study finds that rocks of the Birimian Supergroup are the most prolific, consistent with previous studies, with an average borehole yield of 84.48 m³/day, as compared to average yields of 79.92 m³/day and 66 m³/day, respectively, for rocks of the Voltaian Supergroup and granites of the Eburnean and Tamnean Plutonic Suites. The spatial variation of the major ions in the basin mimics the presumed groundwater flow regime, with the hydrochemistry increasingly getting mineralised as it flows from the upland high-elevation areas (recharge areas) in the northeast and southwest (characterised by Ca/Na-HCO₃ facies), to discharge areas (characterised by Na-Cl) in low-elevation areas in the central and southern sections. The groundwater hydrochemistry is dominated by silicate mineral weathering and ion-exchange processes in the groundwater system. However, carbonate mineral dissolution, anthropogenic pollution, seawater intrusion, and dissolution of evaporite play some role, especially in the extreme south of the basin. The recharge and transition zones in the groundwater flow regime present the best water quality compared to the discharge zones. Further insights into the hydrogeology of the basin were gained through model calibration. The process resulted in a computed horizontal hydraulic conductivity range of 0 – 15 m/d, with an average of 0 – 4 m/day. The simulations revealed enhanced abstractions caused by demand from population growth at an annual rate of 3.6 % over a 20-year period could increase groundwater abstraction from a baseline rate of 10,765,365 m³/year to approximately 24,489,637 m³/year. This projected demand represents about 16% of the basin's baseline annual groundwater recharge. Despite the increase, the simulations suggest minimal impact on overall groundwater volumes and flow patterns within the basin. However, coupling enhanced abstractions with reduced recharge rate caused a decline in groundwater

recharge by 0.026%, a slight decline in groundwater levels, and a reduction in groundwater contribution to stream flow by 8% and 21% respectively, compared to the baseline period. The observations made in these forecasts suggest abstractions at the current rate over 20 years without changes to the recharge rate pose risks to stream flows and ecosystems, especially under drier climate conditions



DEDICATION

This thesis is dedicated to the cherished memory of my mother, Madam Grace Atubpoka. Her wisdom and guidance have been my compass, providing direction throughout my life. Though you are no longer with us, your enduring spirit and sweet memories remain forever in my heart.



ACKNOWLEDGEMENT

I am deeply grateful to the remarkable individuals who have played pivotal roles in shaping this research. Their unwavering support, expertise, encouragement, and dedication have been my guiding lights throughout this research journey.

First and foremost, my esteemed thesis advisors deserve my profound gratitude. Prof. Sandow Mark Yidana, Dr. Emmanuel Obuobie, Prof. Simon Stisen, Prof. Larry Pax Chegbeleh, and Dr. Ida Karlsson Seidenfaden—your expert guidance and profound knowledge have been instrumental. Your unwavering commitment to my growth as a researcher has left an indelible mark on my work.

Special thanks are due to Dr. William Agyekum, Emeritus Professor Kurt Klitten, Dr. Elikplim Abla Dzikunoo, and Mr. Emmanuel Ayizeme for their technical assistance. I would also like to extend my deepest appreciation to the Groundwater Division of the CSIR-Water Research Institute, the Earth Science Department at the University of Ghana, and the Community Water and Sanitation Agency for providing essential data and technical support for this work.

A debt of gratitude goes to the Ministry of Foreign Affairs of Denmark/Danida Fellowship Centre. Through the ‘Building Climate Resilience into Basin Water Management’ (CREAM) Project, their generous sponsorship shaped the contours of my research.

To my family, friends and loved ones: your unwavering belief in my potential, endless patience, and steadfast encouragement have sustained me. You are my constant source of strength.

Lastly, I acknowledge the collective contributions of all those whose works and insights have enriched my research. Each one of you has left an imprint, and for that, I offer my sincere thanks.

TABLE OF CONTENTS

DECLARATION	i
ABSTRACT.....	ii
DEDICATION.....	v
ACKNOWLEDGEMENT	vi
TABLE OF CONTENTS.....	vii
LIST OF FIGURES	xii
LIST OF TABLES	xv
LIST OF ABBREVIATIONS.....	xvi
CHAPTER ONE.....	1
INTRODUCTION	1
1.1 Background.....	1
1.2 Problem Statement.....	4
1.3 Justification of Study	6
1.4 Research Objectives.....	7
1.5 Thesis Structure	8
1.6 Study Area	9

1.7 Geology and hydrogeology.....	12
CHAPTER TWO	17
GROUNDWATER RECHARGE ESTIMATION FROM MULTIPLE INDEPENDENT METHODS IN THE FRACTURED HARD ROCK AQUIFERS IN THE DENSU RIVER BASIN, GHANA	17
2.1 Introduction.....	17
2.2 Materials and Methods.....	20
2.2.1 Conceptual recharge.....	21
2.2.2 Chloride mass balance method	23
2.2.3 Water table fluctuation method.....	24
2.2.4 Baseflow separation methods	26
2.3 Results.....	27
2.3.1 Chloride mass balance (CMB).....	27
2.3.2 Water table fluctuation (WTF).....	28
2.3.3 Recharge estimates from baseflow filters	33
2.4 Discussions	35
2.5 Conclusion	37
CHAPTER THREE	39

UTILISING HYDROGEOLOGICAL AND HYDROCHEMICAL DATA TO DEVELOP A
CONCEPTUAL UNDERSTANDING OF GROUNDWATER RESOURCES IN THE DENSU
RIVER BASIN, SOUTHWESTERN GHANA..... 39

3.1 Introduction..... 39

3.2 Methodology..... 42

 3.2.1 Borehole and hydraulic tests data 42

 3.2.2 Sampling and analysis..... 42

 3.2.3 Mass balance and statistical modelling..... 44

 3.2.4 Irrigation quality assessment..... 46

3.3 Results and discussions..... 47

 3.3.1 General hydraulic characteristics..... 47

 3.3.2 Conceptual lithostratigraphy..... 52

 3.3.3 Spatial patterns of groundwater hydrochemistry 55

 3.3.4 Irrigation quality assessment..... 62

 3.3.5 Hydrogeochemical processes controlling groundwater chemistry 67

 3.3.6 Groundwater saturation state and mineral stability 74

 3.3.7 Conceptual groundwater flow..... 79

3.4 Conclusion 82

CHAPTER FOUR.....	84
ASSESSING THE POTENTIAL IMPACTS OF ABSTRACTION AND RECHARGE USING NUMERICAL GROUNDWATER FLOW MODELLING FOR THE DENSU RIVER BASIN, GHANA	84
4.1 Introduction.....	84
4.2 Materials and methods	87
4.2.1 Data collection and analyses	87
4.2.2 Conceptual model and boundary conditions.....	88
4.2.3 Numerical model setup and calibration	93
4.2.4 Scenario analysis.....	97
4.3 Results and discussion	99
4.3.1 Model calibration and performance	99
4.3.2 Hydraulic conductivity field	100
4.3.3 Steady state groundwater flow.....	102
4.3.4 Transient state groundwater budget.....	105
4.3.5 Scenario analysis.....	109
4.3.6 Conclusion	112
CHAPTER FIVE	114

CONCLUSIONS AND RECOMMENDATIONS	114
5.1 Summary of main findings.....	114
5.2 Scientific contribution and study limitations	117
5.2 Recommendations.....	118
REFERENCES	120



LIST OF FIGURES

Figure 1.1: Map of the Densu River Basin (a) showing elevation, surface water and towns, (b) spatial distribution of average annual rainfall, (c) geology (adopted from Duodo, 2009), and (d) sub-basin	11
Figure 1.2: Average monthly rainfall for the (a) Mangoase, (b) Asuboi, (c) Parkro, and (d) Ashaladja sub-basins of the Densu River Basin (1981 - 2022)	12
Figure 2.1: Conceptual model showing groundwater recharge and storage mechanisms in the Densu River Basin	22
Figure 2.2: Groundwater fluctuations for selected boreholes in the Densu River Basin.....	30
Figure 2.3: Spatial distribution of groundwater recharge in mm/year (a, b, c) and percent of average annual rainfall (d, e, f) based on the CMB (a&d), WTF (b&e), and BFF (c&f)	32
Figure 2.4: Average groundwater recharge (mm/month) based on baseflow filters	34
Figure 3.1: Relationship between borehole yield and depth in the Densu Basin	51
Figure 3.2: Semivariogram models for (a) borehole yield, and (b) borehole depth	51
Figure 3.3: Spatial distribution of (a) borehole yield, (b) depth, and (c) transmissivity	52
Figure 3.4: Relationship between weathered thickness, borehole yield, and elevation.....	54
Figure 3.5: General lithostratigraphy of boreholes in the (a) Birimian Supergroup, (b) granites, and (c) Voltaian Supergroup in the Densu Basin	54

Figure 3.6: Conceptual (a) solid and (b) cross-section of the lithostratigraphy of the Densu River Basin	55
Figure 3.7: Q-mode hierarchical cluster analysis showing spatial variation in groundwater	57
Figure 3.8: Spatial distribution of selected physicochemical parameters; (a) pH, (b) TDS, (c) Cl ⁻ , (d) HCO ₃ ⁻ , (e) Total hardness, and (f) Fe in the Densu Basin	61
Figure 3.9: Irrigation quality assessment using (a) USSL, and (b) Wilcox diagrams	65
Figure 3.10: Spatial distribution of irrigation quality assessment indices; (a) sodium adsorption ratio (SAR), (b) percent sodium (Na%), (c) permeability index (PI), and (d) magnesium ratio (MR)	66
Figure 3.11: Bivariate plots of (a) (Ca ²⁺ +Mg ²⁺ - (HCO ₃ ⁻ +SO ₄ ²⁻) vs (Na ⁺ +K ⁺)-Cl ⁻ , (b) CAI-I vs CAI-II, (c) Na ⁺ vs Cl ⁻ , (d) Ca ²⁺ vs SO ₄ ²⁻ , (e) Total ions vs Cl ⁻ , (f) Ca ²⁺ +Mg ²⁺ - HCO ₃ ⁻ +SO ₄ ²⁻ , (g) NO ₃ ⁻ vs Cl ⁻ , and (h) NO ₃ ⁻ vs Total cations.....	73
Figure 3.12: Biplots of selected saturation indices and pH	76
Figure 3.13: Mineral stability diagram for (a) CaO-SiO ₂ -Al ₂ O ₃ -H ₂ O, (b) NaO ₂ -SiO ₂ -Al ₂ O ₃ -H ₂ O, (c) KO ₂ -SiO ₂ -Al ₂ O ₃ -H ₂ O and (d) MgO-SiO ₂ -Al ₂ O ₃ -H ₂ O systems	78
Figure 3.14: (a) 3D topography and (b) conceptual flow based on groundwater hydraulic head	81
Figure 3.15: Conceptual hydrogeology of the Densu River Basin	81
Figure 4.1: Conceptualisation and boundary conditions of the model domain	91

Figure 4.2: (a) Biplot of computed versus observed hydraulic head, and biplot of computed versus observed depth to groundwater level 100

Figure 4.3: Horizontal hydraulic conductivity field for (a) Layer 1, and (b) Layer 2 102

Figure 4.4: Steady state (a) model-computed 3D view and (b) flow patterns of groundwater hydraulic head..... 105

Figure 4.5: Time series plot of model-computed and observed hydraulic data for the transient period 107

Figure 4.6: Time series plot of average groundwater recharge in the basin 108

Figure 4.7: Groundwater recharge trend for the wet (MIROC5) and dry (MOHC) precipitation projections..... 112



LIST OF TABLES

Table 2.1: Summary statistics of recharge estimates from the CMB method. Standard deviation in brackets.	27
Table 2.2: Groundwater recharge estimate from the WTF method for selected boreholes and years	31
Table 3.1: Summary statistics of aquifer hydraulic properties	50
Table 3.2a: Descriptive statistics for Cluster 1a	57
Table 3.2b: Descriptive statistics for Cluster 1b.....	50
Table 3.2c: Descriptive statistics for Cluster 1c.....	57
Table 4.1: Summary of groundwater recharge studies in the Densu River Basin	90
Table 4. 2: Overview of calibration parameters.....	95
Table 4.3: Model performance for the calibration period (June 2020 – June 2023) and the evaluation period (July 2023 – April 2024).....	100
Table 4.4: Transient groundwater budget over the 2020 – 2023 period.....	109



LIST OF ABBREVIATIONS

BFF	Baseflow filters
CBE	Charge Balance Error
CMB	Chloride Mass Balance
CSIR-WRI	Council for Scientific and Industrial Research - Water Research Institute
CWSA	Community Water and Sanitation Agency
DANIDA	Danish International Development Agency
IPCC	International Panel on Climate Change
RMSE	Root Mean Squared Error
SAR	Sodium Adsorption Ratio
USGS	United States Geological Survey
USSL	United States Salinity Laboratory
WHO	World Health Organisation
WRC	Water Research Commission
WTF	Water Table Fluctuation



CHAPTER ONE

INTRODUCTION

1.1 Background

Groundwater plays a crucial role in the delivery of potable water to the world's population, and most importantly in developing countries, arid areas, and places where surface water bodies are limited, unsuitable and unavailable. Groundwater supplies 25% of consumptive water globally, of which 50% is for drinking and 40% for industrial use (Hao et al., 2018). The dependence on groundwater is even more profound in most developing countries in Africa, particularly Ghana, where a large portion of the population relies on groundwater for various purposes (Kortatsi et al., 2008; Foster et al., 2020; Agyemang, 2025).

Inadequate investments and a lack of institutional capacity to treat the available surface waters and construct the needed infrastructure for storage and distribution have led to various governments adopting less expensive approaches to supplying potable water to settlements, especially rural communities. This is usually in the form of boreholes with hand pumps or, in a few cases, mechanised boreholes which serve as town water supplies from a centralised storage. In Ghana, about a quarter of the urban communities and 90% of the rural population depend heavily on groundwater for their household water needs (Yankey et al., 2011). Similarly, in the Densu River Basin, groundwater is of immense importance in delivering the potable water requirements of urban and rural communities, supporting socioeconomic development, and maintaining ecosystems. According to the Water Resources Commission (WRC), the Densu River Basin is one of the most populated river basins in Ghana, with a population density of 359 persons/km² as

compared to the national average of 77 persons/km² (WRC, 2007; Ghana Statistical Service, 2021). The basin supplies about 300,000 m³ of water daily to the western parts of Accra, the capital town of Ghana (WRC, 2007), through the Weija dam. Historically, the Densu River served as the main source of water for some communities within the basin, and the Weija dam, which supplies raw water to the water treatment plant of Ghana Water Company Limited (GWCL), a public company responsible for water supply in urban settlements in Ghana. However, population growth, climate variability, and urbanisation, coupled with poor agricultural practices and waste disposal methods, have stressed both the quality and quantity of available water resources within the basin (Adomako et al., 2011a; Bam et al., 2011; Yidana et al., 2018). Similarly, the interaction of groundwater with aquifer materials during transit or storage undoubtedly affects its hydrochemistry and general quality (Loh et al., 2019; Chegbeleh et al., 2020) and may have implications for its suitability for various uses.

There have been reports of massive pollution of the surface water resources from the Densu River and the subsequent closure of the GWCL water treatment plant at Weija, which led to a ban on farming activities along the banks of the Densu River (Graphic, 2001). The WRC (2007) identified the Densu River Basin as the most vulnerable basin in Ghana and under significant pressure due to the increasingly high population density, inadequate waste infrastructure, and lack of environmental awareness, which threaten water resources. They recommended resorting to groundwater supply in some parts of the basin as one of the major solutions to the ever-increasing water demand and also as a complementary approach to the sustainable management of surface water resources of the Densu River.

Notwithstanding the challenges which could potentially limit the availability of water resources in the basin, water demand from the basin is expected to rise in response to climate change/variability, population growth, and industrialisation in parts of Greater Accra. These rising water demands and the need for a sustainable water supply, especially to rural communities which are usually dispersed and remote, pose a serious challenge. Also, the public water supply system to urban centres by the GWCL has proven inconsistent and unreliable in recent times. These challenges have shifted the interest to intensify groundwater exploration and exploitation in the basin. Groundwater has proven to be the most efficient and cost-effective approach to rural water supply in Ghana since it is easily sited close to demand centres and usually requires little or no treatment prior to consumption/use, unlike surface water sources (Loh et al., 2019; Akurugu et al., 2020). Despite the numerous advantages groundwater presents as a complementary and sole source of water for some uses, not much is known about the groundwater system in the Densu River Basin for sustainable management of the resources, so as to avoid over-exploitation.

This study is aimed at providing deeper insights into the general hydrogeology of the basin and how stresses like climate change, population growth, and industrialisation will impact groundwater resources in the Densu River Basin. It seeks to, for the first time, incorporate recharge estimations (Chapter 2), hydrogeochemistry (Chapter 3), and numerical groundwater flow modelling (Chapter 4) in the basin, as an initial step to comprehensively characterise the hydrogeological properties of the underlying aquifers of the basin.



1.2 Problem Statement

Climate variability and change, and their attendant consequences such as rainfall variability and rising temperatures, are expected to impact negatively on the available water resources for both domestic and industrial purposes, and affect groundwater recharge rates, among others (WRC, 2007). Water resources have been predicted by most scholars to be at the centre of the impacts of climate change (Kusangaya et al., 2014; Nkhonjera, 2017; Asare-Nuamah & Botchway, 2019). The IPCC (2022) holds that potential impacts of climate change on water resources are expected to increase in magnitude, diversity, and severity if the observed climate change in the last 100 years persists into the future. Freshwater sources, including surface and groundwater, have been predicted to be the most affected by climate change, in terms of quality and quantity. This is very true for arid and semi-arid areas, where the impacts of climate change on water resources are greatly felt.

The IPCC (2022) further projects that Africa will be disproportionately affected by climate change. The projected warming in Africa is estimated to be 1.5 times higher than the global average. Such unusually elevated increases in temperature are already being experienced in several regions in Africa, particularly the Sahel and Southern Africa, as exemplified by more frequent El Niño-linked droughts and heat waves. The impacts of climate change in Sub-Saharan Africa are likely to be severe as a result of extreme poverty, malnutrition, and hunger, as well as low adaptive capacity (Mazvimavi et al., 2011; Kusangaya et al., 2014).

Several studies in Ghana have examined the potential impacts of climate change on water resources (Zougmore et al., 2014; Agodzo et al., 2023; Dinko & Bahati, 2023), with a consensus that climate change will affect both the quality and quantity of available water resources in the region.

However, literature shows limited research has been carried out in the Densu River Basin in terms of climate change and anthropogenic impacts on groundwater resources in the basin (Adomako et al., 2011a; Bam et al., 2011; Yidana et al., 2018). Population growth and urbanisation are expected to put more stress on the available water resources. These stresses will be caused by rising pollution of surface water bodies and increased reliance on groundwater for clean water supply within the basin. Abstractions of groundwater from the aquifer in excess of replenishment may lead to a critical case of unsustainability of the resource. Similarly, groundwater resources are also known to be vulnerable to geogenic sources of pollution such as the dissolution of soluble salts, fluoride minerals, low pH, etc, a problem that has serious impacts on human health (Kortatsi et al., 2008).

Hence, an evaluation of groundwater, in terms of availability, distribution, and quality, is needed to enhance the understanding of the groundwater resource and to support the formulation of future plans for the development of water resources. To do so, it is imperative to answer the following questions:

- ❖ What are the spatiotemporal variations of groundwater recharge rate across the basin?
- ❖ How can hydrogeological and hydrochemical data be integrated to develop a comprehensive conceptual understanding of the basin?
- ❖ What aquifer types underlie the basin, and what are their hydraulic characteristics?
- ❖ What are the principal controls on, and spatial variation in groundwater hydrochemistry, and what do they indicate about groundwater flow and recharge in the basin?

- ❖ How will different abstraction and/or recharge rates as a consequence of climate change, population growth, and urbanisation affect the groundwater system and sustainability of the resource?

1.3 Justification of Study

The Densu River Basin is characterised by aquifer systems with heterogeneous fractured crystalline rocks, weathered zones, and sedimentary formations with varying hydraulic properties, which to a large extent govern groundwater occurrence, movement, and quality. Understanding these hydrogeological conditions is essential for interpreting groundwater flow dynamics and hydrochemical evolution. Tay and Kortatsi (2008) analysed groundwater quality in the basin using hydrochemical data, while Adomako et al. (2011a) characterised the hydrochemistry of the basin using geochemical and multivariate statistical analysis. Even though these approaches offer valuable insights, they fail to directly quantify flow rates or recharge, characterise flow dynamics or the inherent aquifer properties. Also, Yidana et al. (2014) used a transient numerical model to estimate recharge rates in the basin and other hydraulic properties. While individual approaches offer valuable insights, combining numerical modelling, recharge estimation, and hydrogeochemistry provides a more holistic approach to the characterisation of the groundwater system in the basin. The integrated approach adopted in this study provides a quantitative understanding of flow dynamics and helps evaluate scenarios, enhances the reliability of recharge estimates, and provides additional constraints on model parameters and processes. This research holds significant importance for the comprehensive approach adopted for understanding and managing groundwater resources to provide a thorough evaluation of groundwater availability, quality, and sustainability in the Densu River Basin. This approach is crucial for the development

of efficient and practical strategies to effectively manage water resources to meet various needs while addressing challenges posed by climate change and population growth on water demand and availability. The findings from this study will be valuable to policymakers, water resources managers, private sector businesses, and other key stakeholders as they can be used to inform the development, utilisation, management, and conservation of groundwater resources. This will enhance the sustainability of the resource.

1.4 Research Objectives

The study seeks to characterise the hydrogeology and hydrochemistry of the Densu River Basin and evaluate the sustainability of groundwater resources under increasing pressures from climate change and variability, population growth, and urbanisation.

The specific objectives are to;

- ❖ Estimate groundwater recharge using multiple methods based on different and independent data types to understand its spatiotemporal characteristics in the basin;
- ❖ Develop a conceptual hydrogeological understanding of the basin, integrating hydrogeological and hydrochemical data;
- ❖ Develop and calibrate/validate a transient 3D groundwater flow model for the basin and assess the impacts of scenarios of abstraction and climate change on the groundwater resource.



1.5 Thesis Structure

This thesis is organised into five chapters to facilitate a comprehensive exploration of the subject matter. Chapter 1 gives an overview of the research topic and area, its significance, and objectives. The next three chapters (2-4) all relate to journal papers or manuscript drafts generated during this thesis.

A large portion of Chapter 2 is published in a peer-reviewed journal as a review paper (Akurugu et al., 2022), drafted from a literature review on the topic and study area. The chapter contains a description of the study area, including the geology, hydrogeology, and climate. Some of the content in this chapter is repeated in relevant portions in chapters 2, 3, and 4. This is because those three chapters have been organised as stand-alone and ready-to-publish chapters.

Chapter 2 delves into the application and comparison of different recharge estimation methods, utilising independent datasets capable of giving deep independent insights into recharge characteristics for efficient and sustainable management of groundwater resources in the basin. The strengths and weaknesses of the methods applied are also discussed, and the complementary advantages of using multiple methods are revealed in how the weaknesses in one method are offset by another.

Chapter 3 explores the conceptual hydrogeologic framework of the Densu River Basin, which encompasses the hydrochemistry and conceptual groundwater flow analyses. A detailed understanding of the hydrogeological properties and groundwater hydrochemistry provides crucial information for informed and practical sustainable management of the resource. The suitability of the groundwater for domestic and irrigation purposes and the hydrochemical processes influencing

same have also been assessed in this chapter. Assessment of essential aquifer parameters, borehole logs, and hydrochemical data was conducted in an attempt to construct a holistic conceptual understanding of the hydrogeology of the Densu River Basin.

Chapter 4 presents the conceptualisation, development, calibration, and validation of a transient 3D numerical groundwater flow model, and predictions made using the same based on scenarios of various stresses to assess the impacts on groundwater resources in the basin. The conceptualisation and input parameters to the numerical model were built based on information and analysis in the preceding chapters and a review of the literature.

Chapter 5 summarises the key findings and significance of the research, and outlines potential future research directions to further explore the groundwater dynamics within the Densu River Basin based on the limitations of this study.

1.6 Study Area

The Densu River Basin is located in south-western Ghana, between latitudes 5°30' and 6°20' north, and longitudes 0°10' and 0°38' west (Figure 1.1). It is bordered to the north by the Afram and Pra basins, the coastal basins and the Gulf of Guinea to the south, the southern Volta and Afram basins to the east, and the Ayensu basin to the west. The basin is highly populated by rural and urban settlements, with over a million people and a population density of about 359/km², about five times the national average (Ghana Statistical Service, 2021). The high population density is mainly due to its proximity to the Accra metropolitan area, the national capital (WRC, 2007). The basin has a land mass of about 2,500 km², spanning 13 districts, and three regions of Ghana; about 72%, 23% and 5% of the basin lies within the Eastern, Greater Accra and Central Regions, respectively.

The Densu River takes its source from the Atewa-Atwiredu hills and flows downstream in an easterly direction towards Koforidua, where it gradually changes its course and flows southwards into the Weija dam (Figure 1.1a). The dam stores water for supply to the western parts of Accra, and surplus water discharges into the Densu delta (Sakumo lagoon), and finally into the Gulf of Guinea (Yidana et al., 2014). Generally, the basin features gently undulating terrain with elevations ranging from about 0 to over 777 m.a.s.l. The northern part, particularly around the Atewa Range, consists of upland areas, with steep elevations reaching 777 m.a.s.l., characterised by dissected hills and rolling lands. The basin slopes southeastward toward the Weija Reservoir, supporting a dendritic drainage pattern. Low-lying areas dominate the central and southern portions, with elevation between 0 and 65 m.a.s.l., and a slope of about 2%, where broad alluvial plains are more prone to flooding and pollution. The highly variable relief influences both surface runoff and groundwater flow dynamics across the basin (WRC, 2007).

The climate of the area is wet semi-equatorial in the north and dry equatorial in the south, towards the coast. Rainfall is bimodal in both climates, with a mean annual rainfall of approximately 1400 mm in the north and 700 mm in the south (Figure 1.1b), which occurs between April - June, and September – November (Figure 1.2). Relative humidity is highest during the rainy season, reaching an average of 93%, and declines gradually to around 41% in the dry season, during the harmattan (Adomako et al., 2011a). Air temperatures are usually high in the basin, averaging 27 °C and ranging between a minimum of 23 °C during the harmattan in December and a maximum of 32 °C in March (Akurugu et al., 2022).

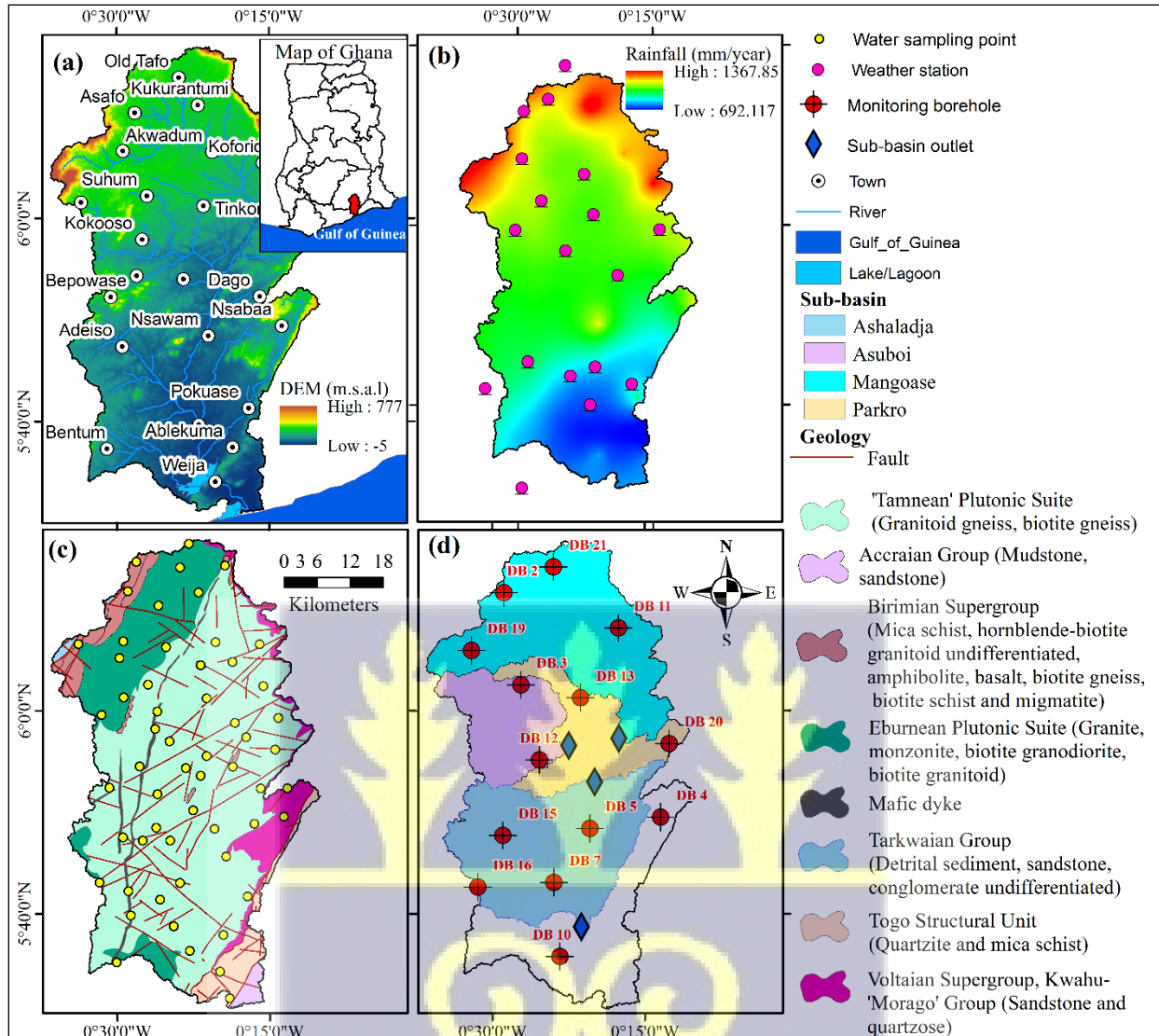


Figure 1.1: Map of the Densu River Basin (a) showing elevation, surface water and towns, (b) spatial distribution of average annual rainfall, (c) geology (adopted from Duodo, 2009), and (d) sub-basin

The climate in the north has given rise to a moist semi-deciduous forest, whereas the south is characterised by a dense growth of bushes of the coastal savanna. The forested zone of the basin, which contains some of the timber resources in Ghana, has been depleted, leaving very little of the original forest, mainly due to cocoa farming. The depletion of the forest cover has left behind a

secondary forest cover, which is referred to as a derived savanna (Mantey et al., 2011). The area is characterised largely by well-drained ochrosols, which are typically red, reddish brown, or orange-brown, and are largely low in nutrients, particularly nitrogen and phosphorus. However, the forested ochrosols in the north of the basin are relatively rich in nutrients.

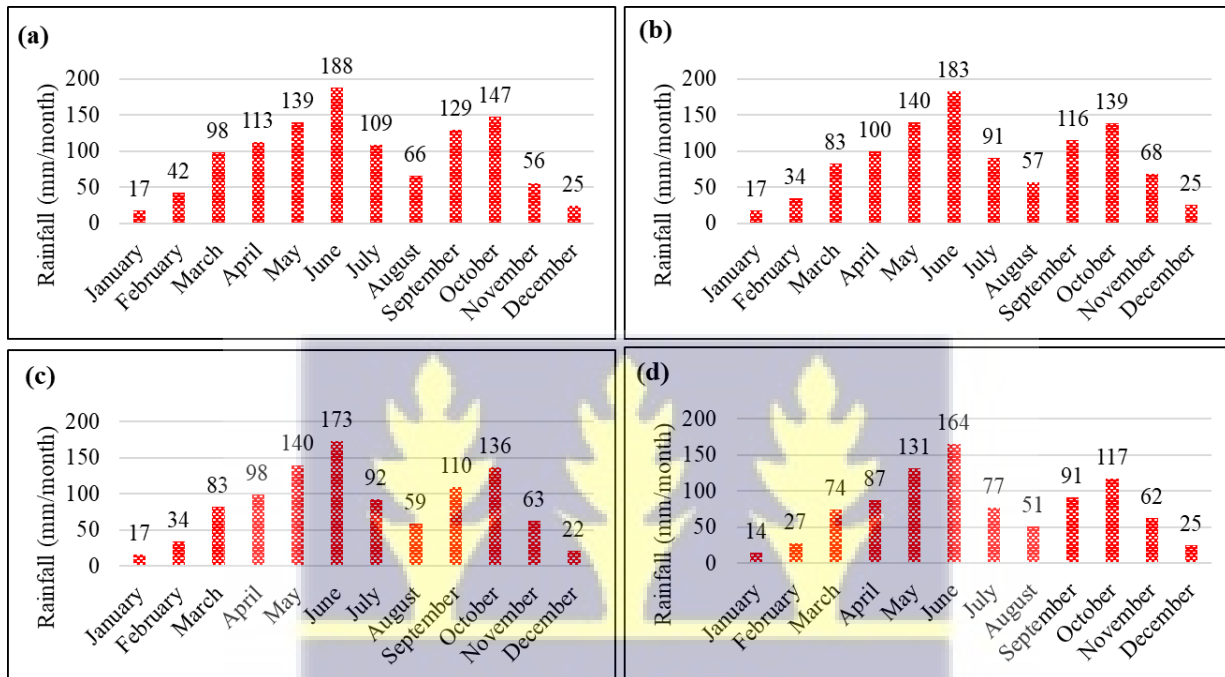


Figure 1.2: Average monthly rainfall for the (a) Mangoase, (b) Asuboi, (c) Parkro, and (d) Ashaladja sub-basins of the Densu River Basin (1981 - 2022)

1.7 Geology and hydrogeology

The Densu River Basin is underlain largely by the Basement Complex, comprising Precambrian crystalline igneous and metamorphic rocks. These rocks are mainly the Birimian, Granites, Tarkwaian, Accraian and Palaeozoic consolidated sedimentary formation of the Voltaian Supergroup (Figure 1.1c). The sedimentary formation, mainly the Kwahu-Morago Group (Kortatsi, 1994; Dapaah-Siakwan & Gyau-Boakye, 2000; Adomako et al., 2011b), consists of

basal sandstones, medium-grained mudstones, and shales. Rocks of the Togo Structural Unit, on the other hand, are highly folded and jointed and form the chain of hills known as the Akwapim-Togo Ranges, which extend from the coast of Accra to the Togo border. The Togo structural Unit in the Densu Basin consists of metamorphosed arenaceous and argillaceous sedimentary strata, typically composed of quartzite and micaceous schist. The Tarkwaian Group underlies a small portion of the basin in the northwest. It comprises detrital sediment, mainly sandstone and conglomerate, undifferentiated, which is typically intruded by thick laccoliths or dikes and sills of epidiorite with folds along the axes that trend northeast. Rocks of the Accraian Group, which underlie the extreme south of the basin, have undergone post-depositional igneous activity and major block faulting. Common rock types in this group include shale, sandstone, and grit (Dapaah-Siakwan and Gyau-Boakye, 2000). Rocks of the Birimian Supergroup occur in the extreme northwest of the basin. It comprises two major lithostratigraphic units of early Proterozoic age, which are the Birimian Sedimentary Basins and Birimian Volcanic Belts (Kesse, 1985). The Eburnean tectono-thermal event, which stabilised the West African Craton, caused the Birimian Supracrustal rocks to become folded and metamorphosed under greenschist-facies conditions, and intruded by granitoids of the Eburnean and Tamnean Plutonic Suites.

The Basement rocks are characterised by little/negligible pore spaces, permeability, and transmissivity; as a result, aquifers within these rocks exhibit low yields (Cook, 2003; Darko & Krásny, 2007). Therefore, groundwater occurrence in the basin is controlled by the occurrence and pervasiveness of secondary structural entities such as joints, fractures, and weathered zones which produce openings for groundwater recharge, flow, and storage (Darko et al., 2003; Yidana et al., 2014). The occurrence and pervasiveness of these secondary structural entities have resulted in the

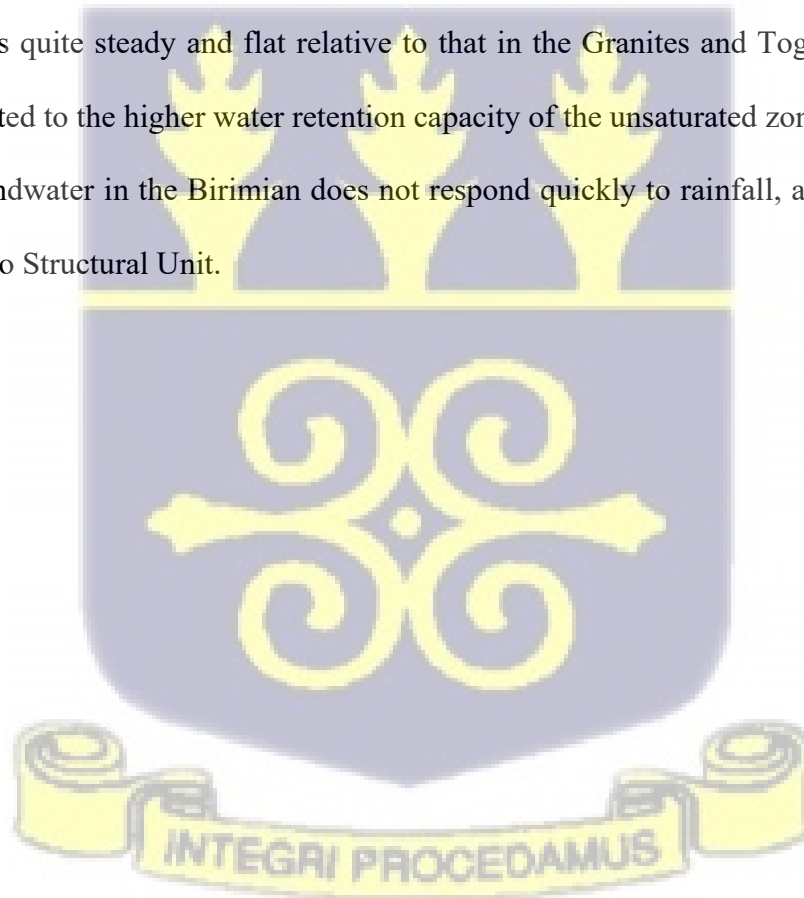
development of the weathered zone aquifers and the fractured zone aquifers. These two main aquifer types contain the alluvium (very thin and non-existent in most places), saprolite, saprock, fractured and fresh bedrocks, within which groundwater occurs (Banoeng-Yakubu et al., 2011). Aquifers within the weathered zone occur at the base of the saprolite and in the upper parts of the saprock and complement each other in terms of groundwater delivery. The weathered zone varies from 0 to 100 m, thickest in the forested areas, averaging 60 m, and thinnest in the arid zones, averaging 10 m. The fractured zone aquifers, on the other hand, usually occur at some depth beneath the weathered zone. The weathered and fractured zone aquifers are usually discontinuous and limited in area (Kortatsi, 1994).

As a result of the complexity of weathering and the occurrence of secondary structural entities, the hydrogeological properties are highly variable. Aquifers within the Birimian are highly productive in terms of groundwater delivery, owing to downward folding, which can serve as reservoirs for groundwater accumulation and deep weathering. Borehole yield varies between 0.7 and 9.0 m³/h with an average of 3.7 m³/h. Relatively, the granites deliver less water as a result of the less weathered conditions and fractures, except for the northern parts of the basin, where groundwater delivery in the granites is relatively high (Darko et al., 2003). Borehole yield within the granites varies from 0.1 to 30.0 m³/h, with a mean value of 2.0 m³/h. Darko et al. (2003) observed no correlation between yield and borehole depth in the granites in the Densu Basin but noted that borehole yield declined beyond 60 m. They concluded that drilling beyond 60 m in the granites may not improve the yield. Aquifers in the granites are generally unconfined to semi-confined, and yield is controlled by the degree of weathering and continuity of the formation's structures (Adomako et al., 2011a, b).

The Togo Structural Unit along the south-eastern border of the basin is highly fractured, jointed and folded, and the contact zone between it and the Voltaian and granites offers highly conducive conditions for high groundwater accumulation. Borehole yield in the Togo Structural Unit ranges between 0.6 and 6.0 m³/h, with an average of 2.8 m³/h. Analyses of hydrogeological data from the database of the CSIR-Water Research Institute revealed that borehole depths in the Densu Basin range between 23.0 and 40.0 m in the Birimian, 9.1 and 103.0 m in the granites and 28.0 and 97.0 m in the Togo Structural Unit. Similarly, the average thicknesses of the weathered zones are between 5.0 and 27.0 m, 1.0 and 32.0 m and 3.0 and 36.0 m, respectively, in the Birimian, granites and Togo Structural Unit. Static water levels in the basin, on the other hand, vary from 0.8–16.9 m, 0.1–13.5 m and 1.1–17.9 m in the Birimian, granite and Togo Structural Unit, respectively. However, due to the discontinuous nature of groundwater occurrence in the granites, the static water levels may vary widely and not necessarily fall within the stated bounds.

Hydraulic conductivity and permeability of the rock determine, to a large extent, the amount of vertical groundwater recharge rate. The hydraulic conductivity field established by Yidana et al. (2014), through the simulation of a transient groundwater model in the basin, ranged between 2 m/d in the middle portions of the basin and over 40 m/d in some parts of the south. The Togo Structural Unit (southeast of the basin) have been described as highly folded and jointed, creating unique conditions for groundwater flow and high storage (Adomako et al., 2011a, b; Yidana et al., 2014). Pumping test analyses in the basin revealed transmissivity for the granites, Birimian and Voltaian to be 0.5–86.8 m²/day, 31.8 m²/day and 0.38 m²/day, respectively. Transmissivity values for 24 boreholes in only the granites were obtained. The range of 0.5–86.8 m²/day, with a mean of 8.9 m²/day, showed a fairly heterogeneous hydrogeological environment in the granites, which is

characteristic of crystalline geologic formations. As the only study, Yidana et al. (2014) present a spatial distribution map of the hydraulic head. Their study suggests hydraulic heads were highest in the northern parts where the Densu River takes its source and rainfall is highest, and lowest in the southern parts of the basin (Fig. 1.1) where rainfall is lowest (WRC, 2007). Groundwater in the basin has therefore been observed to flow in the north-south direction (Alfa, 2010; Yidana et al., 2014, 2018), in accordance with the general hydrogeological principle; groundwater flows from high elevation to low elevation areas (Akurugu et al., 2020). Alfa (2010) further noticed that, on average, hydraulic heads in all the geologic formations showed an annual fluctuation of about 2 m between the wet and dry seasons. Head fluctuation in the Birimian Supergroup, according to Alfa (2010), was quite steady and flat relative to that in the Granites and Togo Structural Unit, which he attributed to the higher water retention capacity of the unsaturated zone of the Birimian. Therefore, groundwater in the Birimian does not respond quickly to rainfall, as compared to the Granite and Togo Structural Unit.



CHAPTER TWO

GROUNDWATER RECHARGE ESTIMATION FROM MULTIPLE INDEPENDENT METHODS IN THE FRACTURED HARD ROCK AQUIFERS IN THE DENSU RIVER BASIN, GHANA

2.1 Introduction

Groundwater remains one of the most critical freshwater resources worldwide, especially for drinking and domestic purposes. It accounts for 98 - 99% of all liquid fresh water on earth (Margat & Van der Gun, 2013) and supports farming, sanitation, industry, and drinking water supplies. Globally, over 1.5 billion people depend on groundwater for their potable water supply (Clarke et al., 1996). The demand for groundwater resources is expected to grow in the wake of population growth, industrialisation, pollution, and climate change (Lutz et al., 2010; Howard et al., 2016; Belhassan, 2022), especially in arid and semiarid climates (Hoogesteger, 2022; Zamani et al., 2022). A proper understanding of groundwater recharge, the process through which groundwater is replenished, is crucial to the efficient and sustainable management of the resource (Pulido-Velazquez et al., 2020). Recharge and the mechanism of its occurrence have direct implications for groundwater quality and suitability (Adhikari et al., 2022; Sadeak et al., 2023). The rate and spatiotemporal pattern of groundwater recharge, for example, have implications for the effective management of the resource, including protection from contamination. However, the estimation of groundwater recharge is one of the most difficult and uncertain components of the groundwater resources assessment framework. This is mainly due to the complex nature of groundwater recharge processes and the lack of direct methods of measurement.

Notwithstanding, several methods (e.g. water budget, numerical modelling, water table fluctuation, empirical methods, baseflow separation, Darcy's methods, chloride mass balance, tracers techniques, satellite data analysis, etc) have been devised and used in many studies (Chen & Lee, 2003; Yeh et al., 2007; Adomako, Maloszewski, et al., 2010; Healy & Scanlon, 2010; Qablawi, 2016; Duah et al., 2021) for characterisation of quantitative groundwater recharge. The application of a recharge method should be based on a conceptual understanding of the recharge processes in the site and the fundamental theory, assumptions inherent in the method being applied, and the adaptability of the method to different environmental settings and water management goals (Lafare et al., 2021) to ensure consistency and modification of same if need be (Healy & Cook, 2002; Healy & Scanlon, 2010).

Several texts in the literature (Lerner et al., 1990; Healy & Scanlon, 2010; De Vries & Simmers, 2002; Scanlon et al., 2002) recommend the application of multiple methods in recharge estimates since errors associated with these estimates are hardly quantifiable. Results from multiple methods and consistency of same do not necessarily imply accuracy, however, may give qualitative insight into some measurement errors or improper conceptualisation of the site for which a recharge method is applied (Scanlon et al., 2002; Singh et al., 2019; Seidenfaden et al., 2023).

The different groundwater estimation methods vary in complexity and data requirements; from simple empirical formulas (Mandel & Shiftan, 1981; Cheeturvedi, Sinha & Sharma, 1988; Guttman & Zukerman, 1995) to advanced complex numerical modelling approaches which require several data types and skills in their implementation (e.g., Cooley, 1979; Sanford et al., 2004; Tiedeman et al., 1997; Yidana et al., 2015). The chloride mass balance (CMB) and water table fluctuation methods are two of the most widely used approaches for estimating groundwater

recharge globally (Geneviève et al., 2020; Crosbie & Rachakonda, 2021; Malík et al., 2021). The CMB method is popular for its robustness over several climatic zones and cost-effectiveness; in its basic form only requires analysis of chloride levels in groundwater and rainfall. The CMB method is relatively easy to accurately implement in basins that meet the basic assumption that atmospheric deposition is the only source of chloride in groundwater, discounting the contribution of chloride from the aquifer, vadose zone, dry deposition, etc. Uncertainty from the method arises from upscaling point estimates to basin/regional scales, or where other processes influence the chloride levels in the groundwater system (Akurugu et al., 2020; Crosbie & Rachakonda, 2021). The WTF, on the other hand, is straightforward and insensitive to the mechanism of recharge in the unsaturated zone (Healy & Cook, 2002). It assumes that a rise in the water table in unconfined aquifers is due to recharge. The most uncertain parameter in the WTF method, given that the water table elevations are measured accurately, is the specific yield (S_y), especially with the assumption that S_y is constant throughout the entire aquifer and within the area under consideration. This constitutes a weakness of the method since practically S_y varies variously across different soil materials and vertically within aquifers (Geneviève et al., 2020). There are various implementations of the WTF method, varying from the conventional graphical approach (Obuobie et al., 2012; Duah et al., 2021) to the rise and corrected rise methods (Nimmo et al., 2015). Analysis of streamflow datasets is another way of understanding groundwater recharge. Inherent in streamflow data are the baseflow and quick flow components, which give great insight into groundwater recharge dynamics and a catchment's hydrological response to storm runoff and changing water dynamics. Simple recursive digital filters (Lyne & Hollick, 1979; Chapman & Maxwell, 1996; Eckhardt, 2005; Tularam & Ilahee, 2008) have been adopted in estimating

baseflow, a derivative of groundwater recharge, in several studies (e.g. Chemingui et al., 2015; Huet et al., 2016; Kissel & Schmalz, 2020; Andualem et al., 2021). These methods are hereafter referred to as baseflow filters (BFF).

Multiple studies have tried to compare the results of recharge estimations from different methods (e.g., Lee et al., 2010; Somaratne et al., 2014; Crosbie & Rachakonda, 2021; Seidenfaden et al., 2023), routinely finding large spreads (uncertainties) in recharge estimation results. However, only very few studies have been published on tropical African regions (Walker et al., 2019). This study aims to use different data types to estimate groundwater recharge using multiple methods that each rely on different and independent data types; the water table fluctuation (WTF) based on groundwater levels, chloride mass balance (CMB) based on chemical analyses of chloride content, and two baseflow separation (BFF) methods based on stream discharge measurement in the Densu River Basin Ghana. Each of these methods relies on different and independent data types, which provide independent insights into groundwater recharge in their respective unique ways but collectively aid a comprehensive understanding of the spatiotemporal characteristics, dynamics, and mechanisms of recharge in the fractured hard rock system of the Densu River Basin.

2.2 Materials and Methods

This study adopts three independent methods for estimating groundwater recharge and baseflow in the Densu River Basin. The ESPERE Tool (Lanini et al., 2020), which is a numerical tool used to rapidly and simultaneously estimate aquifer recharge using several different methods was adopted in this study. The groundwater recharge methods used in ESPERE are the water table fluctuation (WTF) method and two baseflow filters (BFF); (Chapman & Maxwell, 1996; Eckhardt,

2005). The study also adopted point estimates from the chloride mass balance method, which were spatially interpolated over the basin. Given the current state of the science, it is challenging to directly measure and assess the accuracy of any recharge method; hence, outputs from multiple methods complement each other and build confidence in the results. Although Healy and Cook (2002) admonish that consistency of results should not be mistaken for accuracy.

2.2.1 Conceptual recharge

Healy and Scanlon (2010) recommend the development of conceptual models of recharge processes applying a particular estimation method, to help understand where, when, how, and why recharge occurs the way it does at a particular place and time. The conceptual model aims to identify the most significant recharge contributions to the groundwater system and serves as a guide for choosing suitable methods of estimation. The accuracy of recharge estimates relies on the adequate conceptualisation of the recharge mechanisms in the domain, the input data, and the validity of the assumptions of the estimation method.

The conceptual model of this study is based on the river network, regolith, topography, geology, and climate, which appear to be the main factors influencing recharge in the basin. The study area is characterised by weathered and fractured crystalline aquifers, which are mostly unconfined to semi-confined. The northeast and northwest of the basin are characterised by hills and mountain ranges, with somewhat thick forest cover, and a wet semi-equatorial climate, as such records the highest rainfall in the basin. Key hydrological processes that influence groundwater storage in the basin are illustrated in Figure 2.1 through multiple flow paths. These include: infiltration and percolation of water to the saturated zone, groundwater discharge to rivers and vice versa, shallow

subsurface flow toward river channels, abstraction through wells, and evapotranspiration losses. Groundwater recharge in the basin occurs as the influx of water to the saturated zone through infiltration from soils and surface waters. Besides the probabilistic pattern of rainfall occurrence, undulating topography, which is characteristic of the northern and some central sections of the basin, may also greatly influence groundwater recharge. The orographic influence of the mountains causes higher rainfall and groundwater recharge in the mountainous areas. Generally, the temporal and spatial variability of precipitation, climate, soil, topography, vegetation, and land use impact the amount of recharge that may occur in a place (Lerner et al., 1990; De Vries & Simmers, 2002).

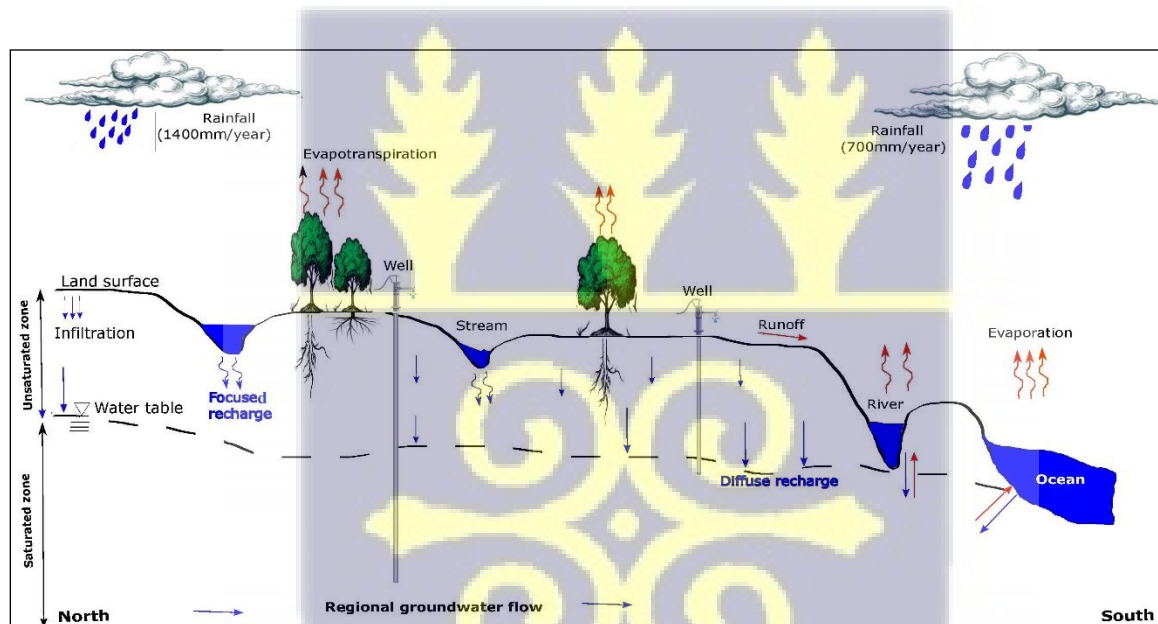


Figure 2.1: Conceptual model showing groundwater recharge and storage mechanisms in the Densu River Basin

Several ephemeral streams and perennial rivers abound in the Densu Basin (Figure 1a), making focused recharge a probable recharge mechanism in the area. Ephemeral streams can contribute

significantly to groundwater recharge in dry areas (Healy & Scanlon, 2010), such as the southern section of the basin, which is characterised by a dry equatorial climate. Ephemeral streams usually contain water after rainfalls for relatively shorter periods, which is lost as evapotranspiration or through the stream bed as potential or actual recharge. A river, especially perennial, may lose or gain water along its reaches at some point of flow or time of year. Hence, water in a river that contributes to recharge at some point may be discharged at some other point due to the spatiotemporal variability of hydrological processes (Scanlon et al., 2002; Kang et al., 2021); this point is critical in the selection of an appropriate recharge method in time and space.

2.2.2 Chloride mass balance method

Chloride is generally conservative and does not actively participate in biogeochemical reactions; hence serves as a good tracer for recharge studies (Mullaney et al., 2009; Somaratne & Smettem, 2014). The chloride mass balance (CMB) method is based on the assumption that all the chloride in groundwater results from atmospheric deposition; chloride in the atmosphere moves with infiltrating water into the groundwater system. Chloride data from 60 boreholes and hand-dug wells were collected in the study area and used with average chloride data in rainwater for point estimates of groundwater recharge based on Equation 2.1.

Due to the high climatic variation in the study basin, the average annual rainfall for each sampled point was extracted from a gridded rainfall map spanning 1981 - 2022 (Figure 1b), which was developed for the basin based on the 5 x 5 km gridded data from Gyasi-Agyei et al. (2023). The average chloride amount in rainfall was estimated at 1.13 mg/l based on historical chloride data from some of the weather stations in the basin (Duah et al., 2021), which was used for all point

estimates in this study. Bicarbonate ions are abundant in groundwater, but chloride generally occurs in small amounts in groundwater; but is abundant in seawater. The ionic ratio of chloride and bicarbonate was used to constrain groundwater samples that may have been influenced by other sources of chloride, such as seawater intrusion, which is plausible in the coastal areas in the extreme southeast of the basin.

$$R = \frac{Cl_{(p)}}{Cl_{(gw)}} \times P \quad (2.1)$$

Where R is groundwater recharge rate (mm/year), $Cl_{(p)}$ is the average chloride amount in rainfall (mg/l), $Cl_{(gw)}$ is the chloride amount in groundwater sample (mg/l), and P is the average annual rainfall (mm/year).

2.2.3 Water table fluctuation method

HOBO water level loggers U20 series, with a range of 0 - 30 m, were installed 15 m below the static water levels in 14 monitoring wells and programmed to measure hourly. Two barometric loggers with a range of 0 - 9 m were also installed in Suhum (DB 3) and Nsawam (DB 5) (Figure 1d) to measure atmospheric pressure used to compensate for the water logger readings. The monitoring wells were placed such that they were evenly distributed as well as representative of the various geologic formations in the basin. Monitoring was carried out from 2020 to 2023. Historical water level monitored data from 2004 to 2008 were also analysed in this study. The hourly time series static water level data were averaged to daily records, plotted as graphs, and visually inspected. Data series with obvious seasonal fluctuations and apparent responses to rainfall, with no missing records of more than 5 continuous days, were considered for further

analysis. Precipitation data from the monitoring stations extracted from a bias-corrected 5 x 5 km gridded precipitation data for the respective groundwater monitoring periods (Gyasi-Agyei et al., 2023) were used alongside the groundwater data for this analysis. The ESPERE tool requires specific yield, daily rainfall, and groundwater level data for recharge estimation using the water table fluctuation (WTF) method. This study adopted the corrected RISE implementation for the WTF method, which takes into account the unrealised recession, a simplified form of the Episodic Master Recession method by Nimmo et al. (2015). Different specific yield values were tested with each borehole guided by the hydrogeology and records from Johnson (1967) and Sinha and Sharma (1988).

The water table fluctuation method assumes that groundwater recharge is the cause of any rise in the water table in unconfined aquifers per unit time, and the recharge rate is proportional to the specific yield of the aquifer (Healy & Cook, 2002; Mensah et al., 2014; Yang et al., 2018). The WTF technique is best applied to shallow unconfined aquifers and water tables that display sharp rises and declines in water levels (Healy & Cook 2002). Groundwater recharge is estimated as the product of the water level rise and the specific yield of the aquifer material at each time step as follows:

$$R = \frac{\Delta h}{\Delta t} \times S_y \quad (2.2)$$

where S_y is the specific yield of the unconfined aquifer, Δh is the change in water table height, and Δt is the period for the change in water table height.

2.2.4 Baseflow separation methods

Baseflow in the context of groundwater recharge analysis may be considered as a lower end bound of actual groundwater recharge. This is because part of the recharge is lost to evapotranspiration, inter-basin flow, groundwater abstraction, etc (Healy & Scanlon, 2010; Zomlot et al., 2015). Two digital filter-based baseflow separation methods, Chapman and Maxwell (1996) and Eckhardt (2005), were implemented in this study using the “Estimating Effective Rainfall and Aquifer Recharge by Different Methods - ESPERE” tool (Lanini et al., 2020). These two methods assume baseflow is the low-frequency part of streamflow that responds slowly to the precipitation and is sustained by groundwater, whereas interflow and overland flow, which constitute quick flow, are the high-frequency part that responds quickly to the precipitation. Streamflow gauge stations in the basin (Figure 1d) were used as outlets for sub-basins for the baseflow analysis. Four sub-basins were delineated for the basin: Mangoase, Asuboi, Parkro, and Ashaladja. Daily streamflow data with gaps of less than 5 continuous days, as required by the ESPERE tool, were analysed. This resulted in the analyses of streamflow and rainfall records for the years 2006-2007 for Ashaladja, 1971-1993, 1997, 2003-2008 for Asuboi, 2003-2011 for Mangoase, and 1973-1975, 1995, 2004-2008, 2011 for Parkro. In contrast to the WTF and CMB methods, which are considered point estimates of recharge, the BFF method is regarded as catchment average recharge rates for the area upstream of the streamflow gauge location.



2.3 Results

2.3.1 Chloride mass balance (CMB)

Based on the CMB method, annual groundwater recharge across all 60 available chloride sampling points for the Densu River Basin varies from 1 – 338 mm, with an average of 34 mm and a standard deviation of 55 mm (Table 2.1). These ranges of values are comparable with recharge estimates by other studies in the Densu River Basin. The high standard deviation of 55 mm/year suggests the groundwater recharge values are widely dispersed, indicating several factors control the mechanism and amount of recharge in the basin. The CMB estimates represent long-term groundwater recharge for the basin, employing rainfall data for the period 1981 – 2022.

The CMB recharge estimates are generally low in the middle and south of the basin, with an average of about 3% of the average annual rainfall. The low values in the south are attributable to the effects of seawater intrusion and sea spray, which impact the groundwater up to 30 km inland. The effect of this is high levels of chloride in the groundwater and relatively low recharge estimates. Therefore, uncertainties associated with recharge estimates using the CMB method in the basin would likely impact the lower bound values. However, the recharge estimates appear to be in tandem with the distribution of rainfall in the basin, decreasing southwards.

Table 2.1: Summary statistics of recharge estimates from the CMB method. Standard deviation in brackets.

	Recharge (mm/year)	Recharge%	Rainfall (mm/year)
Mean	34 (55)	3 (5)	1094 (121)

Minimum	1	0	792
Maximum	338	24	1318

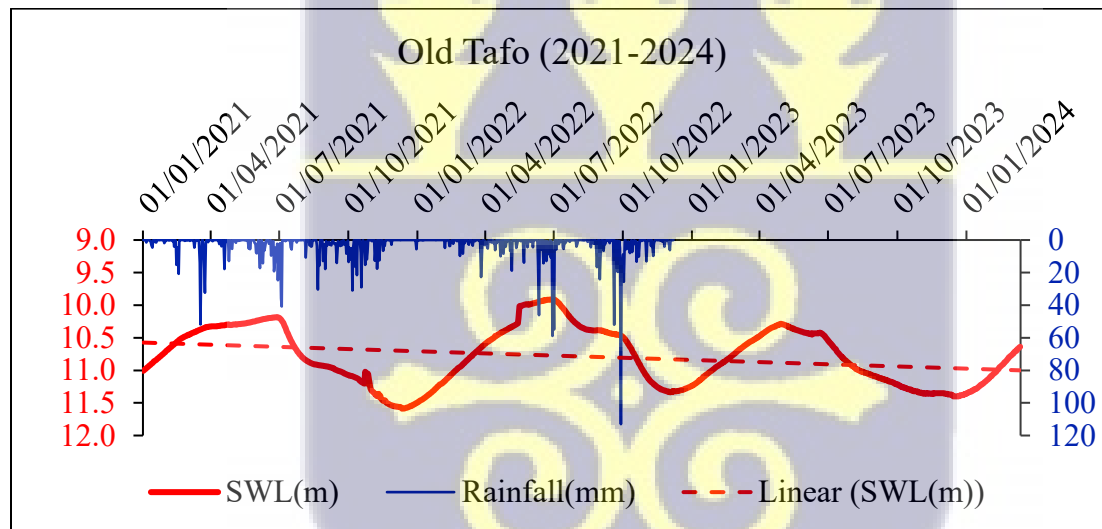
2.3.2 Water table fluctuation (WTF)

Groundwater hydrographs were compared with rainfall records for the same period to understand the behaviour of the water table to rainfall for aquifers in the Densu River Basin (Figure 2.2). The groundwater level fluctuations in the basin did not vary much within the various geological formations, ranging from 0.4 - 7 m/year, with an average fluctuation of 2.5 m/year. The highest fluctuations of 5 - 7 m/year occurred at Nsawam and Suhum, both located in the Granitoids. The highest rainfall occurs within the major and minor rainfall seasons in the basin (Figure 1.2), which are between April-June and September-November, respectively. However, groundwater level rise in all the monitored boreholes displayed an average of 2.5 months' delay to rainfall events. The average 2.5-month lag time is the period within which the soil moisture is refilled after the preceding dry season, which also suggests the groundwater recharge process is slow and gradual (Obuobie et al., 2012).

Recharge for each of the monitoring wells was estimated for selected years with no large gaps of missing records based on Equation 2.2 by multiplying the groundwater level rise by the specific yield values of the aquifer material in which the wells are situated. The average groundwater recharge ranged from minimum, maximum, and areal average values of 27, 327, and 150 mm/year for specific yield values of 0.01, 0.05, and 0.03, respectively. These estimates represent 3 – 28% of the annual rainfall (Table 2.2). The highest recharge rate of 327 – 149 mm/year, averaged over

five years, based on Sy values of 0.04 – 0.02 using the WTF method, was estimated at Adjomoku, located in rocks of the Birimian Supergroup. These high recharge estimates at Adjomoku are consistent with the high rainfall amounts in the north and the relatively porous hydraulic properties of rocks of the Birimian Supergroup.

The other monitoring boreholes in the north and central sections of the basin present similar recharge estimates in the same order of magnitude within the given specific yield values (Table 2.2 & Figure 2.3b). Recharge estimates from the WTF method appear to show a decreasing trend towards the south of the basin, with Ablekuma CP in the extreme south of the basin recording the lowest recharge estimate of 68 - 27 mm/year based on specific yield values of 0.05 - 0.02, in tandem with the rainfall pattern in the basin.



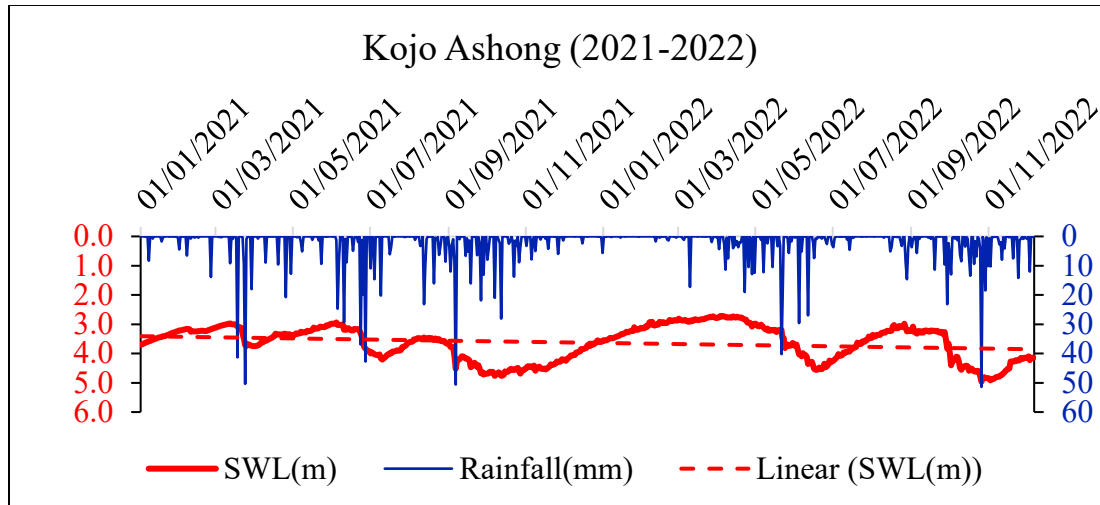


Figure 2.2: Groundwater fluctuations for selected boreholes in the Densu River Basin



Table 2.2: Groundwater recharge estimates from the WTF method for selected boreholes and years

Borehole	Period of record	Specific yield (Sy)	Average recharge (mm/year)	% Annual rainfall
Tafo (DB 1)	2006	0.05 - 0.03	320 – 160	22% - 12%
Old Tafo (21)	2021-2022	0.05 - 0.02	103 - 41	10% - 4%
Adjomoku (DB 2)	2005-2006, 2008, 2021-2022	0.04 - 0.02	327 - 149	24% - 13%
Suhum (DB 3)	2006, 2008, 2021-2022	0.02 - 0.01	256 – 186	22% - 16%
Akrabo (DB 13)	2021-2022	0.05 - 0.02	166 - 66	16% - 6%
Yaw Amoahkrom (DB 12)	2021-2022	0.05 - 0.02	166 - 66	15% - 6%
Nsawam (DB 5)	2021	0.05 - 0.02	283 – 113	24% - 11%
Pokrom Nsabaa (DB 4)	2005-2006, 2008, 2021	0.02 - 0.01	220 - 126	23% - 14%
Kojo Ashong (DB 7)	2005-2007, 2021-2022	0.05 - 0.02	178 – 106	21% - 13%
Dankwah (DB 16)	2021-2022	0.05 - 0.02	89 - 35	9% - 4%
Domeabra (DB 10)	2021-2022	0.05 - 0.02	72 – 29	10% - 4%
Ablekuma CP (DB 9)	2005	0.05 - 0.02	68 - 27	9% - 4%

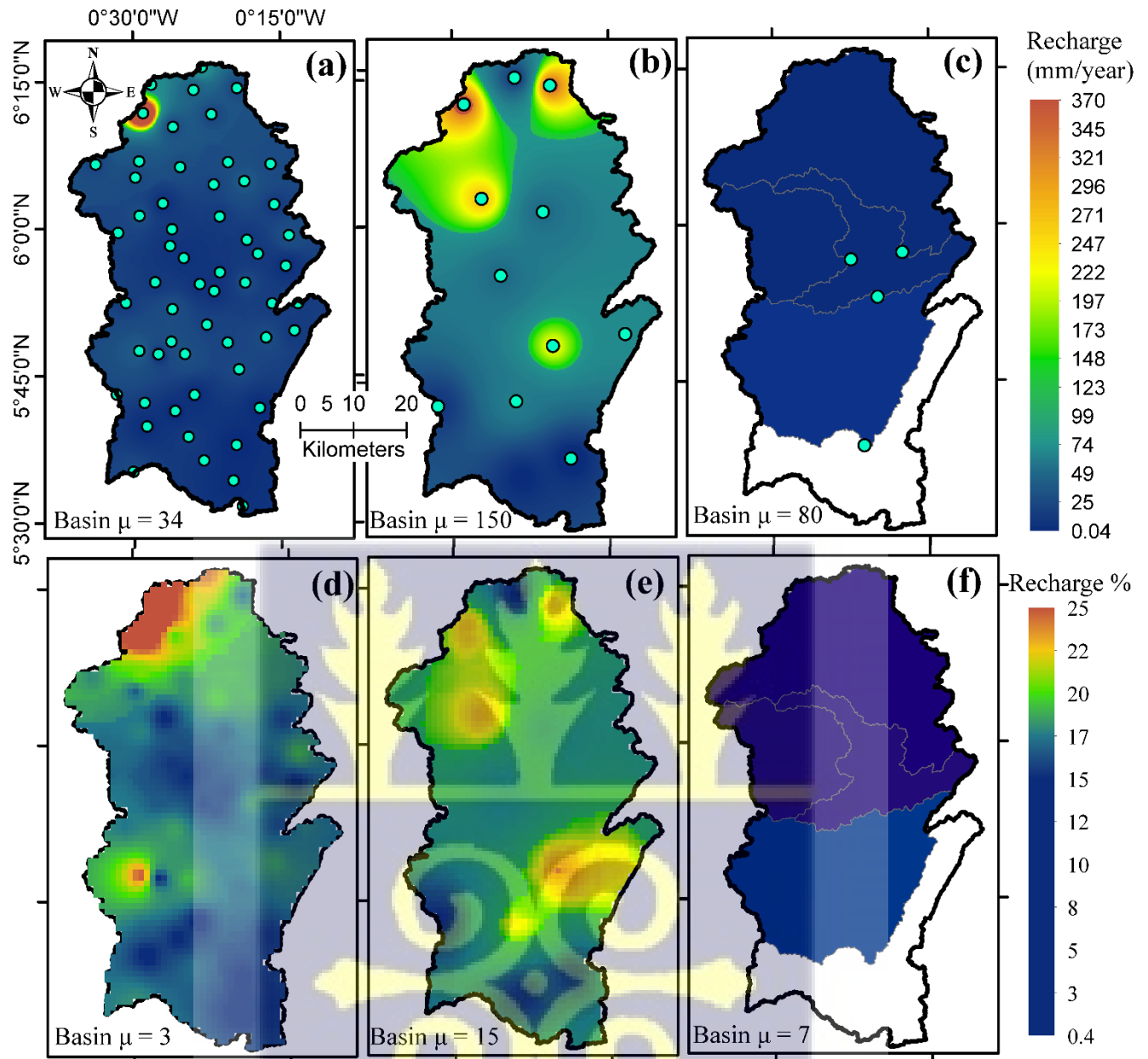


Figure 2.3: Spatial distribution of groundwater recharge in mm/year (a, b, c) and percent of average annual rainfall (d, e, f) based on the CMB (a&d), WTF (b&e), and BFF (c&f)

2.3.3 Recharge estimates from baseflow filters

The Chapman and Maxwell (1996) and Eckhardt (2005) baseflow filters were applied to daily streamflow data in four gauge stations to estimate monthly and annual recharge for the Densu River Basin for periods between 2003 and 2011. The average recharge for each sub-basin was computed by dividing the total average baseflow by the total area of the sub-basin, delineated by using the gauge stations as the sub-basin outlet. These methods revealed groundwater recharge using the Chapman and Maxwell (1996) and Eckhardt (2005) filters, respectively, to be 68 and 78 mm/year, 48 and 28 mm/year, 71 and 96 mm/year, and 105 and 146 mm/year for the Mangoase, Asuboi, Parkro, and Ashaladja sub-basins, respectively (Figure 2.3). These estimates represent, for the Chapman and Maxwell (1996) and Eckhardt (2005) filter methods, 6 and 7%, 5 and 3%, 6 and 9%, and 9 and 13% respectively, for the Mangoase, Asuboi, Parkro, and Ashaladja sub-basins. Recharge estimates in the Mangoase, Asuboi, and Parkro sub-basins are averages over nine, six, and five years, respectively, whereas the estimate for Ashaladja is for only the year 2007. As such, more credence may be put on those averages over those from the one-year record. The total average for the entire basin for the two methods is 73 and 87 mm/year for the Chapman and Maxwell (1996) and Eckhardt (2005) filters, respectively, representing 7% and 8% (Figure 2.3c&f). Estimates from the Chapman and Maxwell (1996) method are lower than those from the Eckhardt (2005) method except in the Ashaladja sub-basin, in line with the key assumption that baseflow cannot exceed streamflow in the Chapman and Maxwell (1996) method. The highest average monthly groundwater recharge occurs in June and peaks around October in all the sub-basins, reaching maximums of 16, 15, 14, and 25 mm/month for the Chapman and Maxwell (1996) method, and 19, 8, 20, and 35 mm/month using the Eckhardt (2005) method, respectively, for

Mangoase, Asuboi, Parkro and Ashaladja sub-basins (Figure 2.4). These recharge estimates do not show any obvious spatial correlation with the hydrogeology or hydroclimate of the basin, except that those estimates from the Mangoase, Asuboi, and Parkro sub-basins are in the same order of magnitude.

Generally, the average recharge estimates from the analysis of baseflow data from the two digital filter methods are lower than average estimates from the other recharge methods applied in this study. This corroborates the assertion that baseflow is a lower derivative of total groundwater recharge, some of which may have been lost through groundwater evaporation, inter-basin exchanges, abstractions, etc, resulting in the relatively lower recharge estimates from these baseflow methods (Lee & Risley, 2002; Bayou et al., 2021; Crosbie & Rachakonda, 2021).

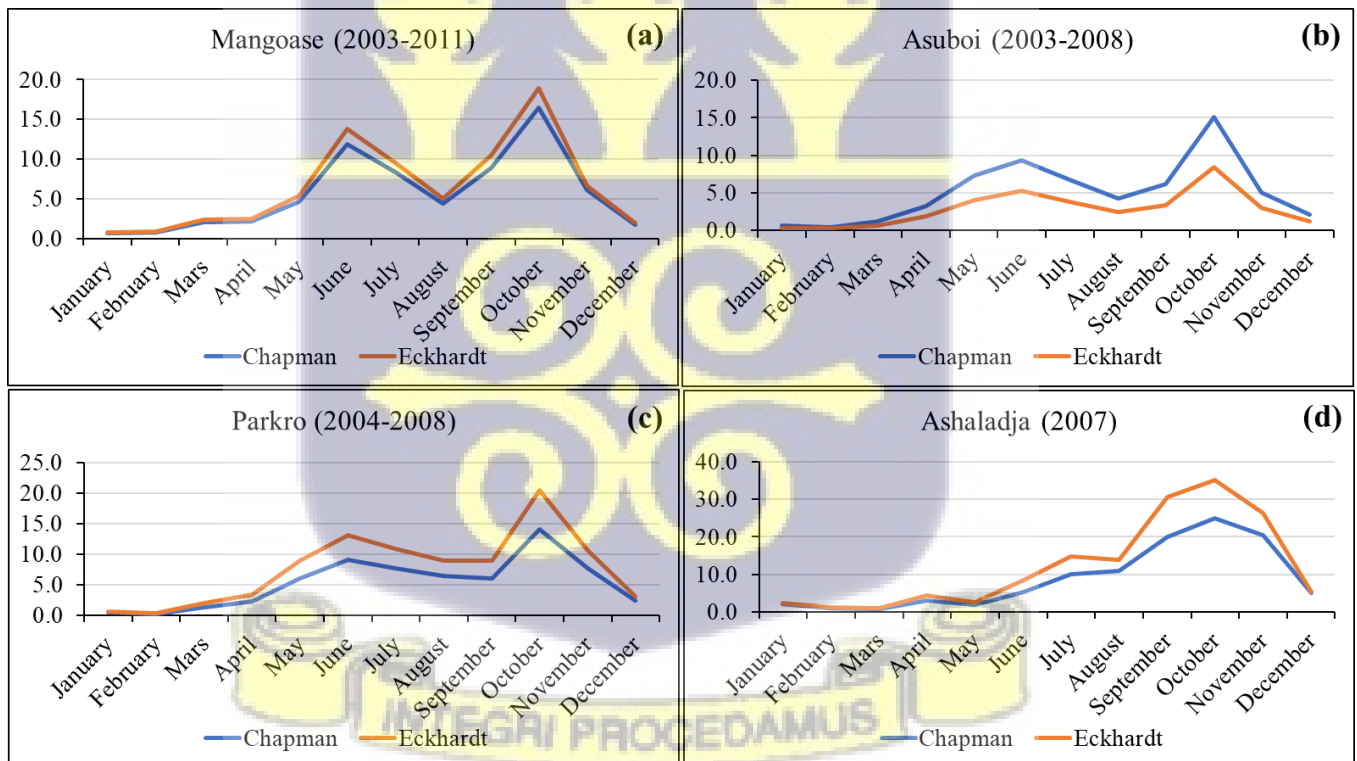


Figure 2.4: Average groundwater recharge (mm/month) based on baseflow filters

2.4 Discussions

Three methods of groundwater recharge quantification have been applied to the Densu River Basin in southern western Ghana. Direct recharge and baseflow methods with point and basin/sub-basin scale approaches were applied. The study highlights the significance of applying multiple methods in assessing groundwater recharge based on different datasets at different spatio-temporal scales. Adopting multiple methods provides the opportunity to interrogate the inherent uncertainties associated with applying a single method. The CMB estimates are generally considered point estimates, whereas the WTF estimates are considered to cover areas up to 100 m² (Delin et al., 2007; Jie et al., 2011; Geneviève et al., 2020). The recharge estimates from these two methods are assumed to be local in scale due to the high spatial variability of aquifer hydraulic properties. However, a sufficient number of point estimates over the entire basin may provide considerably representative recharge values for the entire area (Geneviève et al., 2020). However, recharge estimates from the baseflow analysis are considered to be on the basin or sub-basin scale.

Groundwater recharge point estimates interpolated over the basin using the CMB method ranged from 1- 338 mm/year, with an average of 34 mm/year representing less than 1 to 24% and 3%, respectively, of the average annual rainfall. The CMB estimates in this study compare well with the results by Duah et al. (2021) in the basin, who reported an average groundwater recharge of 0.4 - 320 mm/year using the CMB approach, from a smaller sample of ten boreholes. However, in their study, the estimates represented 0.04% – 19% with an average of 4% of the average annual rainfall. The difference in percent recharge from this study mainly arose from the different rainfall data used. The standard deviation of 55 mm/year in this study suggests groundwater recharge values are widely dispersed, suggesting several factors control the mechanism and amount of

recharge in the basin. This level of spatial variability in recharge may also lead to variations in groundwater availability and quality across different locations in the basin. The lower bound estimates using the CMB method may have been influenced by other sources of chloride in the groundwater besides atmospheric deposition, leading to high chloride levels in the groundwater and low recharge estimates based on Equation 2.1. Therefore, less credence should be placed on such values, which occur in the extreme south of the basin and patches in the central and northern sections. Notwithstanding, the CMB estimates are comparable to estimates from the WTF method.

The WTF method estimates ranged from 27 – 327 mm/year, with an average of 150 mm/year, for specific yield values of 0.01 – 0.05 and 0.03, respectively, which represent 3 – 28% and 15% of the average annual rainfall, respectively. The highest recharge estimate of 327 mm/year by the WTF is comparable to 338 mm/year by the CMB method, both of which are located in the extreme northwest of the basin (Figure 2.3), a high elevation and rainfall area, characterised by a relatively denser vegetation cover and relatively permeable geologic material of rocks of the Birimian Supergroup. This is in line with assertions by some studies (Adomako et al., 2010; Duah et al., 2021; Akurugu et al., 2022) that identify some parts of the north as the recharge zone in the basin. The spatial pattern here also shows some semblance to the CMB and WTF methods (Figures 2.3a&b), with patches of high recharge estimates in the middle and northern sections of the basin. Recharge estimates from the WTF method, like the CMB method, also display a decreasing southward trend, with a minimum value of 68 - 27 mm/year estimated at Ablekuma CP in the south of the basin (Figure 2.3b). This represents 4 - 9% of the average annual rainfall and is highly comparable with recharge estimates by the baseflow filters (Figure 2.3c&f), which averages around 7 - 8% of the average annual rainfall. The average recharge values in this study are slightly

higher than recharge estimates conducted in the basin (Alfa et al., 2011; Water Resources Commission, 2007; Yidana et al., 2014). The recharge rates in this study do not differ significantly from estimates from other parts of the country, especially the Volta basin (Obuobie et al., 2012; Mensah et al., 2014; Akurugu et al., 2020). In the African continent, MacDonald et al. (2021) also observed recharge to range between 34 – 280 mm/year for Ghana, and 3 - 43 mm/year for the entire continent based on recharge estimates from multiple methods and statistical modelling of same to predict unsampled locations.

Monthly analysis of recharge estimates from the baseflow filters revealed that recharge accumulation is gradual in the basin beginning around March/April, the beginning of the rainy season, and peaking around June and October. Although the major rainy season peaks around May/June in the basin, the highest groundwater recharge occurs in the peak of the minor rainy season in October (Figure 1.2). This is probably due to the 2.5-month lag time between rainfall and recharge, and the saturation state of the soil, which allows much recharge to occur following the preceding wet season that occurred a little over two months ago. About 90% of the groundwater recharge is accumulated between May and November annually; as such, these periods are the periods within which large volumes of water may be abstracted without significant impacts on the water table.

2.5 Conclusion

Three methods for quantifying diffuse groundwater recharge have been applied to the Densu River Basin in southwest Ghana. The point recharge estimates obtained with the CMB technique, which were interpolated over the basin, gave the lowest average estimate of 38 mm/year, corresponding

to an average of 3% of the average annual rainfall, whereas the WTF method estimated the highest average value of 150 mm/year, corresponding to an average of 15% of the average annual rainfall. The lowest estimates from the WTF techniques are highly comparable with the baseflow estimates, which range from 4 - 9% of the average annual rainfall. And since the lower bound estimates from the CMB method are considered to be highly uncertain, and probably influenced by saline waters, groundwater recharge in the basin would most likely fall between the upper bound estimates from the CMB and WTF methods and the average minimum estimates from the WTF and baseflow analyses. As such, the overall recharge in the entire basin using the three methods is estimated to range from 27 - 338 mm/year, representing 4 – 28% of the average annual rainfall, with an areal average value of ~ 15% of the average annual rainfall, which agrees with the findings of similar studies in the region. The WTF and CMB methods are particularly sensitive to specific yield values and chloride levels in groundwater, respectively, and one must consider that when discussing results from such techniques.

The highest estimates obtained were in the northern and high-elevation areas, whereas the lowest estimates occurred around the south and low-elevation areas in the basin. Recharge accumulation is gradual in the basin beginning around March/April, the beginning of the rainy season, and peaking around June and October. Although the major rainy season peaks around May/June in the basin, the highest groundwater recharge occurs in the peak of the minor rainy season in October, which is attributable to the 2.5-month lag time between rainfall and recharge. About 90% of the groundwater recharge is accumulated between May and November annually, and this may be the ideal period for large groundwater abstractions in the basin.

CHAPTER THREE

UTILISING HYDROGEOLOGICAL AND HYDROCHEMICAL DATA TO DEVELOP A CONCEPTUAL UNDERSTANDING OF GROUNDWATER RESOURCES IN THE DENSU RIVER BASIN, SOUTHWESTERN GHANA

3.1 Introduction

Globally, groundwater is a vital resource, supporting the water supply needs for domestic, industrial, and agricultural purposes (Varol & Davraz, 2015; Velis et al., 2017; Liu et al., 2023). It constitutes over 85% of all fresh liquid water globally and provides ~50% of irrigation water (FAO, 2019). Groundwater usage is more profound in arid and semi-arid areas where surface water sources are limited, and in low- and middle-income countries where the needed infrastructure for treatment and water supply systems is inadequate (Wada & Bierkens, 2014; Carrard et al., 2019; Loh et al., 2019; Chegbeleh et al., 2020; Li et al., 2021). Groundwater in the Densu River Basin, Ghana, is of great significance in the delivery of water for domestic, industrial, and agricultural use, for urban and rural communities within and outside the basin. Several factors, such as rainfall and other weather conditions, geographical location, the mineral composition and hydraulic properties of host rocks, and geochemical processes within aquifers interact in different ways to determine the unique chemical composition, availability, and storage of groundwater (Wada & Bierkens, 2014; Yidana et al., 2018; Li et al., 2021; Xiao et al., 2023). A better appreciation and understanding of the hydrogeology and processes controlling the availability, distribution, and quality of groundwater is essential for optimal management of the resource. An integrated and

holistic assessment of existing scientific data facilitates this quest and enables managers of water resources to undertake short to long-term strategies for sustainable management of the resource.

Studies aimed at understanding the hydrogeology of any terrain have often relied on several data sources and types and techniques such as hydrochemical and isotopic indicators, water level measurements, water balance analysis, hydraulic testing, and numerical modelling techniques (e.g. Zheng et al., 2012; Yidana et al., 2014, 2015, 2018; Chen et al., 2019; Akurugu et al., 2020; Bloomfield et al., 2020; Evantri et al., 2023; Jovein et al., 2023), among many others. In most cases, a blend of several data types and methods is required for a broader understanding of the complex hydrogeological context (e.g., Burghof et al., 2018; Akurugu et al., 2020; Addai et al., 2023).

Adequate information for useful decision-making on groundwater resources management accrues from a suite of diverse datasets, which are generally difficult to acquire in most developing and third-world economies due to inadequate resources. However, hydrochemical datasets, which are relatively readily available, have also been used in understanding hydrogeological systems and processes. A thorough assessment of hydrochemical datasets provides an indication of the flow geometry (e.g., Ophori and Toth, 1989; Guggenmos et al., 2011; Yidana et al., 2018) and therefore plays an essential role in the initial conceptualisation of the hydrogeological context. Groundwater carries the inherent characteristics of the aquifer, and such characteristics are registered in its hydrochemistry and other tracers. A careful analysis of the hydrochemical data will therefore provide important indicators of the groundwater resources conditions and is indicative of the major segments of the flow system. For instance, the hydrochemical evolution of groundwater as it transits the aquifer material is useful in providing insights into the prevailing factors controlling

the quality of the water and inherent hydrogeochemical processes in the aquifers (Adomako, Osae, et al., 2010; Yidana et al., 2012; Loh et al., 2019; Chegbeleh et al., 2020; Xiao et al., 2023). In addition to indicating the parameters that are responsible for the variations in quality, the hydrochemical tracers provide information useful for determining the state of the groundwater system, especially when combined with data of the physical aquifer parameters and other physiographic information about the terrain.

The Densu Basin is an important hydrological basin in southern Ghana. In addition to increasing population and rapid urbanisation with associated water resource requirements, which place a burden on both groundwater and surface water resources, extensive agricultural activities, illegal mining activities upstream, and other anthropogenic activities threaten both the quality and quantity of groundwater resources. Due to the essential role of groundwater resources, it is important to undertake a holistic assessment of the hydrogeological framework to serve as an important first step in safeguarding the resource for optimal sustainable management. This research, therefore, sought to, for the first time, use both data of hydrogeological parameters and hydrochemical data to develop the conceptual hydrogeological understanding of the basin; which includes to investigate and characterise the hydrogeologic properties and processes influencing groundwater distribution, quality, and flow patterns within the crystalline basement rocks of the Densu River Basin, which has not previously been done. Specifically, the study aims to: 1) assess the hydraulic characteristics of the underlying aquifers and their respective contributions to groundwater availability and delivery; 2) assess groundwater suitability for domestic and irrigation purposes; 3) assess the key hydrogeochemical processes and how they help explain the conceptual understanding of groundwater flow in the Densu River Basin.

3.2 Methodology

3.2.1 Borehole and hydraulic test data

Information and data on the geology, lithostratigraphy, weathering, and pumping test records from boreholes and hydrogeological reports obtained mainly from the database of CSIR-Water Research Institute and Community Water and Sanitation Agency were analysed. Transmissivity and hydraulic conductivity values were estimated from the six-hour constant discharge pumping test and three-hour recovery time-drawdown data for single pumping wells using the Cooper-Jacob method (Cooper & Jacob, 1946), due to its ease of use. Twenty-four (24)-hour constant discharge pumping tests followed by about 12-hour recoveries were conducted on selected boreholes completed in the Birimian and Voltaian Supergroups, and the granitoids, to validate the available records. These long-duration tests were conducted to stress the aquifers and accurately estimate the relevant parameters. Based on the pumping rate in each borehole and the corresponding drawdown, the specific capacity and borehole yield were determined. Depths to the water table were also measured on the field from forty boreholes and shallow wells and used to construct a conceptual groundwater level map, from which flow paths could be deduced. Borehole lithological and geophysical logs were analysed to develop a conceptual framework of the local hydrostratigraphy of the terrain.

3.2.2 Sampling and analysis

Sixty groundwater samples were collected from existing boreholes in the basin from 19th to 23rd November 2020 for major ions and trace element analyses. The sampling campaign was carefully planned to ensure adequate spatial representation of the basin. The locations of the sampled points

are shown in Figure 1.1. The sampling routine followed established standard protocols for water sampling and storage as prescribed in the Standard Methods for the Examination of Water and Wastewater (APHA, 1995). To eliminate stagnant water, the boreholes were purged till EC/pH values attained stable levels. Total Dissolved Solids (TDS), Electrical Conductivity (EC), pH, and temperature were measured *in situ* using Extech EC500: Waterproof ExStik pH/Conductivity Meter from Teledyne FLIR LLC, and later compared with laboratory-measured values as a quality check on the results from the laboratory.

Groundwater for physicochemical analyses was sampled in 1000 ml sterile polyethene bottles, which were thoroughly rinsed with distilled water, followed by the sample, before taking the samples. Samples for trace metals analysis were collected into 500 ml bottles and acidified with concentrated nitric acid to a pH of < 2 , stored at $4\text{ }^{\circ}\text{C}$ in an icebox, and transported to the laboratory of CSIR-Water Research Institute for analysis. These sampling and preservation protocols were intended to preserve the field conditions as much as possible and discourage reactions that would impair the concentrations of the various parameters in transit.

The methods employed for the analyses are atomic absorption spectrophotometry for heavy metals (Mn, Fe, Cu, Zn). The EDTA titrimetric method was used to analyse total hardness (TH), calcium (Ca^{2+}), and magnesium (Mg^{2+}) concentrations, while diazotisation and hydrazine reduction methods were respectively used for the determination of the concentrations of nitrite (NO_2^-) and nitrate (NO_3^-). Potassium (K^+) and sodium (Na^+) concentrations were determined by flame photometry. Phosphate (PO_4^{3-}) concentrations were determined through the stannous chloride method, while fluoride (F^-) and silica (SiO_2) contents were respectively determined through the SPADNS and the molybdosilicate methods. Total alkalinity (Alk) was obtained through the strong

acid titrimetric method, while the concentrations of ammonia (NH₃) were determined through direct nesslerization. Chloride (Cl⁻) concentrations were determined through the argentometric method, and sulphate (SO₄²⁻) by the turbidimetric method.

To determine the internal consistency of the analysis, the Charge Balance Error (CBE) (Equation 3.1) was used. It is globally known that internally consistent analysis should yield CBE values within ±5% (Appelo and Postma, 2005). In addition to the CBE, specific concentrations of hydrochemical and physical parameters were used to determine internal consistency and adequate representation of the resulting data. Based on these, five samples were dropped, and fifty-five samples were considered for further analysis.

$$\text{C.B.E} = \frac{\sum m_c |z_c| - \sum m_a |z_a|}{\sum m_c |z_c| + \sum m_a |z_a|} \times 100 \quad (3.1)$$

Where m_c , m_a , z_c , and z_a are respectively molar concentrations of major cations, major anions, charges of cations, and charges of anions.

3.2.3 Mass balance and statistical modelling

The hydrochemical data were subjected to advanced statistical modelling and mass balance analysis to determine spatial relationships from which inferences could be deduced on the groundwater flow regime and other prevailing processes. The Q-mode hierarchical cluster analysis (HCA) (Holland, 2006) was applied to the data to establish the spatial relations of groundwater in the basin. Q-mode HCA is an unsupervised learning data reduction statistical technique that helps identify similar patterns and relationships in the dataset (Cloutier et al., 2008; Yidana et al., 2018).

It involves computing a distance matrix that measures the dissimilarity between variables and

using a clustering algorithm (in this case, Ward's linkage) to group variables based on similarity. The process requires normal distribution of the data of the variables. Given that the raw hydrochemical datasets were not normally distributed, log transformations and standardization procedures were applied to the original datasets, following the procedure described by Yidana et al. (2018). Log-transformed datasets were standardized to their respective z-scores using Equation 3.2. Data standardization is often recommended so that variables with higher original variances in the distribution of their datasets do not adversely influence the computation of the Euclidean distances in the HCA procedure. The result of Q-mode HCA is a dendrogram that presents the spatial clustering of the samples in a hierarchical fashion based on the similarity and/or dissimilarity of the variable concentrations or derivatives of concentrations.

Speciation and inverse geochemical modelling were undertaken using the PHREEQC program (Parkhurst & Appelo, 2013). PHREEQC is a mass balance geochemical modelling program that employs an optimisation algorithm to find the set of initial conditions such as pH, temperature, aqueous species concentrations, and mineralogy that best match the observed chemical composition of a water sample. The PHREEQC model generates estimated initial conditions with details on the reaction pathways and the relative importance of various reactions in the system. Saturation indices (SIs) of various minerals and gases are calculated (Equation 3.3) to determine whether or not a mineral/species is at equilibrium (SI=0), undersaturated (SI<0), or supersaturated (SI > 0) in the aquifer system at any given point.

$$z = \frac{x - \mu}{s} \quad (3.2)$$

Where z , x , μ , and s are respectively the z-score, measured value, mean, and standard deviation of the parameter.

$$SI = \log \frac{IAP}{K_{SP}} \quad (3.3)$$

Where SI, IAP, and K_{SP} are saturation index, ion activity product of the species, and solubility product of the mineral, respectively.

3.2.4 Irrigation quality assessment

The sodium adsorption ratio (SAR), Na%, permeability index (PI), and magnesium ratio (MR), expressed in equations 3.4, 3.5, 3.6, and 3.7, respectively, were used to assess the quality of the groundwater for irrigation purposes. SAR, Na%, and PI measure the relative ability of a soil to adsorb sodium when the water is used for irrigation and relate the sodium content in the water to the amount of saturating base exchangeable sodium. MR was used to assess the potential of the groundwater to cause soil crumbliness and aggregation, and the potential to supply magnesium and calcium, which are essential nutrients for plant growth and development.

$$SAR = \frac{Na^+}{\sqrt{\frac{Ca^{2+} + Mg^{2+}}{2}}} \quad (3.4)$$

$$Na\% = \frac{Na^+ + K^+}{Ca^{2+} + Mg^{2+} + Na^+ + K^+} \times 100\% \quad (3.5)$$

$$PI = \frac{Na^+ + \sqrt{HCO_3^-}}{Ca^{2+} + Mg^{2+} + Na^+} \times 100\% \quad (3.6)$$

$$MR = \frac{Mg^{2+}}{Ca^{2+} + Mg^{2+}} \times 100\% \quad (3.7)$$

where ion concentrations are all in meq/l.

3.3 Results and discussions

3.3.1 General hydraulic characteristics

Boreholes completed within the granites fall within the depth range of 9.1 m – 103 m, with an average depth of 41.04 m. Borehole yield in this lithology varies widely, ranging from 10.08 m³/day to 614.40 m³/day, with an average of 66 m³/day (Table 3.1). Generally, the depth to aquifer in the granites ranges from 3 m to 72 m with an average of 16.67 m, whereas the average depth to bedrock, which is central to groundwater accumulation, is 11.24 m, and ranges from 1 m to 32 m (Table 3.1). Evidence from outcrops, road cuttings, pits, and borehole logs from various parts of the basin suggests that the depth of weathering in the granite rarely exceeds 13 m. The depth to the aquifer and bedrock suggests that fractures within the granite constitute the main source of groundwater flow to boreholes in the basin. The transmissivity values for the granite are largely variable and range between 0.52 m²/day and 86.83 m²/day, with a mean value of 11.89 m²/day (Table 3.1). This range of transmissivity values suggests a fairly heterogeneous hydrogeologic medium, characteristic of a hard rock environment where fractures, which act as transmission paths, are localised and non-uniform (Figure 3.3c) (Darko and Krasny, 2007).

The granitic gneiss, biotite gneiss, granite, monzonite, and biotite-granodiorite of the Tamnean and Eburnean Plutonic Suites, which constitute the largest lithologies, are generally impermeable and have little inherent primary porosity and storage capacity within the rock matrix. As such, the

accumulation and movement of groundwater are controlled by the pattern and extent of fracturing and/or weathering. Borehole yields are therefore highly variable, dependent on the degree and extent of the distribution of fractures and other secondary structural entities. Where the fractures are unidirectional and unconnected, groundwater fortunes are limited. This condition is prevalent in the southeastern section of the basin around Asikasu and Dantsera in the Upper West Akim and Ga South districts (Darko et al., 2003). However, where the fractures intersect and are well interconnected, particularly with a dense network and thick, vertically conductive overburden, groundwater accumulation and storage are enhanced. These types of aquifers occur between the weathered zone and fresh bedrock and are common in the northern and central sections of the basin, which is characterised by a wet equatorial climate with a moist semi-deciduous forest cover that receives an appreciable amount of rain to guarantee high potential groundwater recharge. Interpolation of borehole yield and transmissivity using ordinary kriging and inverse distance weighting, respectively, shows this spatial pattern. The nugget effect (Figure 3.1) suggests variations in borehole yield (Figure 3.3a) and borehole depth (Figure 3.3b) at distances shorter than the lag distances of 6.3 km and 3.5 km, respectively, which may be attributable to local variation in the geology and/or measurement errors (Simmonds, 2009; Oliver & Webster, 2015). Notable areas are Akrabo, Suhum, Adjomoku, and Nankese, which present some of the highest borehole yields. Another noticeable area of good groundwater accumulation and yield lies at the tectonic contact zone between the granite and Voltaian Supergroup in the southeastern section around Medie, Nsawam, and Ofankor (Figures 3.3a&c), where large volumes of groundwater are extracted for commercial purposes (Darko et al., 2003).

Relatively fewer boreholes are positioned in rocks of the Birimian Supergroup in the Densu River Basin, with a depth range of 25 - 60 m, averaging 33.79 m (Table 3.1). The metamorphosed lava and tuff, and pyroclastic rocks of the Birimian Supergroup are highly folded, foliated, and jointed. Deep weathering along fractures permits water percolation to form large groundwater reservoirs in the extreme north of the basin. Borehole yield ranges between 1.28 and 216 m³/day, with a mean of 84.48 m³/day, affirming the assertion that rocks of the Birimian Supergroup are among the most productive in terms of groundwater delivery in Ghana (Banoeng-Yakubo et al., 2011). The high borehole yield in this formation is also affirmed by Fig. 4a, where the northern section of the basin underlain by the Birimian Supergroup shows relatively high values. The data also suggests high levels of variability in borehole yield in the domain. This accrues from the spatially variable nature of the factors responsible for groundwater resources occurrence in the area; the nature and degree of interconnection of the structural entities are highly variable in the domain.

Generally, rocks of the Birimian Supergroup exhibit deeper weathering, with an average depth to bedrock of about 17.62 m, whereas the weathered profile extends between 5 - 24 m, and the depth to the top of the aquifer varies from 10 m to 31 m, with an average of 19.08 m. The aquifers occur mainly within the fractured bedrock. This is consistent with the regional hydrogeology of the Birimian Province (Dapaah-Siakwan and Gyau-Boakye, 2000; Banoeng-Yakubo et al., 2011).

Rocks of the Voltaian Supergroup present some of the lowest borehole success rates in Ghana based on available data (Banoeng-Yakubo et al., 2011). Boreholes drilled in this formation in the Densu River Basin range from depths of 25 m to 91 m, with an average of 43.15 m. Borehole yield also ranges from 23.04 to 132 m³/day, with a mean value of 55.3 m³/day. The weathered zone is

relatively thin, with an average thickness of 6.4 m, and ranges from 5 – 9 m. This also suggests that groundwater storage and transmission is mainly within the fractured zone.

Generally, borehole yield in the basin appears not to improve with depth (Figure 3.1), which is in tandem with observations made by Darko et al. (2003), where they observed no correlation between yield and borehole depth in the granites and admonished that drilling beyond 60 m in the granites may not necessarily improve borehole yield.

Table 3.1: Summary statistics of aquifer hydraulic properties

Parameter	Granites	Birimian Supergroup	Voltaian Supergroup
Depth (m)	41.04 ± 14.52 (20 – 103, n=237)	33.79 ± 9.95 (25 – 60, n=14)	43.15 ± 18.96 (25 – 91, n=10)
Weathered thickness (m)	11.24 ± 6.91 (2 – 32, n=173)	17.62 ± 6.12 (5 – 24, n=13)	6.40 ± 1.52 (5 – 9, n=5)
Depth to aquifer top (m)	16.67 ± 9.35 (3 – 72, n=108)	19.08 ± 5.99 (10 – 31, n=12)	25.00 (n=1)
Static water level (m)	5.23 ± 3.30 (0.01 – 13.90, n=125)	6.77 ± 4.60 (0.84 – 16.89, n=12)	5.87 ± 5.15 (2.04 – 14.20, n=5)
Yield (m ³ /day)	66.00 ± 82.56 (10.08 – 614.40, n=60)	84.48 ± 57.60 (17.28 – 216.00, n=12)	79.92 ± 39.12 (23.04 – 132.00, n=5)
Transmissivity (m ² /day)	11.89 ± 21.99 (0.52 – 86.83, n=15)	13.12 (n=1)	2.10 (n=1)
Hydraulic conductivity K (m/day)	0.24 ± 0.26 (0.08 – 0.54, n=3)	5.40 (n=1)	1.22 (n=1)
Specific capacity (m ³ /day/m)	7.49 ± 11.42 (0.03 – 75.29, n=53)	—	10.74 ± 13.10 (1.48 – 20.00, n=2)

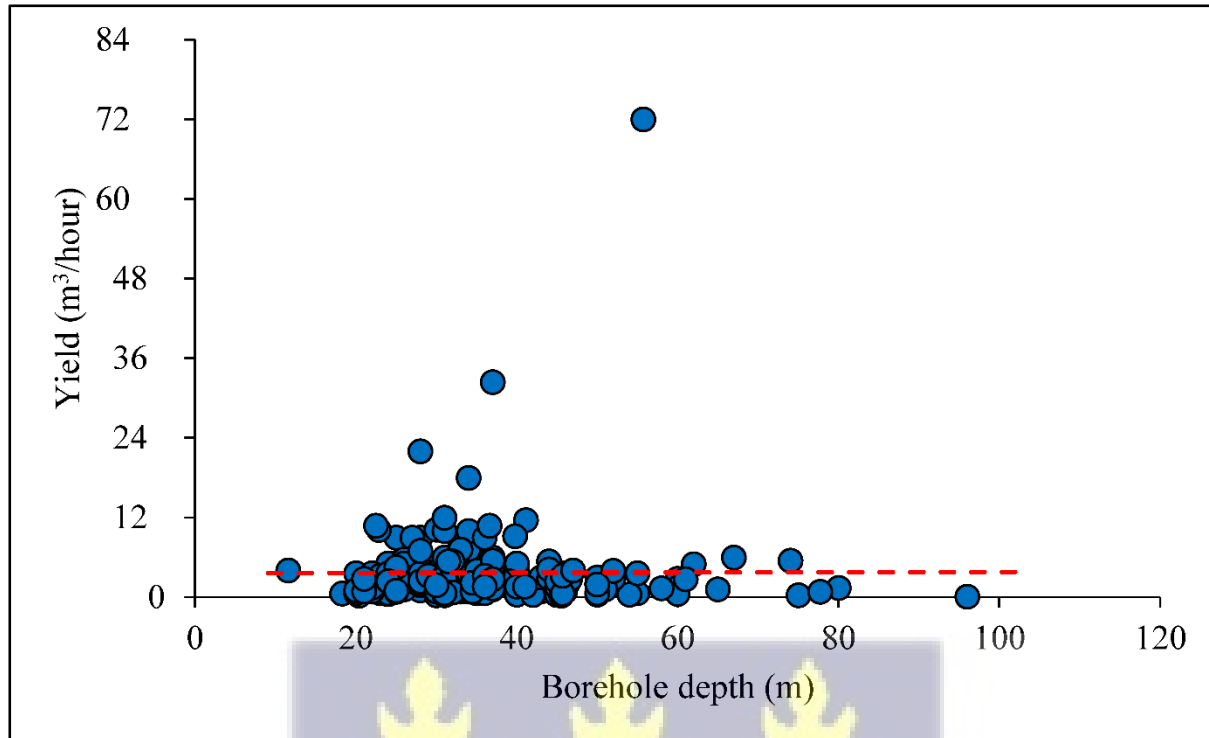


Figure 3.1: Relationship between borehole yield and depth in the Densu Basin

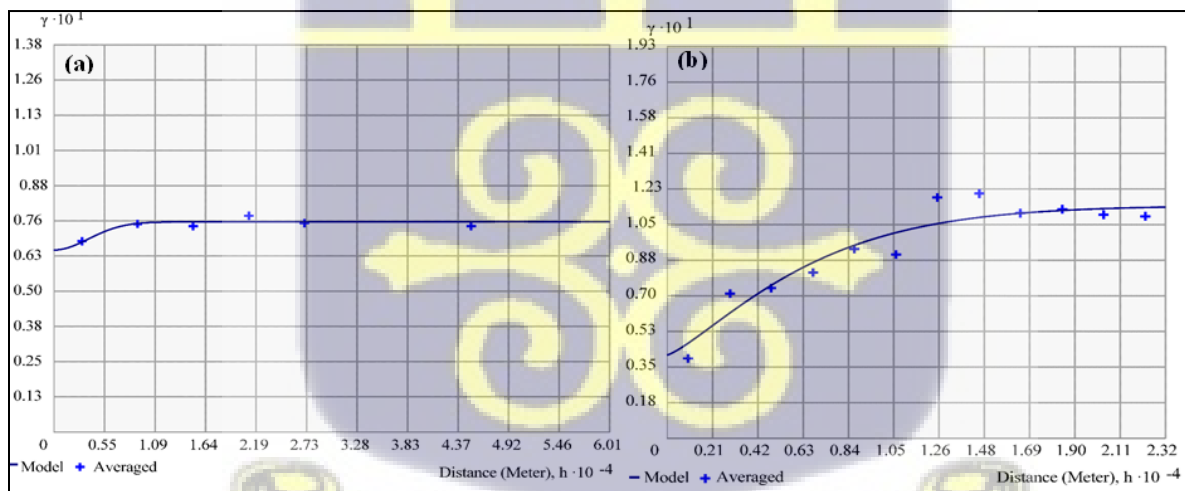


Figure 3.2: Semivariogram models for (a) borehole yield, and (b) borehole depth

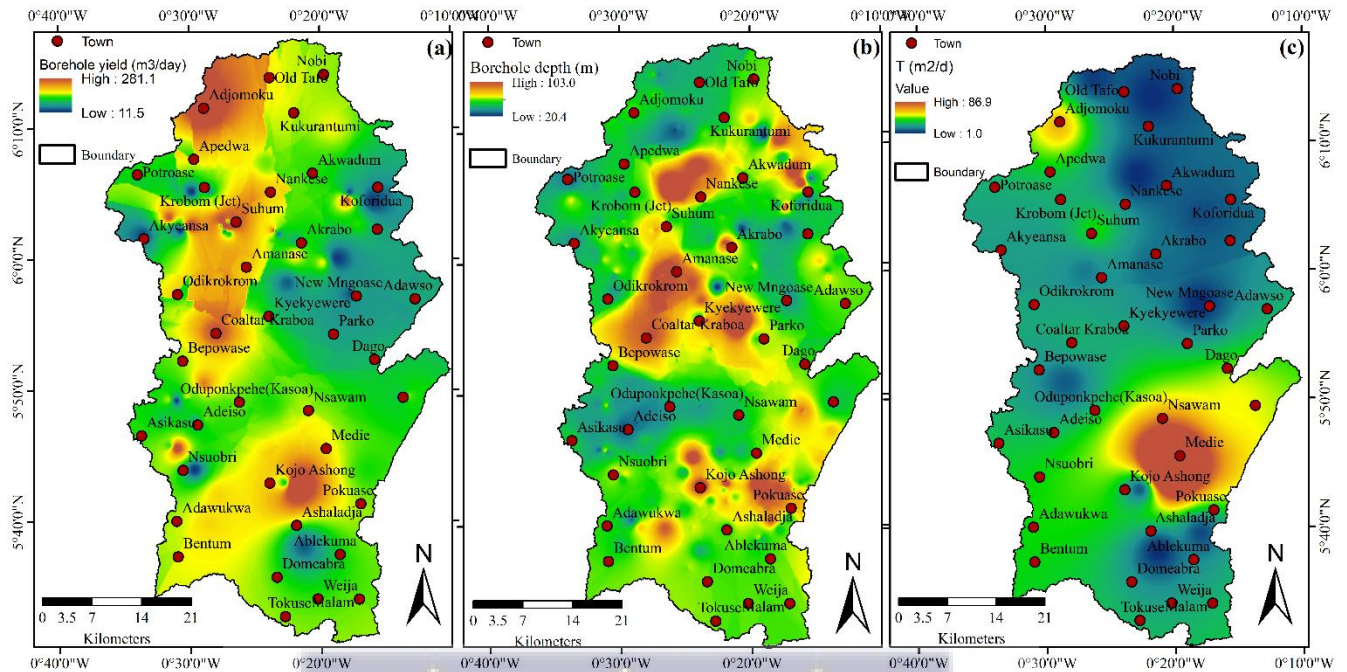


Figure 3.3: Spatial distribution of (a) borehole yield, (b) depth, and (c) transmissivity

3.3.2 Conceptual lithostratigraphy

Profiles of three boreholes drilled through the three main geological units in the basin are presented in Figure 3.5 to give a general sense of the lithostratigraphy of the Densu River basin. The weathering pattern appears to follow a similar trend irrespective of the geologic unit, with widely variable weathered thickness, ranging between 1m and 32 m. The nature of weathering varies from completely decomposed rock to slightly weathered rock, with the fractured bedrock overlying the fresh bedrock.

Most aquifers in the Densu River Basin are encountered at 11 – 35 m and occur within the saprolite, saprock, and fractured bedrock which complement each other in terms of groundwater storage and delivery. The most productive zones in rocks of the Birimian Supergroup are the lower and upper

parts of the saprolite and saprock respectively. Whereas in the granite, the fractured bedrock could be as equally or more productive as the weathered zone depending on the amount and extent of fractures. High elevated areas which act as recharge zones, may also potentially lead to high borehole yields. A correlation of borehole yield and weathered thicknesses with elevation suggests an upward trend in the basin (Figure 3.4). Borehole yield with elevation (Figure 3.4b) on the other hand shows a slight upward trend, which suggests that elevation of the areas has a relatively low impact on borehole yield in the basin.

Aquifers in the basin are generally unconfined to semi-confined, with the main water-bearing zone stretching about 3 m thick (Darko et al., 2003). There are several cases of slightly fractured to unfractured rocks overlying the fractured bedrock in most parts of the basin, suggesting the presence of semi-confined aquifers across the basin.

Based on data from 96 borehole lithological logs, a simplified lithostratigraphic model has been constructed for the basin (Figure 3.6). The saprolite and saprock are lumped as a layer, and the fractured bedrock as a different layer, with the thicknesses defined by the borehole lithological logs. A cross-section of the two layers shows the extreme north of the basin to have a higher weathered zone thickness, especially in rocks of the Birimian and Voltaian Supergroups, and thinnest in the central sections in the granites, with the bedrock outcropping variously (Figure 3.6b).



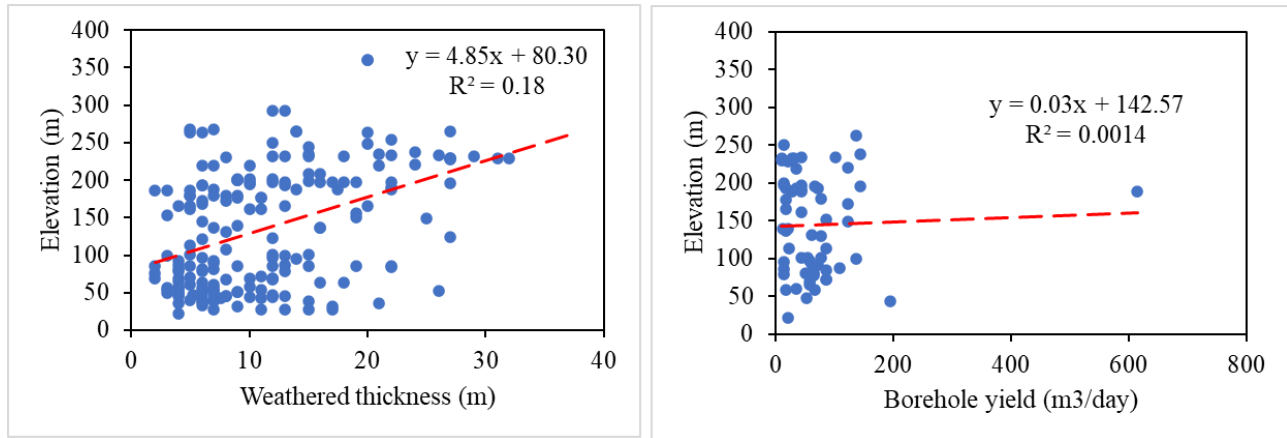


Figure 3.4: Relationship between weathered thickness, borehole yield, and elevation

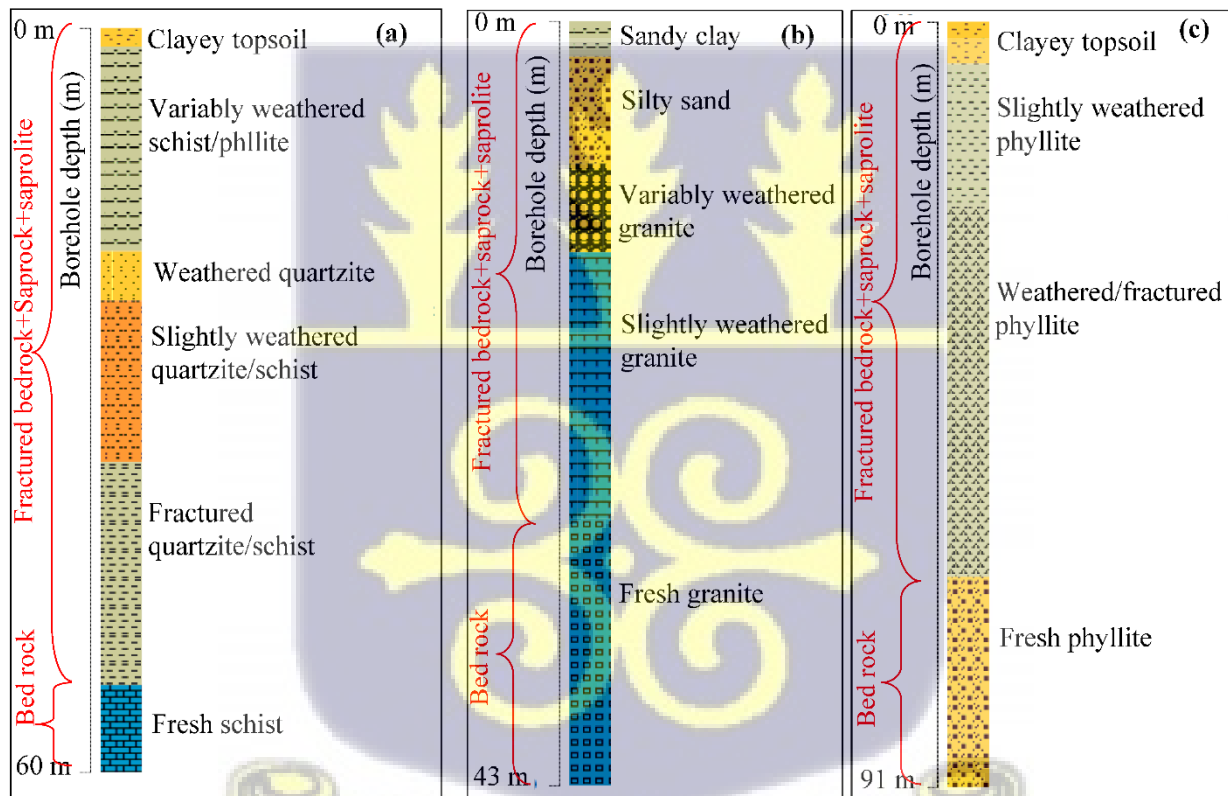


Figure 3.5: General lithostratigraphy of boreholes in the (a) Birimian Supergroup, (b) granites, and (c) Voltaian Supergroup in the Densu Basin

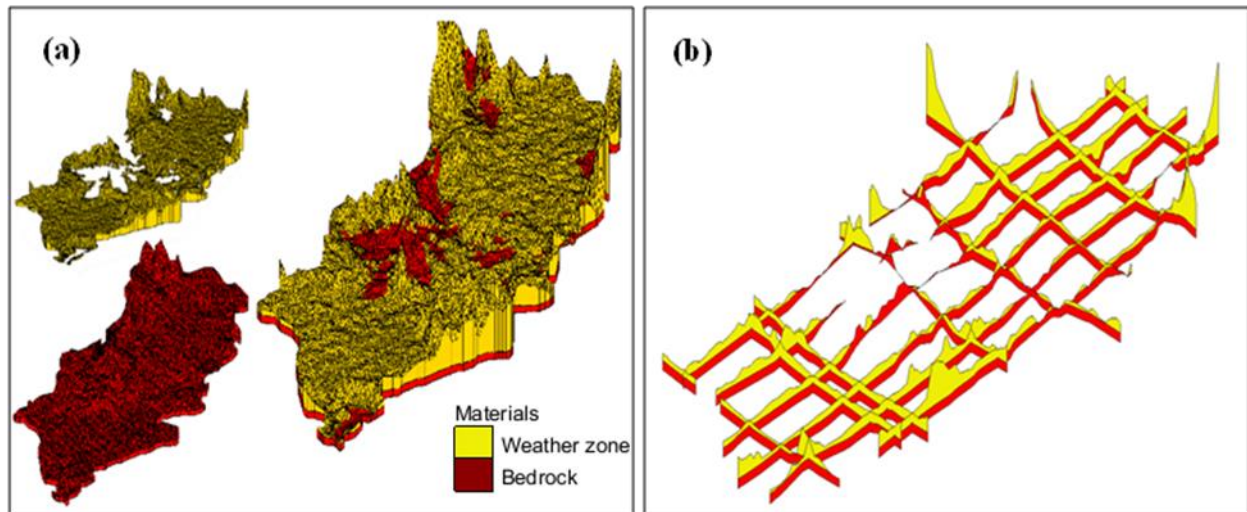


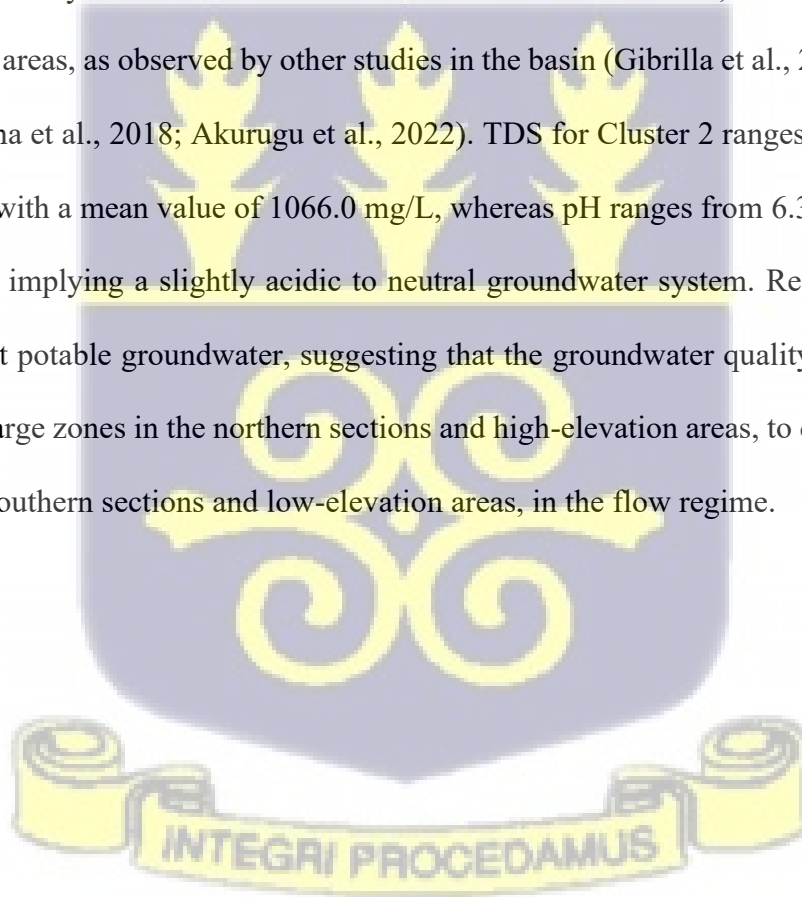
Figure 3.6: Conceptual (a) solid and (b) cross-section of the lithostratigraphy of the Densu River Basin

3.3.3 Spatial patterns of groundwater hydrochemistry

The spatial variation of groundwater hydrochemistry examined using the Q-mode HCA resulted in two clusters (Clusters 1a, 1b, and 2) with a Phenon line drawn at a linkage distance of 6 (Figure 3.7). Cluster 1a members are in relatively high-elevation areas in the basin and are generally weakly mineralised (Table 3.2a). TDS in this group ranges from 57.8 mg/L to 396.0 mg/L, with an average value of 206.4 mg/L. The members of Cluster 1a are also slightly acidic with pH in the range of 5.05 - 8.12, with an average value of 6.34, which are characteristics of recharge areas in the flow regime (Loh et al., 2019; Chegbeleh et al., 2020; Liu et al., 2023). Akurugu et al. (2022) observed TDS in the northern part of the Densu Basin, which they characterised as recharge zones, rarely exceeding 400 mg/L. Except for low pH values in about 55.6% of the samples, and elevated

Fe in one location at Dantsera in the southern part of the basin, Cluster 1a group presents the best water quality for drinking purposes (Table 3.2a). Cluster 1b, on the other hand, is relatively moderately mineralised, with TDS ranging from 322.2 mg/L to 575.4 mg/L, with an average value of 421.7 mg/L. Cluster 1b members are generally located in moderate-elevation areas and are considered transmission zones in the groundwater flow regime. TDS range in Cluster 1b varies slightly from the 40 - 1000 mg/L range proposed by Akurugu et al. (2022), for groundwater in the transmission zones of the flow regime in the Densu River Basin.

Cluster 2 generally represents samples in the discharge zones of the groundwater flow regime. This group is relatively more mineralised than Clusters 1a & 1b members, and is generally located in low-elevation areas, as observed by other studies in the basin (Gibrilla et al., 2010; Adomako et al., 2011a; Yidana et al., 2018; Akurugu et al., 2022). TDS for Cluster 2 ranges from 727.2 mg/L to 1902.0 mg/L with a mean value of 1066.0 mg/L, whereas pH ranges from 6.35 to 7.74, with an average of 6.98, implying a slightly acidic to neutral groundwater system. Relatively, Cluster 2 presents the least potable groundwater, suggesting that the groundwater quality deteriorates as it flows from recharge zones in the northern sections and high-elevation areas, to discharge zones in the central and southern sections and low-elevation areas, in the flow regime.



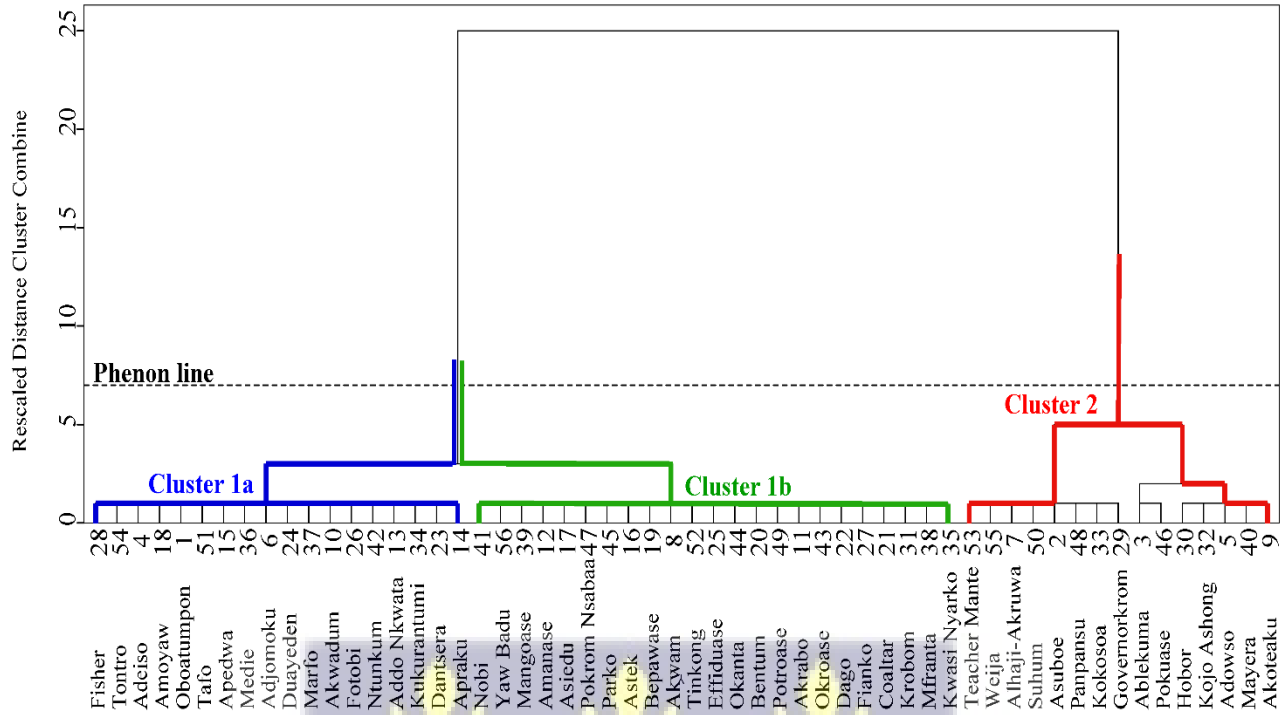


Figure 3.7: Q-mode hierarchical cluster analysis showing spatial variation in groundwater

Table 3.2a: Descriptive statistics for Cluster 1a

	Min	Max	Mean	STD	WHO (2017)	% Potable
pH	5.05	8.12	6.34	0.69	6.50 – 8.50	44.4
TDS	57.8	396.0	206.4	101.8	1000.0	100.0
HCO ₃ ⁻	12.20	200.08	107.22	59.32	-	-
Ca ²⁺	5.7	41.3	20.7	10.1	200.0	100.0
Mg ²⁺	3.2	16.5	9.1	3.9	150.0	100.0
Cl ⁻	3.8	195.3	43.6	43.5	250.0	100.0
Na ⁺	6.0	86.0	34.6	24.4	200.0	100.0
K ⁺	1.0	17.0	3.6	3.6	30.0	100.0
SO ₄ ²⁻	<0.01	51.90	16.74	16.36	250.00	100.0
NO ₃ ⁻	<0.001	1.840	0.778	0.499	50.000	100.0
NO ₂ ⁻	<0.001	0.485	0.035	0.113	3.000	100.0
PO ₄ ²⁻	<0.001	0.212	0.077	0.062	0.700	100.0
F ⁻	<0.005	1.090	0.301	0.360	1.5	100.0
NH ₃	<0.001	0.282	0.036	0.091	-	-

ALK	10	164	88	49	-	-
TH	35.6	146.2	89.3	36.2	-	-
SiO ₂	24.1	97.3	72.2	24.7	-	-
Mn	<0.005	0.269	0.036	0.067	0.400	100.0
Fe	<0.010	0.918	0.095	0.213	0.300	94.4
Cu	<0.010	0.000	0.000	0.000	2.00	100.0
Zn	<0.005	0.083	0.016	0.027	3.00	100.0

Table 3.2b: Descriptive statistics for Cluster 1b

	Min	Max	Mean	WHO (2017)	% Potable
pH	6.51	7.16	6.81	6.5 – 8.50	100.0
TDS	322.2	575.4	421.7	1000.0	100.0
HCO ₃ ⁻	173.24	366.00	234.03	-	-
Ca ²⁺	18.3	81.8	42.8	200.0	100.0
Mg ²⁺	9.4	47.3	21.2	150.0	100.0
Cl ⁻	32.6	116.6	72.2	250.0	100.0
Na ⁺	20.0	110.0	64.4	200.0	100.0
K ⁺	0.8	42.0	9.5	30.0	87.0
SO ₄ ²⁻	8.27	74.30	47.32	250.00	100.0
NO ₃ ⁻	0.001	1.550	0.696	50.000	100.0
NO ₂ ⁻	0.001	0.074	0.012	3.00	100.0
PO ₄ ⁻	0.026	0.261	0.096	0.700	100.0
F ⁻	<0.005	1.000	0.417	1.500	100.0
NH ₃	<0.001	0.425	0.068	-	-
ALK	142	300	193	-	-
TH	120.2	284.0	194.3	-	-
SiO ₂	27.5	98.3	75.7	-	-
Mn	<0.005	0.573	0.057	0.400	95.7
Fe	<0.010	0.338	0.046	0.300	91.3
Cu	<0.010	0.022	0.001	2.000	100.0
Zn	<0.005	0.403	0.030	3.000	100.0



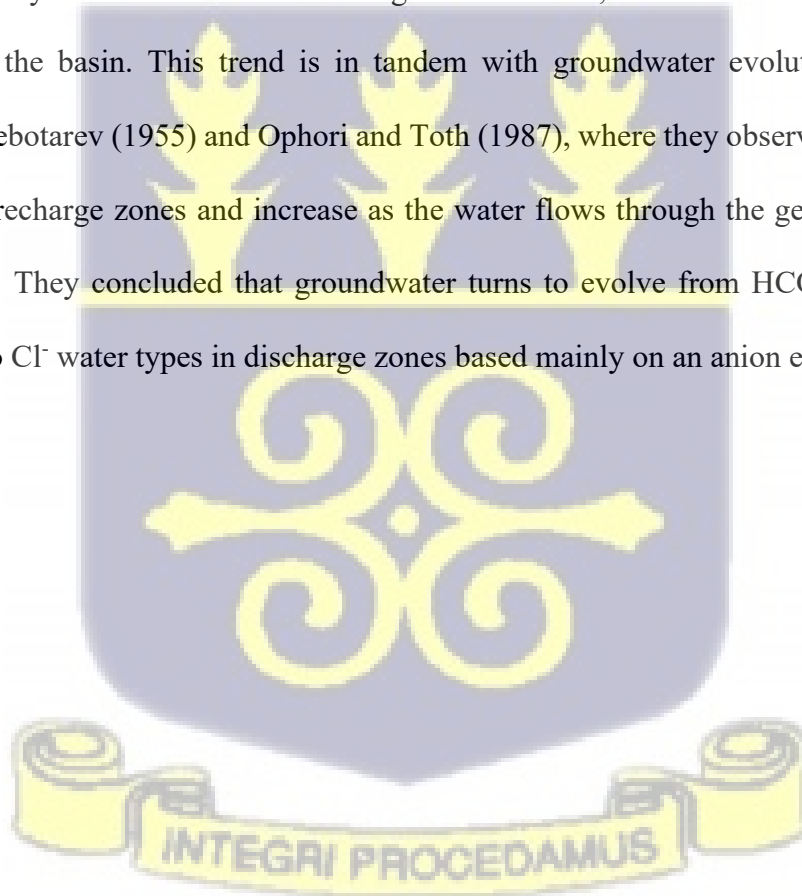
Table 3.2c: Descriptive statistics for Cluster 2

	Min	Max	Mean	STD	WHO (2017)	% Potable
pH	6.35	7.74	6.98	0.36	6.50 – 8.50	93.3
TDS	727.2	1902.0	1066.0	338.0	1000.0	53.3
HCO ₃ ⁻	146.40	536.80	378.04	97.62	-	-
Ca ²⁺	30.2	122.2	69.2	29.4	200.0	100.0
Mg ²⁺	30.0	113.8	58.5	21.8	150.0	100.0
Cl ⁻	133.8	675.5	327.5	150.7	250.0	46.7
Na ⁺	91.0	390.0	195.3	85.3	200.0	66.7
K ⁺	3.8	45.2	10.5	11.5	30.0	86.7
SO ₄ ²⁻	2.35	242.00	82.88	65.61	250.00	100.0
NO ₃ ⁻	0.001	1.320	0.557	0.381	50.000	100.0
NO ₂ ⁻	0.001	0.680	0.080	0.178	3.000	100.0
PO ₄ ²⁻	0.001	0.430	0.098	0.105	0.700	100.0
F ⁻	<0.005	1.710	0.629	0.531	1.500	93.3
NH ₃	<0.001	0.002	0.000	0.001	-	-
ALK	120	440	310	80	-	-
TH	204.6	629.0	413.8	116.5	-	-
SiO ₂	42.8	99.8	77.2	15.3	-	-
Mn	<0.005	4.407	0.442	1.130	0.400	100.0
Fe	<0.010	2.250	0.182	0.574	0.300	93.30
Cu	<0.010	0.048	0.007	0.017	2.000	100.0
Zn	<0.010	0.534	0.074	0.174	3.000	100.0

The data suggest that the study area is dominated by Na⁺ and Ca²⁺ with relatively low levels of Mg²⁺ and K⁺. Among the anions, HCO₃⁻ is the most dominant in the groundwater in the northern and central sections, whereas Cl⁻ dominates in the southern section up to 30 km inland from the ocean. Groundwater in the northern parts and in high-elevation areas is predominantly Na-HCO₃ and Ca-HCO₃ water types, with Na-Cl water types also featuring significantly in these areas, which have been characterised as recharge zones. The middle sections of the basin are characterised by the dominance of Na-HCO₃ and Ca-HCO₃ hydrochemical facies. Altogether, bicarbonate-type waters constitute about 60% of the groundwater in the basin and are found mainly in the northern and middle sections, whereas chloride-type waters constitute the remaining 40%. In general, the

major solute concentrations exhibit similar trends; increasing gradually along the groundwater-inferred flow paths from north to south of the basin (Figure 3.8).

The TDS, which is used as a proxy for groundwater salinity in this study, also increases gradually from the north to the south. In the central section where the groundwater becomes relatively mineralised, relatively high salinity has been observed. The highest TDS values are found in the extreme south, where the basin discharges into the Gulf of Guinea. Generally, salinity in the basin (Figure 3.8b) exhibits a similar spatial trend with Cl^- (Figure 3.8c), and a strong linear correlation with TDS and total hardness ($r = 0.99$ and $r = 0.97$ respectively), confirming the assertions that the groundwater quality deteriorates with increasing mineralisation, and as one moves from the north to the south of the basin. This trend is in tandem with groundwater evolutionary sequences described by Chebotarev (1955) and Ophori and Toth (1987), where they observed TDS to be low in groundwater recharge zones and increase as the water flows through the geologic material to discharge zones. They concluded that groundwater tends to evolve from HCO_3^- water types in recharge areas to Cl^- water types in discharge zones based mainly on an anion evolution sequence and TDS.



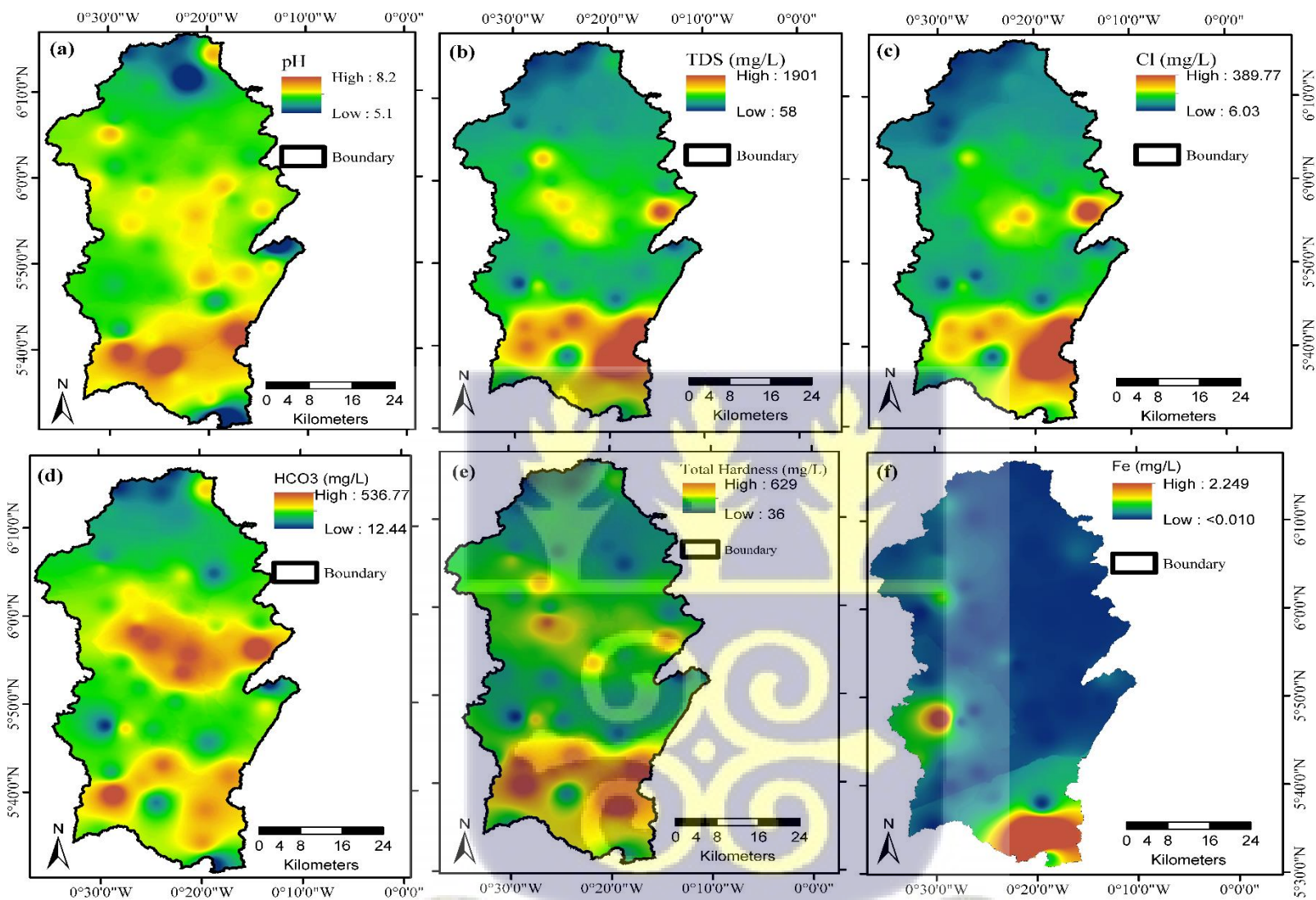


Figure 3.8: Spatial distribution of selected physicochemical parameters; (a) pH, (b) TDS, (c) Cl⁻, (d) HCO₃⁻, (e) Total hardness, and (f) Fe in the Densu Basin

3.3.4 Irrigation quality assessment

The trend of variations in groundwater salinity and sodicity on the Wilcox (1955) and USSL (1954) appears to lend credence to the evolutionary trend of groundwater flow highlighted in the previous sections. Figures 3.9a and 3.9b clearly suggest an evolution trend whereby groundwater sodicity and salinity increase from Cluster 1a through Cluster 1b to Cluster 2. Irrigation water quality appears to deteriorate along the same trend, suggesting that members of Cluster 1a are the best suited for irrigation, followed by members of Cluster 1b. The evolutionary trend is also observed in the spatial distribution (Figures 3.10a&b), where the SAR and Na% gradually increase as the groundwater flows from the north to the south, evolving along its flow paths.

Results from the USSL (1954) analysis also revealed SAR values ranged from 0.61 – 9.67. The higher the SAR value, the greater the potential for soil to adsorb sodium and generate conditions that are inhibitory to crop growth and development. The permeability of soil is impacted by high sodium ions in water used for irrigation, which leads to issues with infiltration. This is because sodium, when present in the soil in an exchangeable form, replaces calcium and magnesium adsorbed on soil clays and leads to soil particle dispersion. The soil aggregates break down as a result of this dispersion. When dry, the soil becomes dense and hard, which affects its structure by reducing the rates at which air and water permeate the soil (Sundaray et al., 2009; Obiri-Nyarko et al., 2022; Manu et al., 2023). SAR values <10 have been known to be suitable for irrigation in well-drained soils such as sandy soils, but even values around 9 may present problems in fine-textured soils (Tadesse et al., 2011; Aboukarima et al., 2018). It is noteworthy that, irrespective of the SAR value, salinity, and other factors can also affect the suitability of water for irrigation purposes. Notwithstanding, about 73% of the samples fell within classes S1-C1 and S2-C2, which

represent low sodicity-low salinity and medium sodicity medium salinity, respectively (Figure 3.9a). These two classes present waters that are suitable for irrigation of all soils with semi-tolerant-to-sensitive crops, without requiring prior treatment (Zaman et al., 2018; Loh et al., 2019; Obiri-Nyarko et al., 2022). SAR values in the study area are generally low, except in the discharge areas and towards the coast in the south of the basin, where SAR values fall within S1-C3, indicating low sodicity-high salinity. The high-elevation areas, designated as recharge zones in this study, in the north and patches across the basin present small SAR values (Figure 3.10a). The high SAR values areas, on the other hand, are designated as discharge zones in this study, which suggests salinisation of the groundwater as it evolves and becomes more mineralised in the flow regime, affecting its suitability for irrigation.

Na%, as used in the Wilcox (1955) diagram, is a measure of the Na⁺ content relative to Ca²⁺ and Mg²⁺ in the groundwater (Equation 3.5). Just like SAR, high Na% levels in water greater than 60% may cause soil dispersion and structure deterioration, leading to reduced soil permeability problems (Kumarasamy et al., 2014; Amer, 2021; Pivić et al., 2022). A reduction in soil permeability may affect the rate and amount of water and air available to plants for proper growth and development. Results from the Wilcox (1955) diagram also revealed that about 91% of the groundwater in the basin presents water of 'Excellent' to 'Permissible' quality for irrigation (Figure 3.9b). The few samples that fell within the 'Permissible' to 'Unsuitable' category may present such problems when used for irrigation. As such, treatment of such waters, before irrigation application, is required to avoid the aforementioned challenges. It is evident from Figure 3.10b that a large portion (about 95%) of groundwater in the study area has Na% less than 60%, corroborating the assertions made by the Wilcox (1955) diagram. The spatial distribution of Na%

shows that the high values occur mainly in the south-eastern and southern parts of the basin, which are within rocks of the Voltaian Supergroup, Togo Structural Unit, and the Accraian Group. The consolidated sedimentary rocks of the Voltaian Supergroup are known to be composed of some soluble salts containing Na (Yidana et al., 2020), and saline water influences from the ocean are predominant in the south of the basin. This explains the high Na% in the south and southeast of the basin. The northern and southwestern sections appear to present the best quality water for irrigation in terms of Na% (Figure 3.9b).

Generally, the groundwater in the study area is of good permeability, as Figure 3.10c suggests 91% of the water presents groundwater of maximum permeability (Class I) and 75% permeability indices (Class II) (Equation 3.6) (Kumarasamy et al., 2014). The dominant Na-HCO₃ and Na-Cl water types in the northern part of the basin influence the permeability indices of those areas due to the exchangeable Na⁺ in the groundwater. The ‘Unsuitable’ waters, based on the permeability index when used for irrigation over a long period, are likely to affect the permeability of the soil (Kumarasamy et al., 2014; Amer, 2021; Pivić et al., 2022). Ca²⁺ and Mg²⁺ are also associated with soil crumbliness and aggregation and are crucial nutrients for plant growth and development. Elevated levels of these ions in water used for irrigation have the potential to increase soil pH, which could limit the availability of phosphorus for plants (Kumarasamy et al., 2014; Abbasnia et al., 2018; Elsayed et al., 2020). Relatively high levels of Mg²⁺ in groundwater could lead to alkaline waters, which may negatively affect crop yield (Vyshpolsky et al., 2008; Ramesh & Elango, 2012; Chakraborty et al., 2022). In this study, the magnesium ratio (MR) (Equation 3.7) ranged from 23-86%. About 53% of the samples were of ‘Suitable’ quality for irrigation (MR<50%) whereas the rest were deemed ‘Unsuitable’ (MR>50%). Low MR values are

pronounced in the northern section of the study area, with small patches of ‘Suitable’ waters in the central and southern sections (Fig. 3.10d).

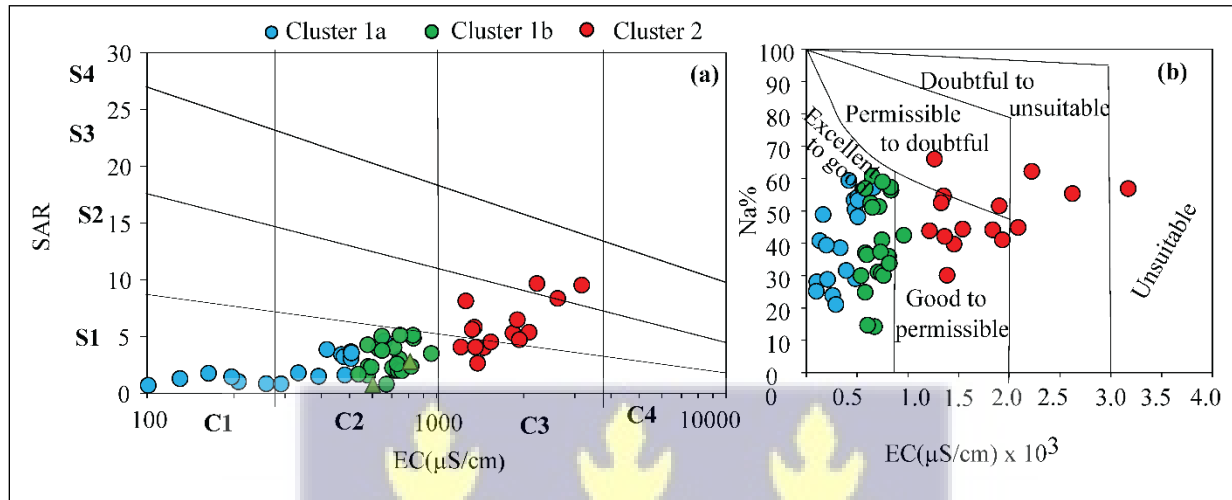
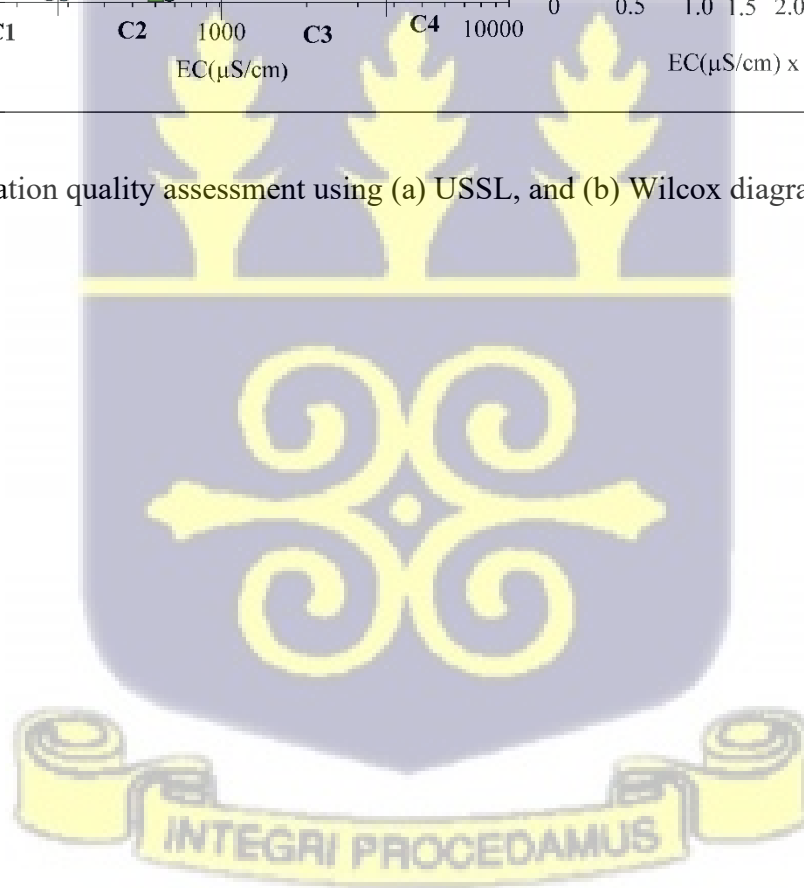


Figure 3.9: Irrigation quality assessment using (a) USSL, and (b) Wilcox diagrams



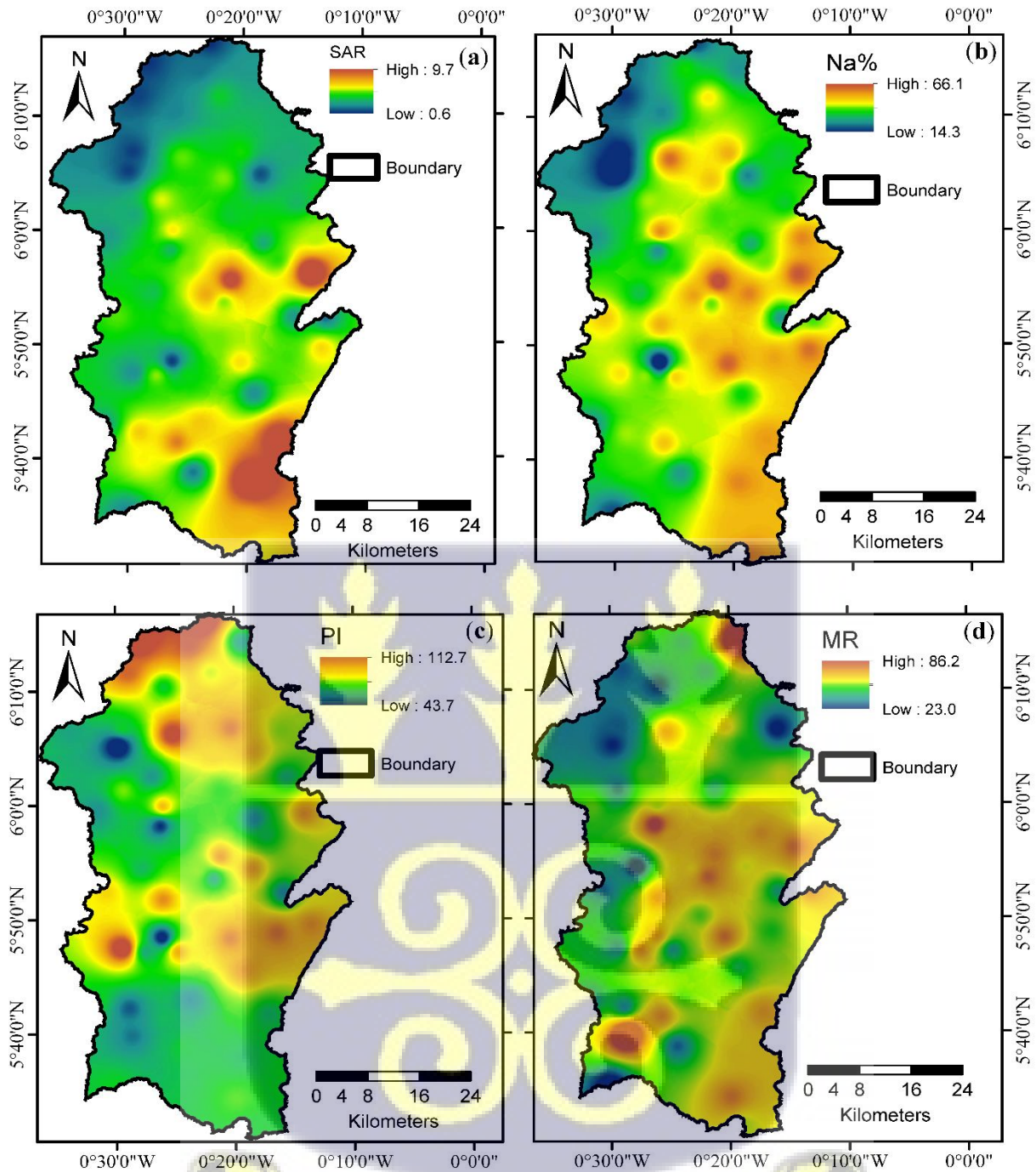


Figure 3.10: Spatial distribution of irrigation quality assessment indices; (a) sodium adsorption ratio (SAR), (b) percent sodium (Na%), (c) permeability index (PI), and (d) magnesium ratio (MR)

3.3.5 Hydrogeochemical processes controlling groundwater chemistry

The dominance of bicarbonate water types, Na-HCO₃ and Ca-HCO₃, in the northern part of the basin suggests the impact of rock-water interactions through CO₂-charged rain (Loh et al., 2019; Tay, 2021). A biplot of Ca+Mg versus HCO₃+SO₄ (Figure 3.11f) suggests silicate mineral weathering plays a significant role in the concentrations of major and minor ions, as well as other parameters in the hydrochemistry of the groundwater in the terrain. The weathering of silicate minerals such as feldspar can release Na⁺ and Ca²⁺ into groundwater. This process occurs over long periods and can be influenced by factors such as temperature, precipitation, and the presence of organic matter and pH (Appelo & Postma, 2005; Priestley et al., 2019). Silicate mineral weathering primarily results in the release of cations and silica into the groundwater system. This process is modulated by the pH, and results in a change in the latter (Figure 3.13a). Samples plotting below the 1:1 line in Figure 3.11f indicate the influence of silicate mineral weathering, where Na⁺, Ca²⁺, Mg²⁺, and HCO₃⁻ are released into solution (Appelo & Postma, 2005; Loh et al., 2016; Akpataku et al., 2019). The granite gneisses which characterise the Tamnean Plutonic Suite in the basin consist of K-feldspars and plagioclase feldspars. As such, the dissolution of minerals such as albite and anorthite are probable sources of Ca²⁺ and Na⁺ in the groundwater.

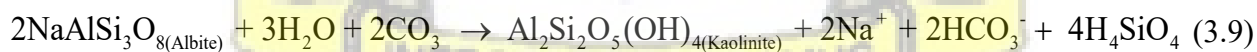
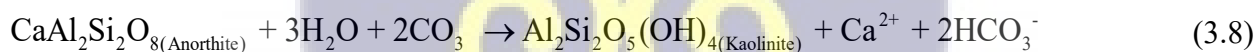
Anorthite (CaAl₂Si₂O₈) and albite (NaAlSi₃O₈) are respectively the calcium and sodium end-members of the plagioclase feldspar series. They may contain significant amounts of magnesium up to 10% Mg²⁺ substitution for Al³⁺ in their crystal structure (Hem, 1985; Appelo & Postma, 2005; Blatt et al., 2006). In the weathering of anorthite and albite, for example, two moles each of HCO₃⁻ are released in solution, whereas one mole each of Ca²⁺ and Na⁺ respectively, are released simultaneously. As such, where silicate weathering is predominant, the bicarbonate ions in solution

are expected to surpass the other cations; from Figure 3.11f, it is observed that a large portion of the groundwater has dominant bicarbonate over Ca and Mg ions. Rocks of the Tamnean Plutonic Suite also contain minor micas and amphiboles, which may explain the relatively low levels of other ions such as Mg^{2+} , Fe, and K^+ in the groundwater. The increase in cation concentration in the groundwater is accompanied by an increase in bicarbonate in the silicate mineral weathering processes (Equations 3.8 & 3.9) with high levels of silica, ranging from 27.5 to 99.8 mg/L. The relatively high levels of silica in the groundwater are consistent with the geology of the basin, dominated by silicate minerals.

Figure 3.11f suggests that, besides silicate weathering, there are other hydrochemical processes at play. Ca-HCO₃ water types are generally associated with rapidly circulating groundwater or groundwater at the early stages of hydrochemical evolution (Appelo & Postma, 2005); both of which are characteristic of the northern section of the basin, where TDS < 400 mg/L. However, about 33% and 27% of the groundwater in the northern section of the basin consists of Na-HCO₃ and Na-Cl water types respectively. In a study conducted in the northern part of the Densu River Basin, Gibrilla et al. (2010) observed TDS ranged from 49-361 mg/L, with slightly acidic to alkaline waters, characterised by Na-Cl, Na-HCO₃, Na-Mg-Ca-HCO₃ water types. Na-HCO₃ and Na-Cl water types are typically associated with deeply circulated groundwaters with much longer residence time (Liang et al., 2018; Chen & Gui, 2021). Since primary evaporites like gypsum and halite are not reported in a large part of the basin, except for rocks of the Voltaian Supergroup in the extreme southeast, the close relation between Na⁺ and Cl⁻ (Figure 3.11c) suggests that, the excess of Na⁺ in the groundwater is probably derived from other processes such as silicate

weathering, ion exchange and sea spray which contribute as the sources of these Na-HCO₃ and Na-Cl water types.

Ion exchange reactions appear to play a critical role in the basin and probably contribute to the high Na⁺ levels in the groundwater. Cl⁻ corrected Na⁺ was plotted against HCO₃⁻, and SO₄²⁻ corrected Ca²⁺ and Mg²⁺ (Martín-Loeches et al., 2020; Zhang et al., 2020) to explore the extent of this process in the groundwater system. For groundwater systems with an active exchange between Na⁺ Ca²⁺ and Mg²⁺, the slope from Figure 3.11a should be -1 (Chegbeleh et al., 2020; Zhang et al., 2020; Islam et al., 2022). As such, a slope of -0.99 indicates that ion exchange is an active process and a contributor to the levels of Na⁺ in the groundwater system. Similarly, two chloro-alkaline indices CAI-I and CAI-II (Equations 3.12&3.13) were also used to assess the occurrence of cation exchange as suggested by Schoeller (1965). As shown in Fig. 13b, a large portion of the groundwater samples presents CAI-I and CAI-II values <0. This suggests cation exchange between Na⁺ and Ca²⁺ and Mg²⁺ in the groundwater, especially in the northern and central sections of the basin as demonstrated by the clusters in Figure 3.11b. Several studies conducted in the basin also identified ion exchange as a factor influencing the basin's hydrochemistry (Gibrilla et al., 2010; Adomako et al., 2011a; Yidana et al., 2018; Akurugu et al., 2022).



Ion exchange;



Chloro-alkaline indices;

$$\text{CAI-I} = \frac{\text{Cl}^- - (\text{Na}^+ + \text{K}^+)}{\text{Cl}^-} \quad (3.12)$$

$$\text{CAI-II} = \frac{\text{Cl}^- - (\text{Na}^+ + \text{K}^+)}{\text{SO}_4^{2-} + \text{HCO}_3^- + \text{CO}_3^{2-} + \text{NO}_3^-} \quad (3.13)$$

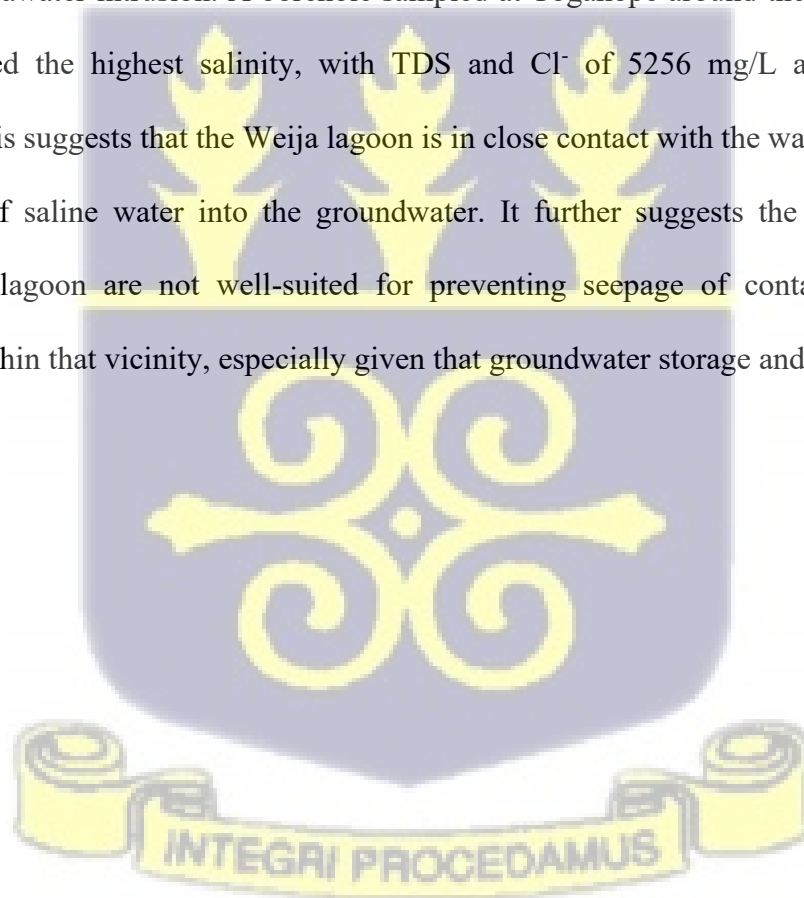
In the central sections of the basin, bicarbonate water types continue to dominate, with Na-HCO₃ being dominant, just like in the northern section. This section of the basin is designated as the transmission zone in the groundwater flow regime, where the groundwater becomes relatively more mineralised, with TDS ranging from 322.2 - 575.4 mg/L, with a mean of 421.7 mg/L (Figure 3.10). The groundwater in this section of the basin maintains its general character from the recharge area, with a continuous dissolution of silicate minerals and ion exchange processes. However, Mg-HCO₃ water types, although in small amounts, feature in this part of the basin, suggesting the dissolution of other silicate minerals such as amphiboles and micas previously not encountered in relatively significant amounts. The groundwater transitions from a bicarbonate-dominated water type, in the recharge and transmission zones respectively in the northern and central sections of the basin, to Na-Cl water type towards the southern portions, with a significant increase in dissolved solutes (TDS 727.2 - 1902.0 mg/L), pointing to longer residence time and

increased water-rock interaction. The southern part of the basin, up to 30 km inland from the ocean, is dominated by chloride water types. This may be a result of a combination of factors such as seawater intrusion, sea spray, and dissolution of evaporites. These areas are characteristically low-elevation areas in the basin and represent the discharge zones in the groundwater flow regime. Adomako et al. (2011a) attributed the elevated levels of chloride to seawater intrusion or dissolution of chloride deposits in the soil zone. The chloride water types in this area, accompanied by the relatively substantial increase in dissolved solutes, are consistent with groundwater at its advanced stage of evolution along the flow paths (Yidana et al., 2012; Younger et al., 2015; Loh et al., 2019; Bloomfield et al., 2020).

Several studies have pointed to anthropogenic pollution as one of the major controls on the groundwater hydrochemistry in the Densu River Basin using mainly nitrate and sulphate levels as the basis (Karikari & Ansa-Asare, 2006; Yidana et al., 2018; Sedenkor et al., 2019; Afrifa et al., 2022). However, this study observed relatively low levels of NO_3^- in the groundwater, which is in tandem with observations made by Adomako et al. (2011a), where all the samples had NO_3^- levels below the WHO (2017) recommended value of 10 mg/L for potable water. The nitrate levels in the groundwater also display a decreasing trend as the groundwater evolves from recharge to discharge areas (Figures 3.11g&h), a trend which was also observed by Adomako et al. (2011b). The declining trend suggests anthropogenic activities, which result in the release of nitrates into the groundwater, do not significantly contribute to the total solute concentration in the groundwater in the basin as it becomes more mineralised (Figure 3.11h), and may be of a lesser influence when it comes to the factors controlling the general hydrochemistry of the basin. However, it must be pointed out that shallow hand-dug wells tapping from shallow aquifers are more prone to pollution

from anthropogenic sources such as fertilizer runoff from farms, domestic wastewater, and leakages from septic tanks (Karikari & Ansa-Asare, 2006; Lutterodt et al., 2018; Abanyie et al., 2020; Wakejo et al., 2022), which may explain why some studies in the basin observed relatively high levels of NO_3^- (Karikari & Ansa-Asare, 2006; Adomako et al., 2011b; Yidana et al., 2018; Afrifa et al., 2022).

The extreme south of the basin, in contact with the ocean, appears to be impacted by seawater intrusion, where saline water from the ocean displaces fresh groundwater, rendering it unsuitable for drinking and other purposes. A ratio $\text{Cl}^-/\text{HCO}_3^-$ greater than 5 suggested 8% of the samples are influenced by seawater intrusion. A borehole sampled at Togakope around the Weija lagoon, an outlier, presented the highest salinity, with TDS and Cl^- of 5256 mg/L and 2392.2 mg/L, respectively. This suggests that the Weija lagoon is in close contact with the water table, allowing easy leaching of saline water into the groundwater. It further suggests the soil and geology underlying the lagoon are not well-suited for preventing seepage of contaminants into the groundwater within that vicinity, especially given that groundwater storage and flow are fracture-controlled.



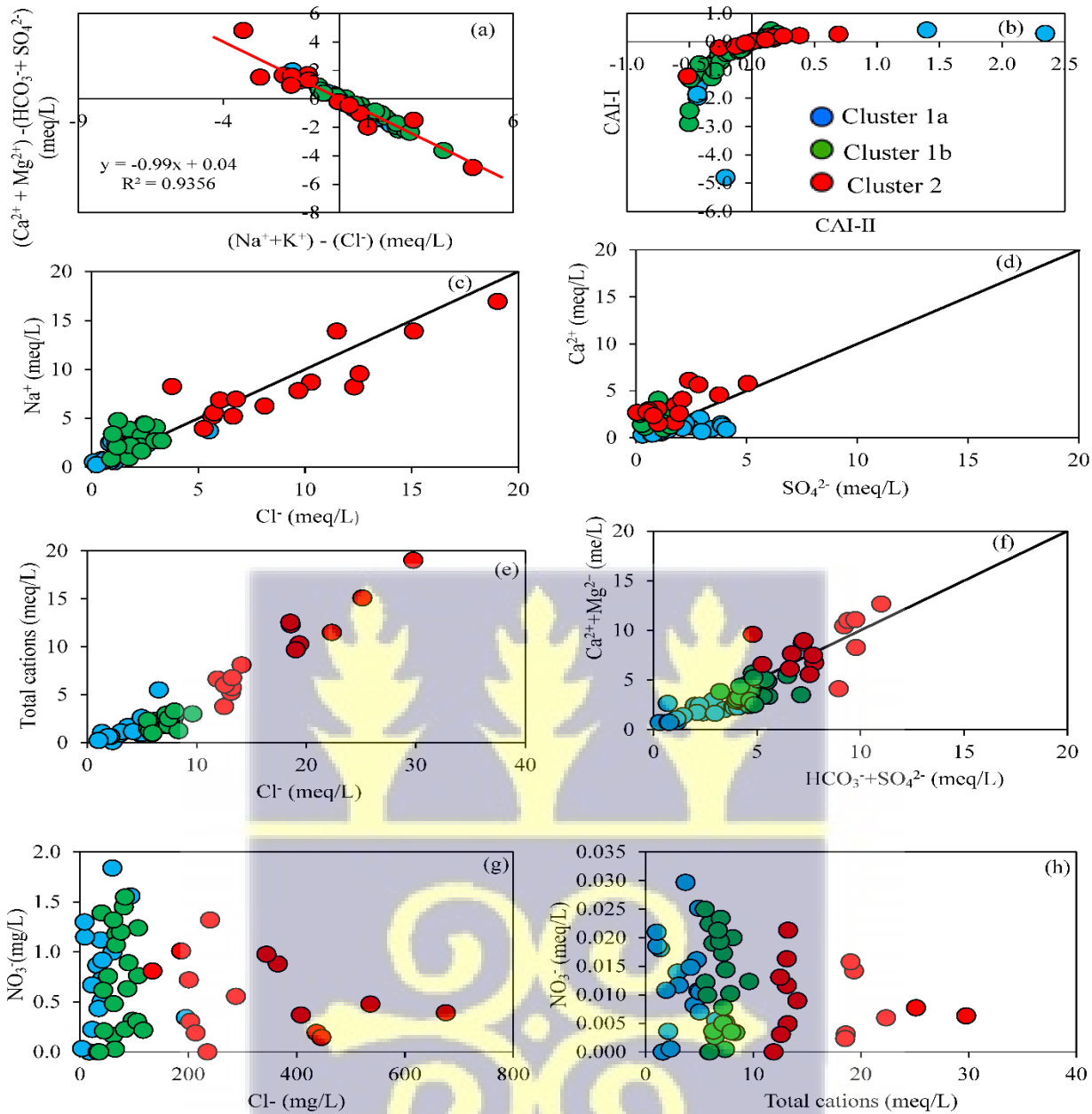


Figure 3.11: Bivariate plots of (a) $(Ca^{2+}+Mg^{2+} - (HCO_3^-+SO_4^{2-}))$ vs $(Na^++K^+)-Cl^-$, (b) CAI-I vs CAI-II, (c) Na^+ vs Cl^- , (d) Ca^{2+} vs SO_4^{2-} , (e) Total ions vs Cl^- , (f) $Ca^{2+}+Mg^{2+} - HCO_3^-+SO_4^{2-}$, (g) NO_3^- vs Cl^- , and (h) NO_3^- vs Total cations

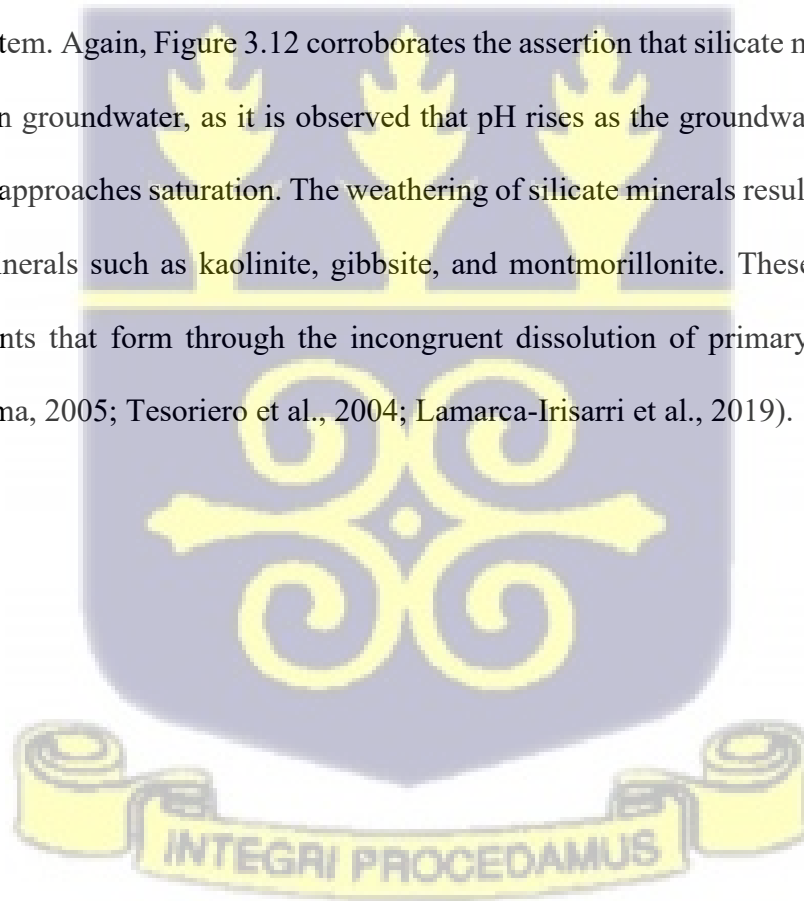
3.3.6 Groundwater saturation state and mineral stability

Mineral equilibrium calculations have proven useful in the absence of reservoir rock samples in assessing the possible reactive minerals in groundwater systems using hydrochemical data (Appelo & Postma, 2005; Gibrilla et al., 2010; Loh et al., 2016; Priestley et al., 2019). Mineral saturation indices (SIs) for some selected silicate and carbonate minerals have been estimated (Figure 3.12) and used to predict whether or not a particular mineral will be at equilibrium, dissolve or precipitate in the groundwater system. Hydrochemical species containing Al were not simulated due to the unavailability of Al data. However, inferences on the same have been made based on mineral stability plots and the probable reaction pathways (Equation 3.3).

The groundwater system generally trends from undersaturation to saturation with respect to most of the minerals, as it becomes more mineralised and as the pH of the water increases (Figures 3.12b, c, e, g, i & k). This suggests that the dissolution of these minerals, if present in the groundwater, continues as the water evolves from the recharge areas through the transition zones till it discharges into the ocean. The samples collected in the discharge areas appear to approach saturation with respect to all minerals, but at varying degrees of magnitude (Figure 3.12). The groundwater system is supersaturated with respect to quartz and chalcedony but undersaturated with respect to amorphous silica, suggesting amorphous silica or some other mineral phase controls the levels of silica in the groundwater in the Densu River Basin.

Although several factors control the dissolution rate of minerals, undersaturated minerals generally have higher dissolution rates than minerals closer to saturation (Hem, 1985; Priestley et al., 2019; Heřmanská et al., 2022). Groundwater systems dominated by silicate rocks are often supersaturated with quartz because quartz is more resistant to dissolution than amorphous silica

(Hem, 1985; Appelo & Postma, 2005; de Ruiter et al., 2021). As such, as the groundwater flows through the rocks, it dissolves the more soluble amorphous silica more easily than it would dissolve the less soluble quartz. However, the undersaturation of the groundwater system with respect to amorphous silica is based on the kinetics of silica dissolution. Although amorphous silica is more soluble than quartz, it also dissolves much faster than quartz. As a result, when the groundwater flows through the rocks, the amorphous silica is dissolved quickly, so the groundwater is unable to reach equilibrium with it. Conversely, quartz dissolves much more slowly, giving the groundwater more time to reach equilibrium with it, resulting in supersaturation with respect to it. Hence, the dissolution rate of the minerals plays a crucial role in determining their state in a groundwater system. Again, Figure 3.12 corroborates the assertion that silicate mineral weathering consumes acid in groundwater, as it is observed that pH rises as the groundwater becomes more mineralised and approaches saturation. The weathering of silicate minerals results in the formation of secondary minerals such as kaolinite, gibbsite, and montmorillonite. These minerals are the insoluble remnants that form through the incongruent dissolution of primary silicate minerals (Appelo & Postma, 2005; Tesoriero et al., 2004; Lamarca-Irisarri et al., 2019).



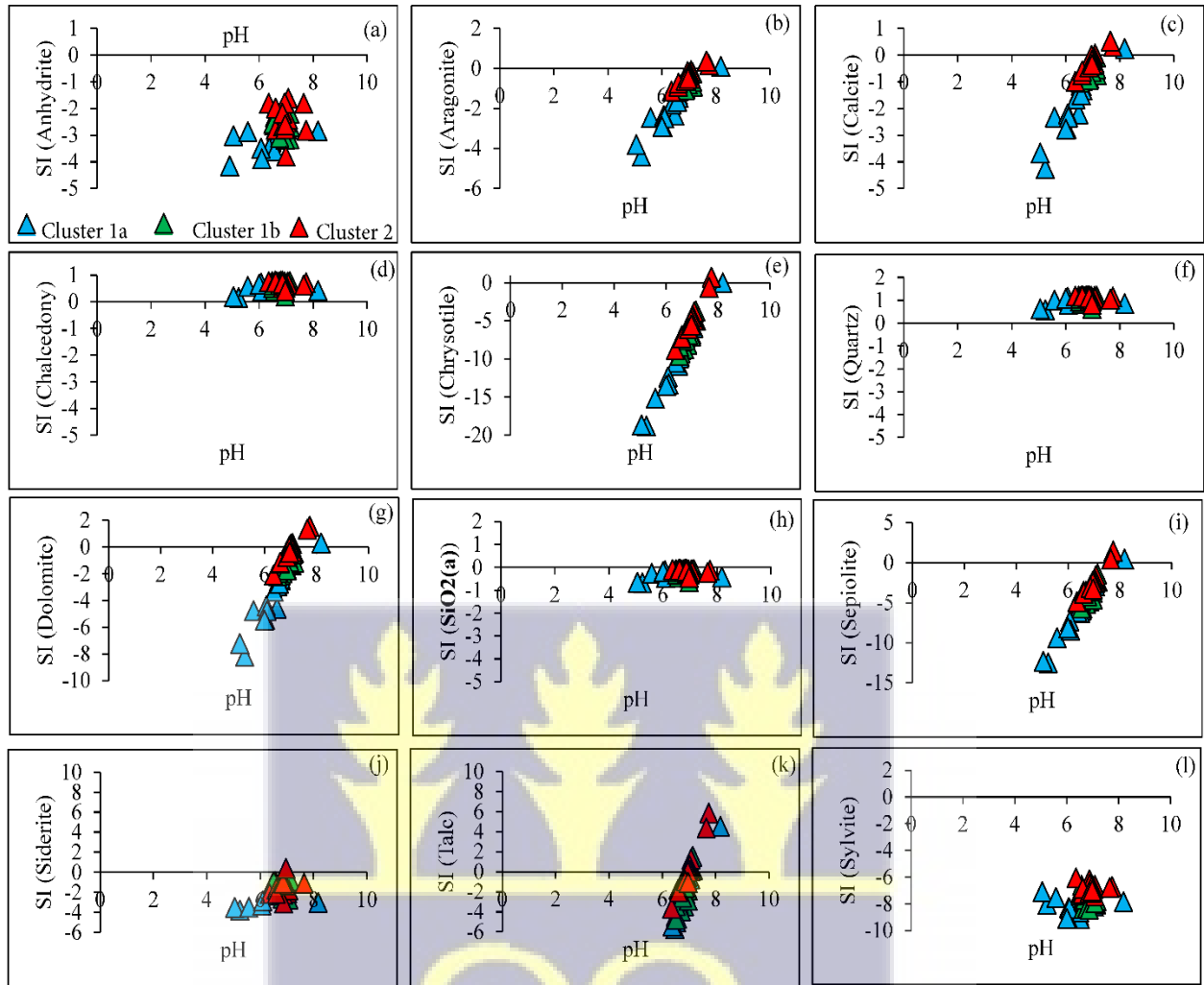


Figure 3.12: Biplots of selected saturation indices and pH

The SIs also suggest the dissolution of carbonate minerals, calcite and aragonite, which approach saturation as the water evolves. Carbonate mineral weathering is a likely process in the basin because small fractions of the basin are underlaid by metasedimentary and consolidated sedimentary rocks of the Birimian and Voltaian Supergroups. However, their overall impact on the general hydrochemistry of the basin may be relatively small. It is noteworthy that the weathering of silicate minerals may also result in the precipitation of carbonate minerals such as

CaCO_3 (Appelo and Postma, 2004), which may also explain CaCO_3 supersaturation in some parts of the basin along the groundwater flow paths.

Mineral stability diagrams provide another way to evaluate the extent of geochemical processes in the groundwater system (Freeze & Cherry, 1979; Appelo & Postma, 2005; Gibrilla et al., 2010; Loh et al., 2016; Priestley et al., 2019). Stability diagrams help to distinguish the stable weathering products, from the silicate minerals likely to dissolve under certain kinetic and thermodynamic conditions. The dominant reactions in the groundwater can be identified by comparing the chemical composition of the groundwater with the mineral stability fields of different minerals. Silicate mineral stability diagrams for $\text{CaO-SiO}_2\text{-Al}_2\text{O}_3\text{-H}_2\text{O}$, $\text{NaO}_2\text{-SiO}_2\text{-Al}_2\text{O}_3\text{-H}_2\text{O}$, $\text{KO}_2\text{-SiO}_2\text{-Al}_2\text{O}_3\text{-H}_2\text{O}$, and $\text{MgO-SiO}_2\text{-Al}_2\text{O}_3\text{-H}_2\text{O}$ (Figure 3.13) systems revealed that the groundwater is stable within the kaolinite field, suggesting the groundwater hydrochemistry is controlled by the thermodynamic equilibrium with this secondary mineral. The secondary minerals are the insoluble remnants of the incongruent dissolution of primary silicate minerals, through the leaching of silica and other minerals in groundwater. In the weathering of albite to montmorillonite, for example, 89% of the silica is retained, decreasing to 33% when it weathers to kaolinite and to 0% when it weathers to gibbsite (Appelo & Postma, 2005), indicating the intensity of leaching of silica and other ions from primary silicate minerals. Therefore, the stability of the groundwater in the kaolinite field suggests the groundwater is probably at the intermediate stage of its advanced evolution, in a hard rock terrain where the mineral dissolution appears relatively slow, given the low levels of dissolved ions (Figure 3.13). The stable kaolinite field also corroborates the ion exchange reaction processes in the groundwater systems made above, since clay minerals like

kaolinite provide large surface areas for such exchanges (Appelo & Postma, 2005; Lazaratou et al., 2020; Akisanmi, 2022).

The silicate mineral stability diagrams and saturation indices corroborate the assertions that silicate mineral weathering of plagioclase, biotite, K-feldspar, amphibole, etc. present in the aquifer system is a major hydrogeochemical process controlling the hydrochemistry of groundwater in the Densu Basin.



Figure 3.13: Mineral stability diagram for (a) CaO-SiO₂-Al₂O₃-H₂O, (b) NaO₂-SiO₂-Al₂O₃-H₂O, (c) KO₂-SiO₂-Al₂O₃-H₂O and (d) MgO-SiO₂-Al₂O₃-H₂O systems

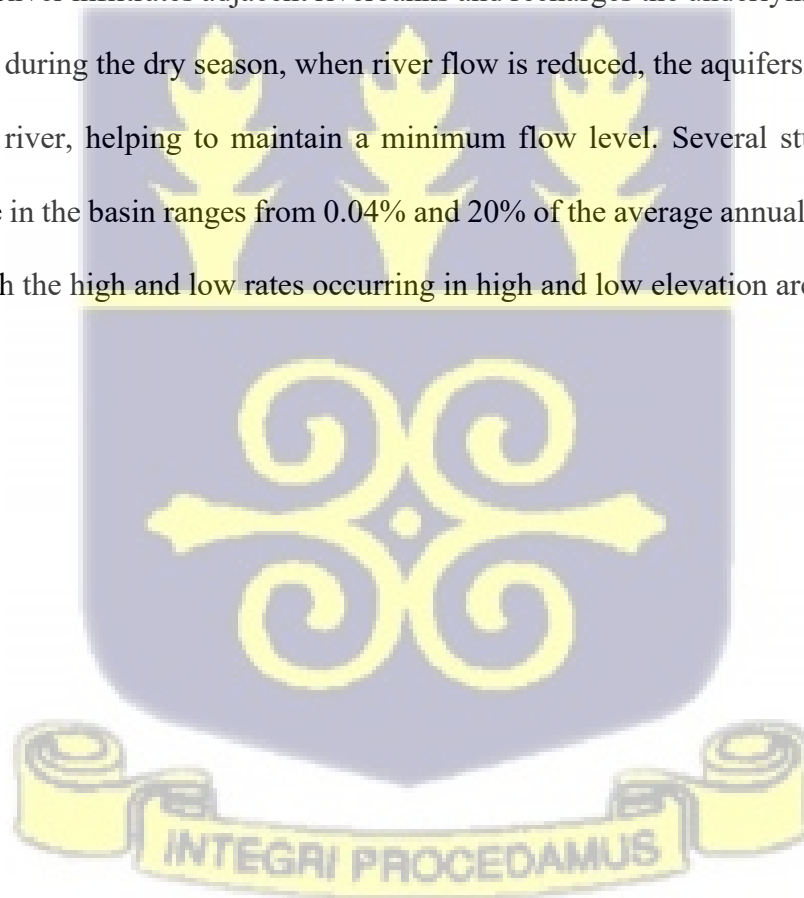
3.3.7 Conceptual groundwater flow

Forty-five (45) water level measurements across the basin have been converted to hydraulic head values by subtracting them from their respective point elevations. The resultant hydraulic heads have been used to construct the conceptual groundwater flow regime, based on the general hydrogeological principle that groundwater flow is orthogonal to the head contours, and guided by the hydrochemistry and topography of the basin. Heads could not be measured at the extreme mountainous north and at the extreme south of the basin due mainly to the unavailability of boreholes or hand-dug wells. The topography of the basin (Figure 3.14a) shows that the highest elevations occur in the extreme northwest and northeast respectively, with patches of high elevations in the central and southeastern sections.

The hydraulic heads vary from 34 – 255 m, with the highest heads occurring around the northwest and northeast of the basin and the lowest in the south, towards the sea. Groundwater flow appears to mimic the topography of the basin, flowing from high to low topographic areas (Figure 3.14), in line with general hydrogeologic principles. The dominant flow pattern is north-south and northeast-southwest, with some localised intermittent flow patterns which are generally undefined, and influenced by the patches of high elevations in the basin. This flow pattern, also observed by some studies in the basin (Alfa, 2010; Yidana et al., 2014; Yidana et al., 2018; Akurugu et al., 2022), is evident in the hydrochemistry of the basin where the low TDS groundwater samples in Cluster 1a are located in the topographic highs and transition to high TDS waters in Cluster 2 in low topographic areas, as the groundwater flows to discharge zones in the basin (Figure 1). This assertion also corroborates the north of the basin and other patches of high elevation in the basin as recharge zones, as relatively low mineralised groundwaters are found in these areas,

characterised by the dominance of bicarbonate freshwater types; Na-HCO₃ and Ca-HCO₃ (Figure 3.15). Whereas the low-elevation areas are characterised by relatively mineralised groundwaters of Cluster 2 group dominated by Na-Cl water type (Figure 3.15).

Groundwater recharge in the basin is largely through vertical infiltration of rainfall through the weathered zone and the fractures, as observed by Adomako et al. (2011a). Field observations also revealed that interaction between the river and the underlying aquifers varies seasonally and influences the amount and nature of recharge processes. During periods of high river flow, and in areas with permeable sediments or fractures in the underlying rocks along the riverbanks, water from the Densu River infiltrates adjacent riverbanks and recharges the underlying aquifers (Figure 3.15). However, during the dry season, when river flow is reduced, the aquifers may contribute to baseflow in the river, helping to maintain a minimum flow level. Several studies in the basin suggest recharge in the basin ranges from 0.04% and 20% of the average annual rainfall (Akurugu et al., 2022), with the high and low rates occurring in high and low elevation areas respectively in the basin.



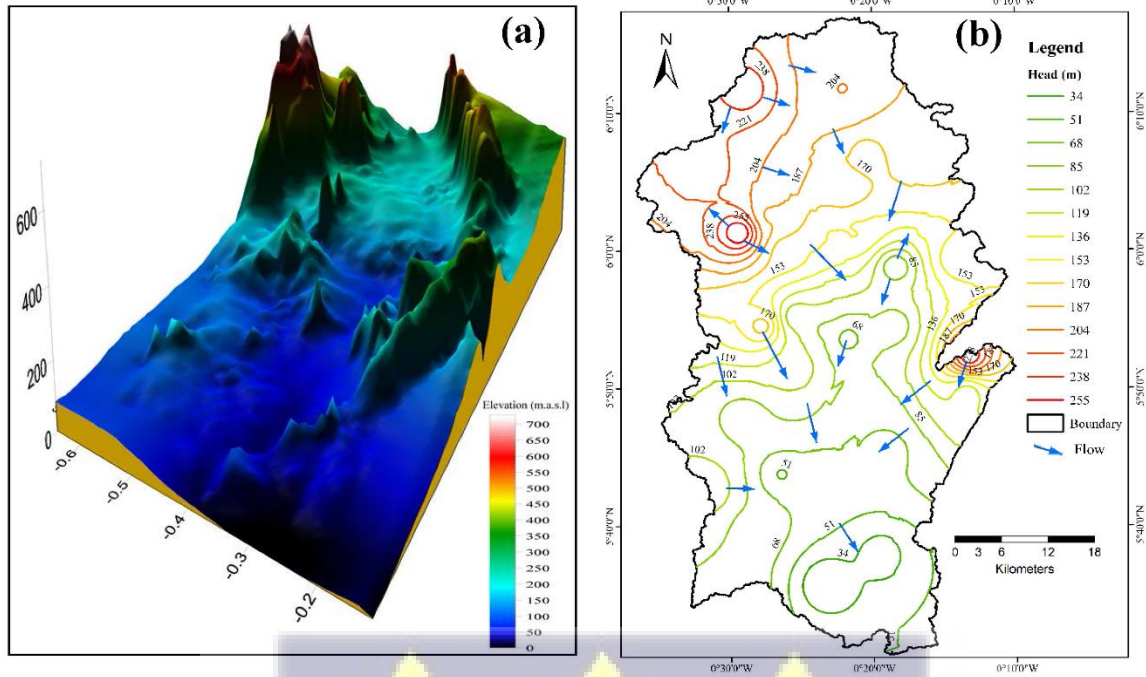


Figure 3.14: (a) 3D topography and (b) conceptual flow based on groundwater hydraulic head

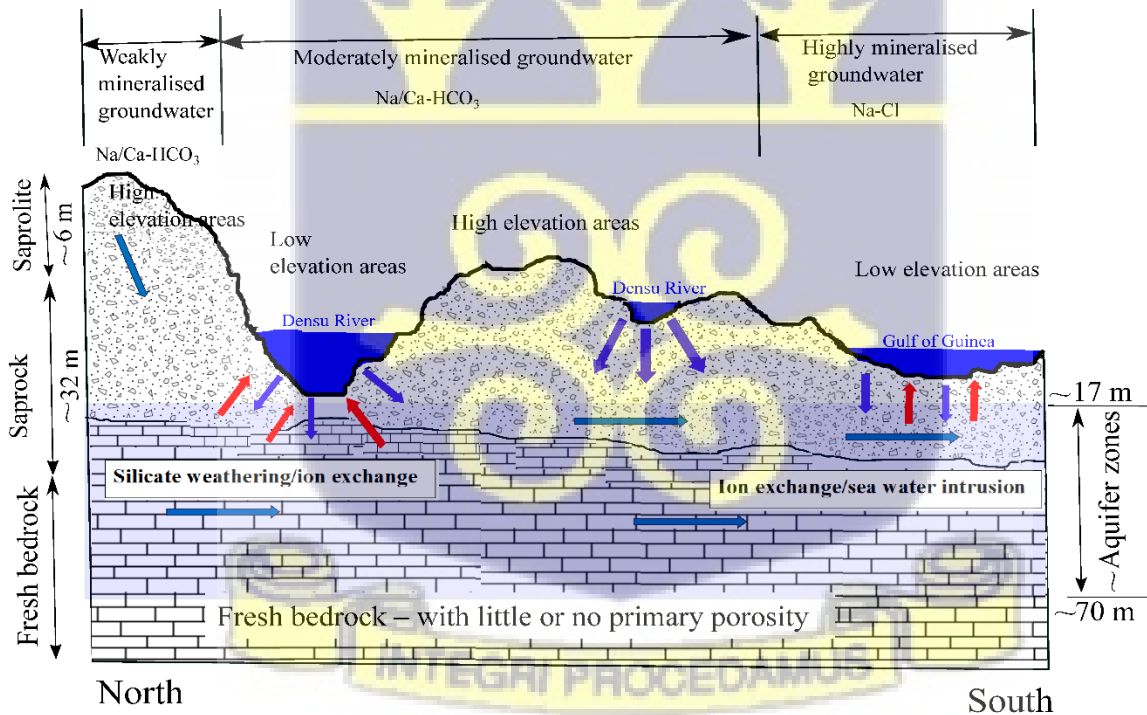


Figure 3.15: Conceptual hydrogeology of the Densu River Basin

3.4 Conclusion

This study attempted to develop a conceptual understanding of the hydrogeologic framework for the data-scarce crystalline basement rocks of the Densu River Basin. Rocks of the Birimian Supergroup were found to be the most productive in terms of groundwater delivery, in tandem with other studies, followed by the rocks of the Voltaian Supergroup and granites of the Tamnean and Eburnean Plutonic Suites. The average yield for the Birimian Supergroup, Voltaian Supergroup, and the granites was 84.48, 79.92, and 66.00 m³/day respectively. Rocks of the Birimian Supergroup displayed relatively deeper weathering, with an average weathered thickness of 17.62 m, compared to 6.40 m and 11.24 m for rocks of the Voltaian Supergroup and granites respectively. Most aquifers in the basin are encountered at 11 – 35 m and occur within the saprolite, saprock, and fractured bedrock which complement each other in terms of groundwater delivery. The most productive zones in rocks of the Birimian Supergroup are the lower and upper parts of the saprolite and saprock respectively. Whereas in the granite, the fractured bedrock could be as equally or more productive as the weathered zone depending on the amount and extent of fractures. A dominant north-south and northeast-southwest regional groundwater flow pattern has been recognised, with local radially concentric groundwater flow patterns which are thought to be influenced by the local topography. The high-elevation areas, identified as recharge zones in this study are characteristically low in dissolved ions and pH, characterised by Ca-HCO₃, and Na-HCO₃ water types, with Na-Cl water types, also featuring prominently. The groundwater becomes more mineralised as it flows from the northern part through the transition zones in the central section to the discharge zones in the south, where it evolves completely to a Cl⁻ water type in the south. Silicate mineral dissolution of probably amorphous silica, albite, anorthite, etc. has been

identified as a major process responsible for the hydrochemical facies identified. Mineral stability diagrams show the groundwater is stable in the kaolinite field, and probably at its intermediate stage of evolution in the hard rock terrain, where the clay mineral kaolinite provides a large surface area for significant ion exchange. Generally, the groundwater is physicochemically potable except in a few places where low pH and elevated Cl^- , Na^+ , Fe, and F- levels render the water unsuitable for drinking. The recharge and transition zones in the groundwater flow regime present the best water quality compared to the discharge zones.



CHAPTER FOUR

ASSESSING THE POTENTIAL IMPACTS OF ABSTRACTION AND RECHARGE USING NUMERICAL GROUNDWATER FLOW MODELLING FOR THE DENSU RIVER BASIN, GHANA

4.1 Introduction

The intensifying effects of climate change on hydrological systems have profound implications for groundwater resources, as shifts in precipitation patterns, rising temperatures, and alterations in seasonal variability have the potential to impact groundwater recharge rates, aquifer storage, and general groundwater availability (Kumar, 2012; Epting et al., 2021; Swain et al., 2022; Veeraswamy et al., 2023). Decreased and extremely inconsistent rainfall patterns, increased evaporation, and frequent and significant drought spells in Ghana have been projected to continue into the future (Issahaku et al., 2016; Yiran & Stringer, 2016; Larbi et al., 2018; Atampugre et al., 2019). Amidst these, rapid population growth, urbanisation, agricultural expansion, and industrialisation, accompanied by pollution continue to exert pressures on available groundwater supplies. The upsurge in anthropogenic activities further complicates the groundwater resources landscape through potential contamination of aquifers from agricultural runoff, industrial discharges, and improper waste disposal.

The Densu River Basin is a critical source of community water supply to the western parts of Accra, the national capital of Ghana, and many other communities for agricultural, industrial, municipal, ecological, and many other uses (Amoako et al., 2010; Adomako, Osaе, et al., 2011; Oti, 2019; Gyimah et al., 2021; Akurugu et al., 2022). Knowledge of the hydrogeological

properties and processes that control the availability and distribution of groundwater resources in the basin is crucial for the proper management of the resource for sustainable use amidst all the pressures on water resources in the basin (Banoeng-Yakubu et al., 2011; Kotb et al., 2021; Akurugu et al., 2022).

Several in situ methods are available for investigating aquifer hydraulic properties in attempts to delineate and estimate groundwater potentials, borehole yields, and aquifer hydraulic properties, amongst others. The traditional pumping test method is one reliable way of estimating aquifer and borehole properties such as specific yield, hydraulic conductivity, transmissivity, and specific capacity. However, this approach requires drilling multiple boreholes, proving costly and time-consuming while only providing point estimates of hydraulic parameters, which do not exactly give a spatial perspective. Similarly, tracer tests employed in aquifer characterisation often yield approximate results due to field limitations. Both methods are impeded by cost, time, and the inability to offer comprehensive spatial insights into hydraulic parameters (Banoeng-Yakubo et al., 2011; Shapoori et al., 2015; Moharir et al., 2017; Ali et al., 2022).

Numerical groundwater models have emerged as powerful tools for addressing complex hydrogeological problems and have proven superior to traditional hydrogeological methods, gaining worldwide attention (Anderson et al., 2015). Numerical groundwater models offer predictive insights into future scenarios, stream-aquifer interaction, irrigation management, over-abstraction of groundwater, land subsidence, seawater intrusion, etc. (El Alfy, 2014; Dibaj et al., 2020; Canul-Macario et al., 2021; De Biase et al., 2021; Nyakundi et al., 2022; Sikdar et al., 2022); and are cost-effective solutions once the model is developed and validated. Unlike traditional hydrogeological methods, numerical groundwater models are capable of giving deeper insights

into groundwater processes by integrating topographic, geological, hydrological, and climate datasets, providing a holistic view of the system's general behaviour (McDonald & Harbaugh, 2003; Anderson et al., 2015). Several numerical simulation models, including FEFLOW (Diersch, 2013), SEAWAT (Langevin et al., 2008), SUTRA (Voss & Provost, 2002), HydroGeoSphere (Brunner & Simmons, 2012), TMVOC (Pruess & Battistelli, 2002), ParFlow (Maxwell et al., 2009), MIKE SHE (Abbott et al., 1986), MODFLOW-SURFACT (Panday & Huyakorn, 2008), and Hydrus (Šimůnek et al., 2016) have been used in hydrological studies. MODFLOW (Harbaugh et al., 2000) is a groundwater model that uses a finite difference numerical code or various implementations of the same. It has been extensively applied in studies relating to groundwater flow, aquifer characterisation, and groundwater resource management forecasts, mainly due to its comparative simplicity and compatibility with most simulated terrains (McDonald & Harbaugh, 2003; Hagan & Darko, 2020).

Generally, numerical simulation models require substantial input data for parameterisation and setup. They also require detailed and accurate observational data for calibration and validation. Thus, data paucity and accuracy pose a hindrance to their adaptation. As a result, relatively few studies exist, especially in Ghana and Africa as a whole. Based on a new and improved observational dataset for the Densu River Basin developed by the Building Climate Resilience into Basin Water Management (CREAM) project (e.g. Chapters Two, Three & Gyasi-Agyei et al., 2023), and an updated hydrogeological conceptualisation of the basin based on new field data, this research sought to develop a new validated physical process-based transient groundwater flow model (MODFLOW). The aim was to simulate groundwater levels in the complex groundwater flow system of the Densu River Basin. The findings of this study will not only enhance our

understanding of the complex hydrogeological dynamics at play in the basin but could also provide vital information that could aid the development of adaptive strategies to safeguard the groundwater resources of the basin.

4.2 Materials and methods

4.2.1 Data collection and analyses

Data on the hydrogeological characteristics of the basin were collected as primary and secondary (historical/reviewed) field datasets. Secondary datasets, including 114 borehole lithological logs, 87 pumping test records, daily water level measurements, daily stream flow records, photographs, and geology maps, were collated from databases of the Council for Scientific and Industrial Research - Water Research Institute, Ghana Hydrological Authority, and Community Water and Sanitation Agency (CWSA). Constant discharge pumping tests, groundwater level monitoring, water sampling and analysis, and water table elevation measurements were conducted across the basin as part of understanding the hydrogeology. Details of these datasets are presented in Chapter Two. The pumping test records also provided data on hydraulic properties such as hydraulic conductivity (K) and transmissivity (T), specific capacity, borehole yield, drawdown, etc.

The collated datasets were thoroughly examined and compared with the existing geological and hydrogeological understanding of the study area. This rigorous process aimed to guarantee consistency and accuracy, ensuring that the datasets were refined and organised into usable formats essential for an adequate domain conceptualisation.

Primary datasets included three pumping tests conducted on selected boreholes, a digital elevation model (DEM) downloaded from the United States Geological Survey (USGS), precipitation data

for the monitoring stations extracted from a newly developed 5 x 5 km gridded precipitation data (Gyasi-Agyei et al., 2023), groundwater abstraction data (Duah et al., 2021), and 45 spot groundwater level measurements across the basin. Furthermore, 14 time series of groundwater levels containing 206,067 observation points covering June 2020 to April 2024, with a resolution of 1 hour to 8 hours, were also analysed in this study. The hourly time series static water level data were averaged to daily records, plotted as graphs, and visually inspected. The time series data were carefully analysed and checked for quality assurance, removing unreliable recordings, outliers, instances of device failures, sudden drawdowns due to nearby pumping, etc. Daily streamflow data from four (4) gauge stations at Mangoase, Asuboi, Parkro, and Ashaladja from 1971 to 2008, with various degrees of missing data, also underwent similar quality assurances for consistency.

4.2.2 Conceptual model and boundary conditions

A hydrogeological conceptual model is a simplified and summarised representation of the groundwater flow and level regime of the domain based on available and general hydrogeological information and understanding of the site. The conceptualisation of the Densu River Basin in this study is based mainly on newer studies in Chapter Two and Akurugu et al. (2022), which outline the hydraulic characteristics of the rocks and aquifers in the basin, and Yidana et al. (2014) who generated a groundwater flow model for the basin. Based on the collated data and studies in the basin, the geology and hydrogeologic framework of the basin were put in a conceptual perspective in a GIS environment using ArcGIS, Golden Surfer®, and Groundwater Modelling System (GMS) version 10.6.2 (Figures 3.14 & 3.15). The hydrochemical and conceptual groundwater flow patterns are well documented in Akurugu et al. (2022) and described in Chapter Two.

Defining the geological framework of the domain being modelled is an important step in conceptual modelling. Drilling through the aquifer succession at specific locations provides valuable information about the local stratigraphy and properties. The borehole lithological log data included borehole IDs, GPS coordinates, depths, aquifer zones, lithology types and thicknesses, structures, and nature of weathering, which are crucial in understanding the geological and hydrogeological framework of the basin and formed the basis for the lithostratigraphy modelling.

GMS provides toolsets for lithostratigraphy modelling based on a robust inverse distance weighting approach. A careful study of the borehole lithological logs revealed two main weathering patterns: the completely decomposed to slightly weathered zone (saprolite + saprock), and the fractured bedrock, as detailed in Chapter Two. Each of the zones displayed relatively similar hydraulic characteristics, irrespective of the local lithology (Figure 3.6). This formed the basis for conceptualising the domain as a two-layer model, with Layer 1 being the weathered zone and Layer 2 covering the fractured bedrock. The domain thickness was based on the thicknesses of each layer, with the top elevation and bottom elevations extracted from the DEM, and interpolated between boreholes. Based on pumping test analysis and literature (Alfa et al., 2011; Yidana et al., 2014; Akurugu et al., 2022), hydraulic conductivity (K) values of 0.00001 - 20 m/day were assigned to Layer 1 and interpolated over the layer, whereas 0.0000001 – 15 m/day was assigned to Layer 2, whilst maintaining a vertical anisotropy of 0.1 m/day between the layers. Analysis of groundwater recharge in the basin revealed that it follows the rainfall patterns in the basin (Figure 1.1). Recharge estimates from the chloride mass balance, water table fluctuation, and baseflow filter methods conducted in the basin and estimates from literature (Table 4.1) were used

to guide recharge values assigned to the model. The assigned recharge in the basin was approximated at an average of 2% to 15% of the annual rainfall.

Table 4.1: Summary of groundwater recharge studies in the Densu River Basin

Source	Methodology	Estimated groundwater recharge	
		mm/year	% of annual rainfall
Chapter Two	Chloride mass balance (CMB)	1 - 338	<0 - 28
	Water table fluctuation (WTF)	27 - 327	3 - 28
	Baseflow methods (BFF)	28 - 145	3 - 13
WRC (2007)	Water balance analysis	112 - 238	10 - 14
Alfa et al. (2011)	Hydrological model; MIKE SHE	120 - 153	8 - 13
Yidana et al. (2014)	MODFLOW model	93 - 192	10.3 - 12
Duah et al. (2021)	CMB and WTF	0.32 - 306	0.04 - 18



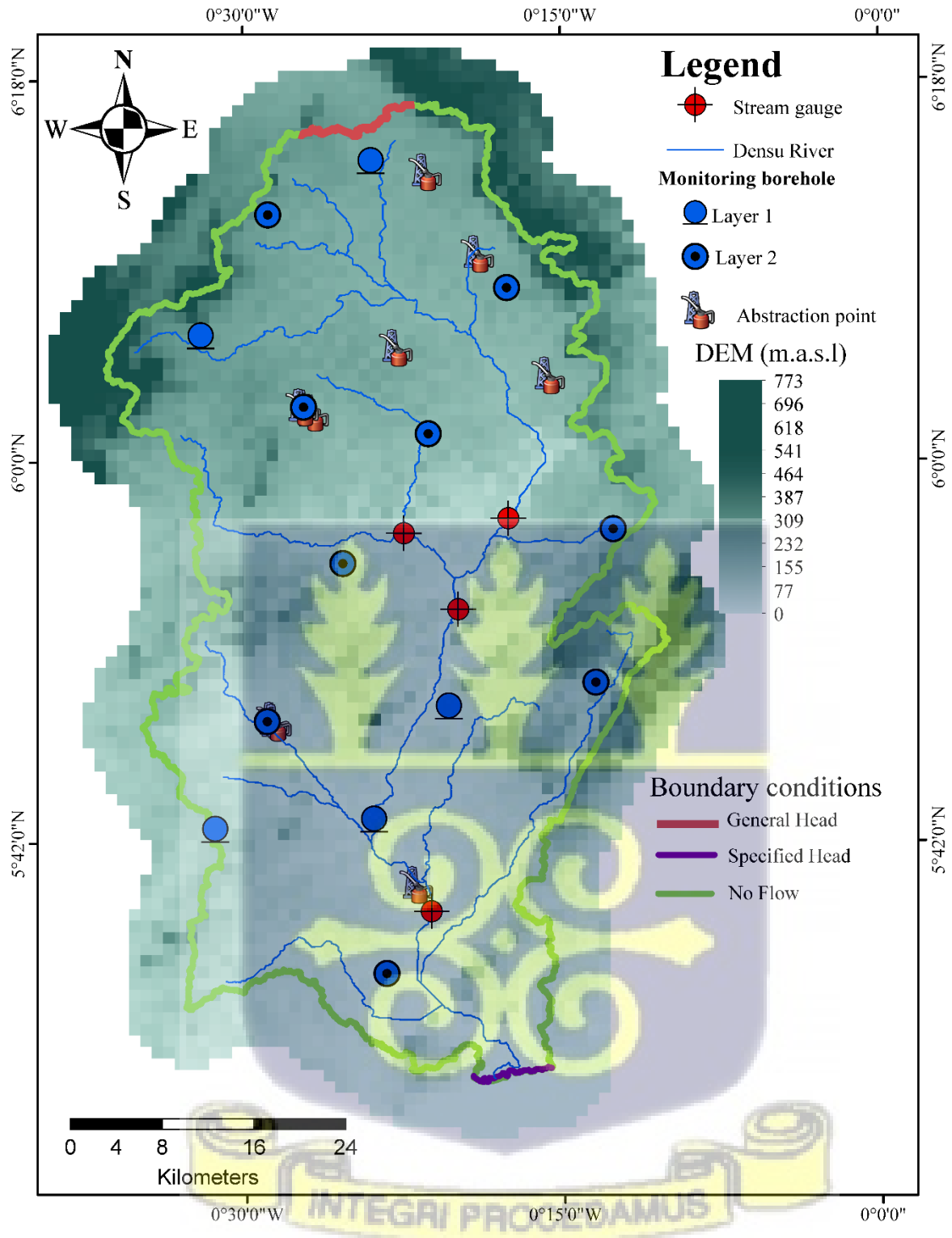


Figure 4.1: Conceptualisation and boundary conditions of the model domain

The top layer, located within the saprolite and saprock, was set as unconfined, reflective of the hydrogeological conditions of the basin, where the water table freely fluctuates in response to changes in recharge, abstraction, evapotranspiration, or other hydrological factors. The bottom layer of fractured bedrock was set as confined to represent the confining layers which restrict the vertical movement of water across the aquifer.

The bottom of the model domain was conceptualised as a No-flow boundary to reflect the fresh bedrock (unfractured) conditions. The lateral bounds of the eastern and western borders of the domain were conceptualised as a No-flow boundary condition, such that flow in and out of the basin through the lateral bounds is limited. Considering the basin as a whole, flow across its lateral boundary would most likely be restricted due to the mountain reaches and probably due to hydraulic constraints such as groundwater divides. Similarly, the contours of hydraulic heads for the basin generally suggest No-flow boundary conditions. As such, assigning No-flow boundary conditions in these parts of the basin would give the model the freedom to simulate the appropriate flow conditions within the model domain without introducing uncertainties associated with flows across the lateral bounds. In the extreme north of the basin, the basin inlet was, however conceptualised as a Head-Dependent flow boundary condition, such that flow in and out of the basin at the basin inlet would depend on the hydraulic head difference. This is to allow for groundwater flow into the basin at the headwaters of the Densu River. Groundwater in the basin would probably discharge into the ocean at the basin outlet in the extreme south. As such, the basin outlet was designated as Specified Head (Dirichlet Boundary), where a known head is assigned and water is simulated as moving in or out of the aquifer at a rate adequate to maintain the head specified.

The Densu River and its major perennial tributaries were digitised and incorporated in the model; however, ephemeral streams were not, since they dry out during the dry season and are thought not to significantly impact the groundwater system. Using the DEM and an average depth of 2 m assigned to the river, the river stages and bottom elevations were computed in ArcGIS and imported into GMS. The frontiers of the river boundary conditions were defined as a function of the riverbed's slope and conductance.

Fifteen groundwater abstraction points, with an estimated total volume of 5,906,430 m³/year, distributed variously across the basin, were implemented for the steady state period. The abstraction volumes were obtained from Duah et al. (2021), and are based on records from the Water Resources Commission (WRC) of Ghana, and the author's estimates from field interviews conducted in the basin. Unfortunately, there seem to be no time-varying records on groundwater abstraction in the basin.

4.2.3 Numerical model setup and calibration

The conceptual model was converted to a 3D numerical model using the modelling platform GMS Aquaveo as the user interface, and groundwater flow was simulated using the cell-centred, finite difference code MODFLOW – 2000 (Harbaugh et al., 2000). The model domain of ~ 2,500 km² was gridded into a 150 x 100 x 2 ijk discretisation, consisting of 45,753 nodes and 30,000 cells. Fourteen hydraulic head datasets averaged from 2020 - 2023 were used. These averages present the long-term average groundwater conditions in the basin and were used to calibrate the model under steady-state conditions to set the basic aquifer parameters, with a calibration target for the hydraulic head set at 2 – 5 m. After calibration, the steady state model was subsequently converted

to a transient model and calibrated using monthly time step groundwater level data of 14 boreholes from 2020 to 2023. Transient calibration was done in a similar fashion as the steady state, except that calibration focused on storage parameters (specific yield and specific storage) and river conductance. Hydraulic head datasets covering July 2023 – April 2024 were used for validation of the model calibration.

Hydraulic conductivity and river conductance were the main parameters calibrated under steady state. The calibration was first performed by a manual trial-and-error method, where small changes were systematically made to the input parameters and run each time in MODFLOW to minimise the error between the observation and prediction values. The manual trial-and-error calibration is performed to provide insights into the model's behaviour and sensitivity to different parameters crucial for determining reasonable ranges for model parameters and understanding the most influential parameters. Therefore, in the coming sections, only automated calibration results (steady state and transient) are reported.

Secondly, an automated calibration using the automated parameter estimation (PEST) method (Doherty, 2004) was performed. The automatic model calibration using PEST requires parameterisation of the model input parameters which involves finding which parts of the model input parameters PEST could optimise. Sensitivity analysis is crucial in groundwater flow simulation which involves assessing and analysing how variations in input parameters impact the model outputs. It reveals the relative importance of the different parameters and their respective influence on the simulation results, thus improving the reliability and accuracy. The PEST calibration which was used in this study incorporates sensitivity analysis automatically, quantifying the influence of each parameter on the simulation outputs. During optimisation,

insensitive parameters are temporarily held at their current values as PEST attempts to compute more desirable values for the sensitive parameters (Doherty et al. 2004). Parameters with higher sensitivity have a higher impact on the model performance and are therefore the target of optimisation in PEST.

The pilot point method was adopted for calibrating hydraulic conductivity in both Layer 1 and Layer 2. The pilot point method offers the flexibility for a complex hydraulic conductivity distribution within the layers if suggested by the observations. They work as a type of surrogate parameter, where hydraulic conductivity is estimated at pilot point locations and thereafter kriged in between points. Forty-two (42) pilot points were evenly distributed across the model domain (Figure 4.2) and assigned initial values (Table 4.2). The pilot point implementation is combined with the regularisation option during calibration. The Tikhonov regularisation option imposes constraints on the (pilot point) parameter such that additional information in the form of prior information equations about the parameter can be added. In this case, the regularisation imposes a homogeneity constraint such that pilot points close to each other do not differ significantly in the absence of other information (observations) directing them otherwise. The regularisation ensures higher stability during the inversion process and allows the number of parameters to greatly exceed the number of observations.

Table 4. 2: Overview of calibration parameters

Parameter	Unit	Starting value	Lower/Upper bound	Sensitivity	Calibrated value
K_Layer1	m/day	0.5	0.00001 - 20	0.0796	0.018 – 6
K_Layer2	m/day	0.5	0.00001 - 15	0.034	0.0027 – 15

General head_conductance	m ² /day/m	0.1	0.1	0.311	1
Recharge_multiplier	N/A	0.10	0.02 – 0.15	1.356	0.0268
River_conductance	m ² /day/m	0.3	0.1 – 0.5	0.09	0.372
Specific_yield	N/A	0.03	0.01 – 0.08	0.025	0.08
Specific storage	1/m	0.0001	0.00001 – 0.001	1.712	0.001

Locations in the model domain with known hydraulic conductivity values obtained from pumping test analyses conducted in the basin were assigned as fixed pilot points so as to prevent parameters from deviating from observed values. Assigning fixed pilot points in regions where crucial hydrogeological features are present, based on field measurements, ideally ensures a better representation of the actual conditions in those areas, leading to an improvement in the model accuracy and reliability for predictions in those specific locations. It potentially reduces the computational burden as compared to trying to estimate parameters across the entire model domain, thereby enhancing efficiency in the calibration process, especially when dealing with large-scale models or when computational resources are limited.

Statistical performance measures used to evaluate the goodness-of-fit of the applied model and calibration in this study are the root mean square error (RMSE) and mean absolute error (MAE), which assess how well the model's predictions compare with the observed values (Equations 4.1 and 4.2 respectively), and the coefficient of determination (R^2), which measures the strength of the linear relationship between the observed and simulated data (Equation 4.3). The use of statistical performance measures is valuable for assessing model performance in groundwater modelling. However, it is advisable to use them in conjunction with other evaluation techniques such as visual

inspection, physical plausibility checks, sensitivity analyses, etc., to obtain a more comprehensive understanding of model strengths and limitations (Anderson et al., 2015; Moriasi et al., 2015).

$$\text{RMSE} = \frac{1}{n} \sqrt{\sum_{i=1}^n (h_i^{\text{obs}} - h_i^{\text{sim}})^2} \quad (4.1)$$

$$\text{MAE} = \frac{1}{n} \sum_{i=1}^n |h_i^{\text{obs}} - h_i^{\text{sim}}| \quad (4.2)$$

$$R^2 = 1 - \frac{\sum_{i=1}^n (h_i^{\text{obs}} - h_i^{\text{sim}})^2}{\sum_{i=1}^n (h_i^{\text{obs}} - \overline{h_i^{\text{obs}}})^2} \quad (4.3)$$

Where RMSE, MAE, R^2 , n , h_i^{obs} , h_i^{sim} , and $\overline{h_i^{\text{obs}}}$ are respectively root mean square error, mean absolute error, coefficient of determination, number of observations, actual observed values, model simulated values, and mean of the observed values.

4.2.4 Scenario analysis

Scenario analysis in groundwater modelling involves evaluating and comparing various scenarios to assess the potential impacts of different conditions, management strategies, or external factors which could impact the groundwater system. Scenario analysis offers water resource managers and researchers an opportunity to gain insights into how the groundwater system responds to various stresses and changes such as population growth, industrialisation, urbanisation, climate change, etc. on groundwater resources, for making informed decisions. The calibrated transient model was used to simulate two scenarios including various stresses on groundwater resources in the Densu River Basin. Accurate estimates of groundwater abstractions in the basin and Ghana, in general, are often unavailable since boreholes are mostly drilled purposely for community water

supply, where such documentations are usually not considered. Groundwater abstraction was therefore based on estimates indicated under section 4.2.2., and recharge estimates used within the calibration period were used as the baseline for future forecasts.

The first scenario (Scenario 1) aims to assess the impact associated with population growth in the basin and the corresponding groundwater demand, given everything else remains the same. This involves increasing the abstraction rate of 10,765,365 m³/year estimated within the transient period by 3.6 % per annum due to the population growth in the basin (Ghana Statistical Service, 2021) over 20 years whilst maintaining the baseline (2020-2023) recharge rates.

The second scenario (Scenario 2) is aimed at simulating the possible consequences of climate change which is likely to cause changes in recharge rates as a result of a decline or increase in rainfall in the basin amidst increased water demands as a result of population growth. Climate change is significantly influencing evapotranspiration rates, temperature, and rainfall amounts, affecting several parts of the ecosystem, key amongst them, water resource availability. Several studies in West Africa and Sub-Sahara Africa in general have observed various degrees of reductions in annual rainfall, with forecasts suggesting a continuing decreasing trend into the end of the century (Sylla et al., 2016; Ayanlade et al., 2022). In this study precipitation projections developed for the Building Climate Resilience into Basin Water Management in Ghana (CREAM) Projections from the climate models MOHC-HadGEM2-ES and MIROC-MIROC5, spanning 20 years (2023-2043) for the basin, were coupled with Scenario 1 with enhanced abstractions to assess the impacts on the groundwater system.

4.3 Results and discussion

4.3.1 Model calibration and performance

The pilot point strategy adopted for hydraulic conductivity calibration allows for adequate representation of the complex distribution of K in the basin. Assigning fixed pilot points (Figure 4.3) in regions where crucial hydrogeological features are present, based on measurements, ideally ensures a better representation of the actual conditions in those areas. Keeping some pilot points fixed during the calibration slightly improved the performance of the model, as opposed to allowing all of them to run freely. This is probably due to the seemingly homogeneous nature of K values around these fixed pilot points (Figure 4.3). Hence, the impact on the model performance is dependent on assigning pilot points as fixed or free, and the location and hydraulic parameter under consideration.

A biplot of the observed and model-simulated hydraulic heads and depths to groundwater levels shows a close match, suggesting a reasonably well-calibrated model with a high coefficient of determination (R^2) (Figure 4.2). The high correlation between the model simulation and observed hydraulic heads (Figure 4.2a) could be a result of the natural correlation between topography and groundwater heads; as a result, it is prudent to also consider the correlation between depths to water table (Figure 4.2b), which also presents a high R^2 value of 0.85. Also, the root mean square error (RMSE), mean absolute error (MAE) and mean error (ME) for the calibrated steady state model are respectively 2.68 m, 1.37 m and 0.06 m (Table 4.3), suggesting adequate agreement between model simulations and observation values.

Table 4.3: Model performance of the hydrological models. The steady state model performance statistics are based on the calibration period of June 2020 – June 2023. The transient model statistics are given for the calibration period (June 2020 – June 2023) and the evaluation period (July 2023 – April 2024).

Model	RMSE	MAE	ME
Steady state	2.68	1.37	0.06
Transient (Calibration)	2.39	1.65	0.20
Transient (Evaluation)	2.45	1.70	0.30

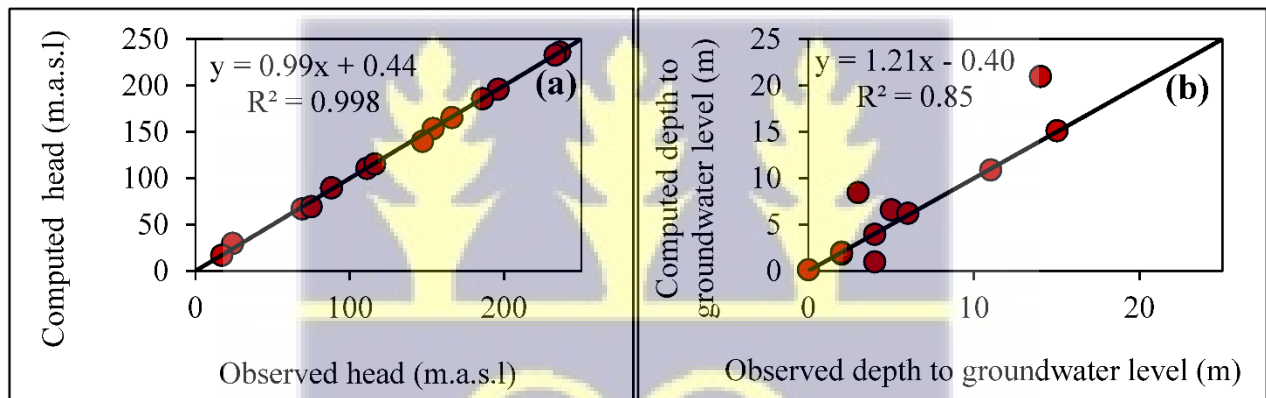


Figure 4.2: (a) Biplot of computed versus observed hydraulic head, and biplot of computed versus observed depth to groundwater level

4.3.2 Hydraulic conductivity field

The calibration of the model shows horizontal hydraulic conductivity (K) ranges from 0.018 – 4.79 m/day for Layer 1, the top layer, and 0.041 – 14.89 m/day for Layer 2, the bottom layer (Table 4.2). The average K values of 0.922 and 2.795 m/d, respectively, were estimated for Layer 1 and Layer 2, except for some patches of high K values in the northwest, central, south, and southwest

of the basin. The K values associated with the three fixed pilot points appear to blend seamlessly with the surrounding hydraulic conductivities (Figure 4.3). The high patches of K values observed in Layer 2 are likely dictated by nearby head observations. The potential for overfitting arises in such situations and may require careful consideration and the need for validation against independent datasets (Fienen et al., 2009). Notwithstanding, limited information is available for validation of the spatial pattern of K in the basin.

The simulation adequately represents the high conductivity observed around Medie in the south, representing the contact between the granites and rocks of the Togo Structural Unit in Layer 2. This range of values in the study agrees well with MODFLOW estimates of K by Yidana et al. (2014) in the basin; however, the spatial pattern in this study differs significantly, again pointing to the high uncertainty associated with the correct prediction of spatial hydraulic properties.



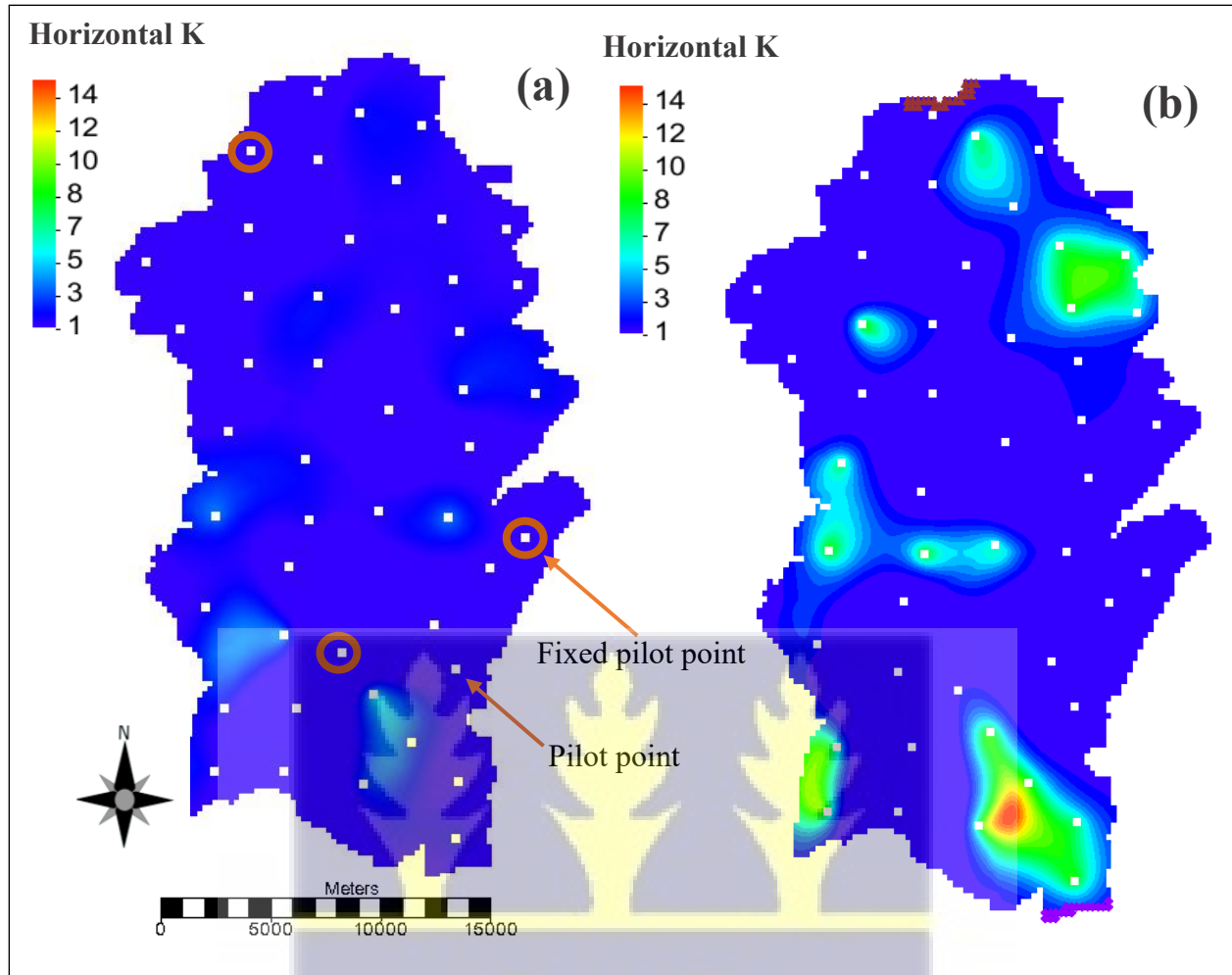


Figure 4.3: Horizontal hydraulic conductivity field for (a) Layer 1, and (b) Layer 2

4.3.3 Steady state groundwater flow

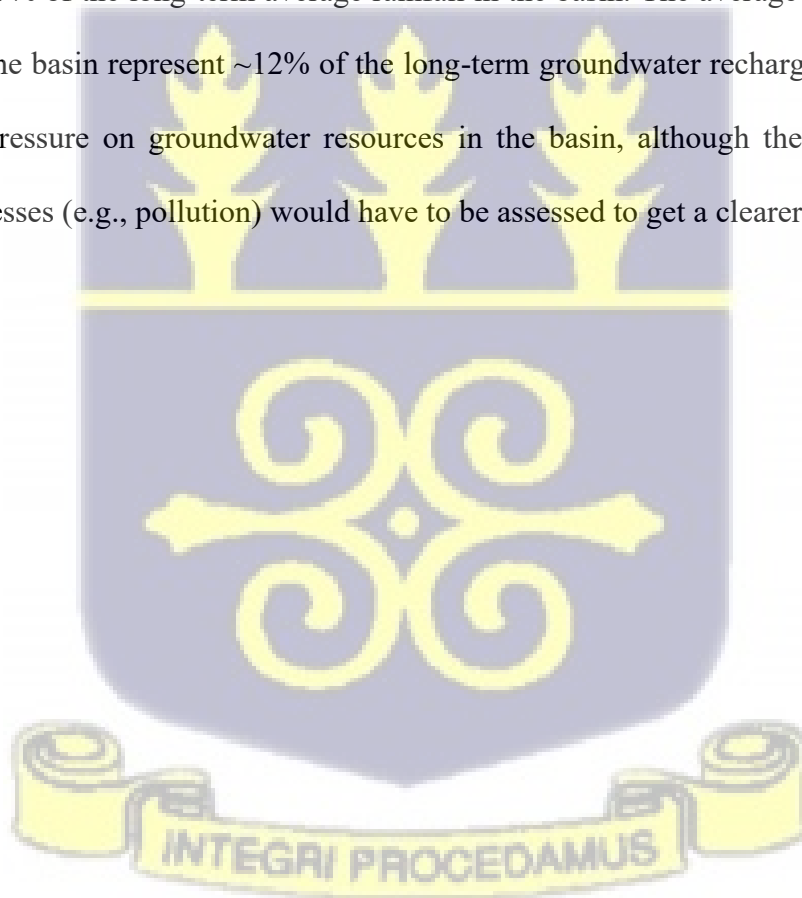
The steady state hydraulic head represents the long-term average groundwater head in the basin. The distribution and flow geometry of the hydraulic head for the basin for the calibrated steady-state model averaged over 2020 – 2023 periods are presented in Figure 4.4. The hydraulic head generally ranges from 0 - 400 m, reaching 630 m in the hills and high topographic areas in the northeast and northwest of the basin. The high hydraulic head locations are generally characterised

as recharge zones in the basin. This is corroborated by the weakly mineralised hydrochemistry of groundwater and recharge estimates in the basin in such locations.

The northern half of the entire basin presents heads between 250 and 630 m, whereas the low heads, between 0 – 120 m, are generally located in the southern half. Groundwater in the north displays a clear northwest –southeast flow pattern. This pattern appears to be dictated by the Atewa-Atwiredu hills in the northwest of the basin, a pattern in line with the flow directions of the Densu River (Figure 4.4b). Groundwater flow from the northern and north-eastern sections converges towards the middle section of the basin and flows southward. A general north-south flow pattern is observable in the basin, in tandem with the literature (Adomako, Gibrilla, et al., 2011; Alfa et al., 2011; Yidana et al., 2014; Akurugu et al., 2022) and the analysis of hydrochemistry in Chapter One. However, towards the middle and southern part of the basin, localised high hydraulic heads in the central, western, eastern, and southern parts, likely influenced by the topography, control some localised undefined flow paths. The general undefined flow patterns in the southern portions of the basin are also influenced by the flat-lying topography, where groundwater flow from one point to another, which is defined by the hydraulic gradient difference, is not significant. This suggests that groundwater flow in areas with relatively flat topography will most likely have relatively indistinctive flow patterns. Generally, the configuration of groundwater flow in the Densu River Basin mimics the topography as observed by several studies (Alfa et al., 2011; Yidana et al., 2014; Akurugu et al., 2022), and in line with the hydrogeological principle that groundwater levels are subdued replicas of the surface topography.

The model-computed water balance for the steady state period in the basin shows total inflow and outflow of about $153 \times 10^6 \text{ m}^3/\text{year}$, with an average difference of $1.28 \times 10^3 \text{ m}^3/\text{year}$ representing 0.0008 %. For a steady state model, the difference between the total inflow and outflow is balanced. Therefore, the marginal percent change in the difference suggests a small water balance error. There is a net inflow of $4.40 \times 10^6 \text{ m}^3/\text{year}$ of groundwater across the General Head Boundary into the basin. This suggests groundwater fluctuations in and at the boundary of the basin at the basin inlet favour net inflow.

The model estimates the average groundwater recharge over the basin as $85.61 \times 10^6 \text{ m}^3/\text{year}$, representing 2.69% of the long-term average rainfall in the basin. The average total groundwater abstractions in the basin represent ~12% of the long-term groundwater recharge. This suggests a relatively low pressure on groundwater resources in the basin, although the impacts of other hydrological stresses (e.g., pollution) would have to be assessed to get a clearer perspective.



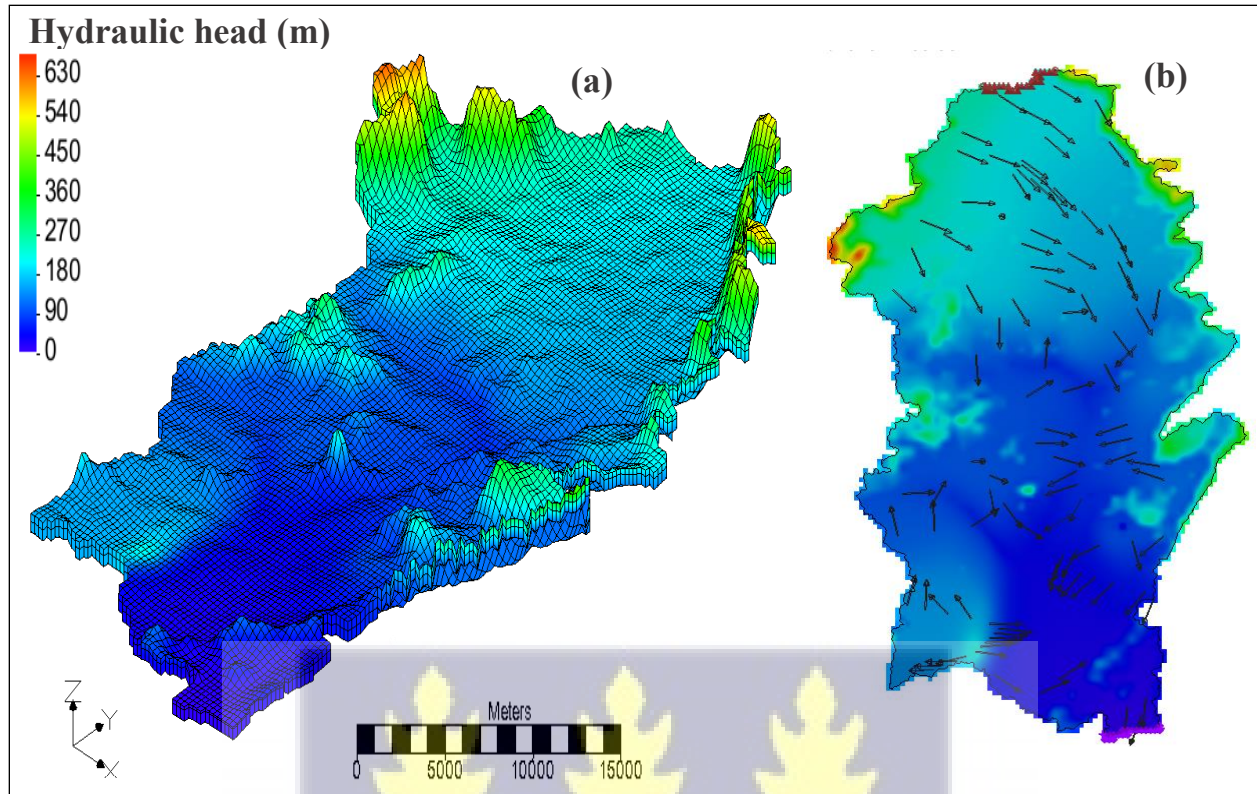


Figure 4.4: Steady state (a) model-computed 3D view and (b) flow patterns of groundwater hydraulic head

4.3.4 Transient state groundwater budget

The calibration period of 2020 – 2023 represents the baseline conditions for the simulations. The transient calibration involved parameterising storage parameters such as specific yield and specific storage, and conductance of the river bed and general head (Table 4.2). The calibration of the transient model yielded RMSE, MAE, and ME of 2.39 m, 1.65 m, and 0.20 m, suggesting a good model performance. The time series plots for the observed hydraulic heads and the model-simulated heads show a good match (Figure 4.5), also suggesting a well-calibrated transient groundwater flow model for the Densu River Basin.

The transient model was evaluated using hydraulic head records from eleven of the fourteen monitoring boreholes spanning July 2023 to April 2024. The evaluation period (07/2023 – 04/2024) presents performance statistics similar to the calibration period (06/2020 – 06/2023), with a slight elevation in the magnitudes (Table 4.3). The evaluation period presented smaller elevations in the RMSE and MAE by 0.06 and 0.05, and a larger increase in ME by 0.1. The deterioration in these performance statistics can be due to the reduction in the number of head observations from 14 to 11, and other uncertainty introduced by data from the evaluation period. The reduction in the number of observation boreholes was due to the unavailability of data in three boreholes (DB 10, DB 11, and DB 19) within the evaluation period. The slight differences in the evaluation statistics between the calibration and evaluation periods suggest the model is capable of fairly accurate predictions of hydraulic heads in the basin at locations where head observations are missing.

Analysis of the observed time series head data within the calibration period revealed a general declining trend in all monitored wells except at Suhum (DB 3) and Kojo Ashong (DB 7), which recorded rising trends. The observed declining trend in groundwater levels in the basin is in line with the observed declining trend in rainfall amounts and consequently groundwater recharge in the basin over the same period in the Densu River Basin (Figures 4.5 & 4.6).



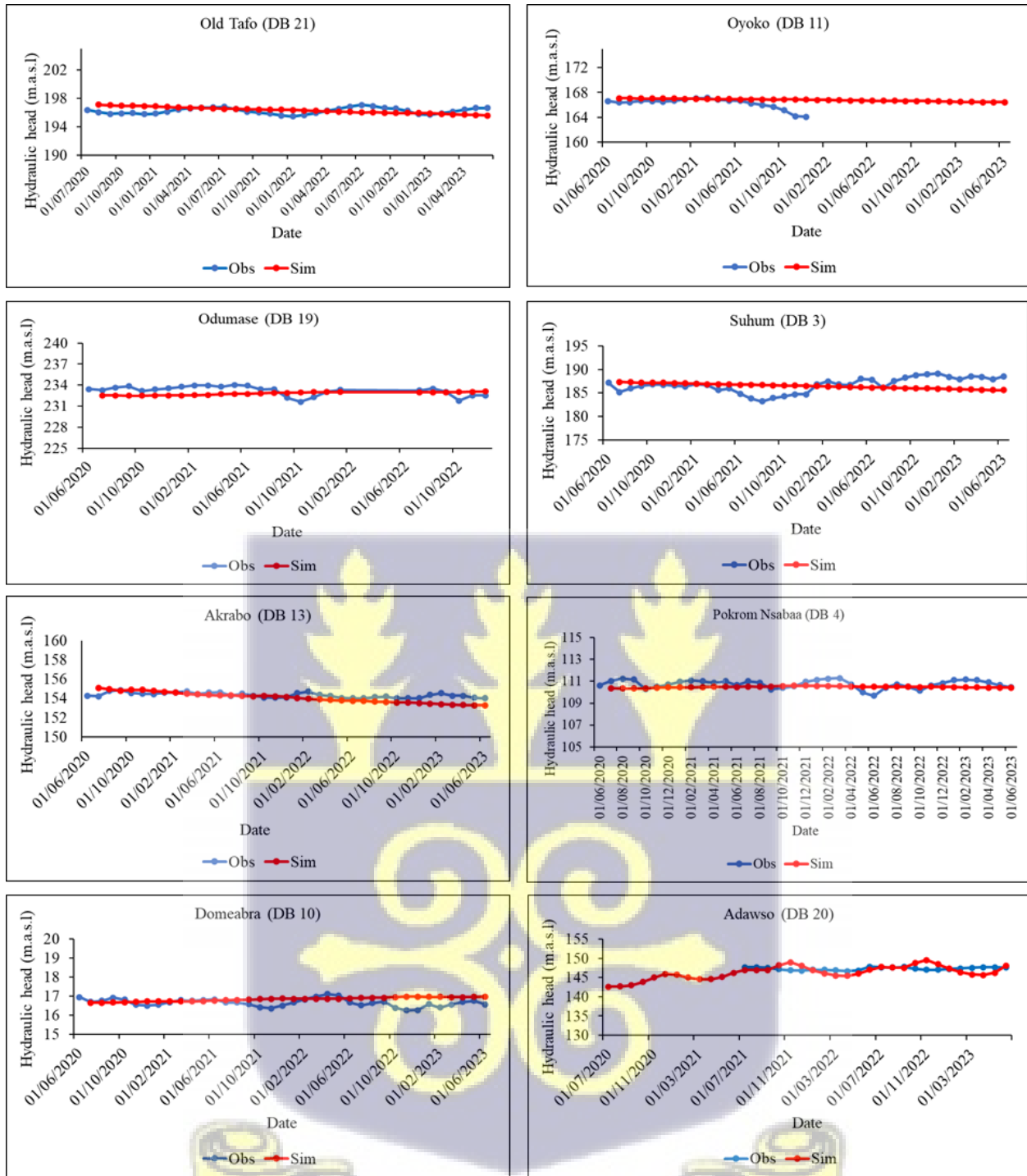


Figure 4.5: Time series plot of model-computed and observed hydraulic data for the transient period

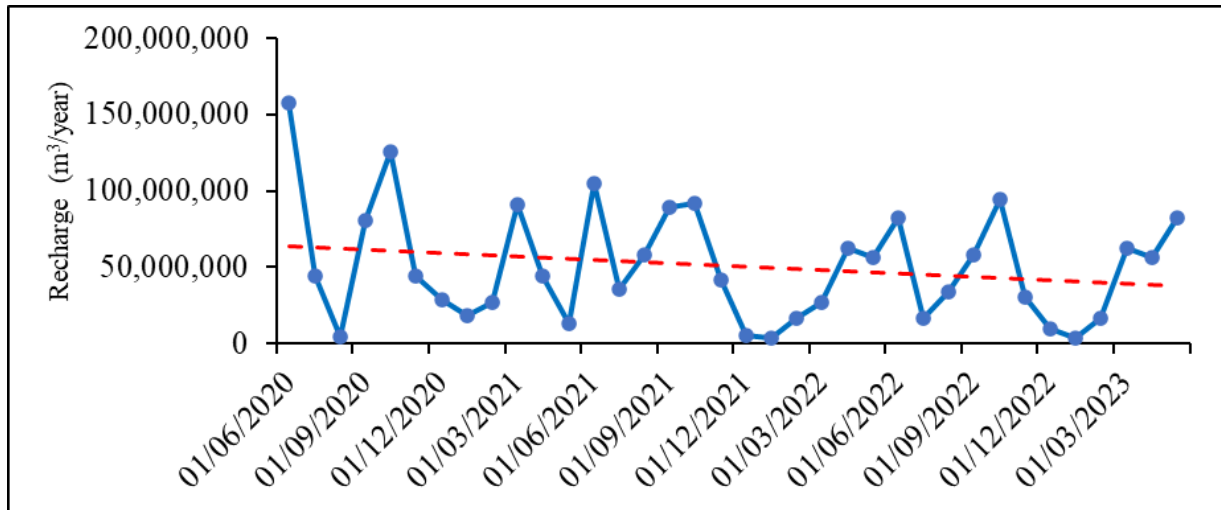


Figure 4.6: Time series plot of average groundwater recharge in the basin

The computed water balance for the transient period in the basin shows a total inflow of about $216 \times 10^6 \text{ m}^3/\text{year}$ and total outflow of $216 \times 10^6 \text{ m}^3/\text{year}$. Groundwater recharge through rainfall constitutes about 72%, and ranges from 3×10^6 and $158 \times 10^6 \text{ m}^3/\text{year}$. Flow from inter-basin exchanges through the General Head boundary constitutes about 1.3% of the total inflow into the basin (Table 4.4). The Specified Head boundary, where assigned heads are simulated as moving in or out of the aquifer at a rate adequate to maintain the head specified, simulated a total outflow of $3 \times 10^6 \text{ m}^3/\text{year}$. Within the transient period, the groundwater system experiences a net loss of $168 \text{ m}^3/\text{year}$, which represents 0.000077% of the total inflow (Table 4.4). The net loss is probably due to the declining rainfall pattern and the corresponding decline in groundwater levels. The transient period recorded a relatively high groundwater recharge rate, peaking at $158 \times 10^6 \text{ m}^3/\text{year}$, which explains the higher total inflows and outflows as compared to the steady state model.

The simulated groundwater contribution to total streamflow estimated by the model over the transient period was approximately $202 \times 10^6 \text{ m}^3/\text{year}$, representing a basin recharge rate of 80

mm/year, which is highly comparable with recharge estimates by the baseflow filter methods (Table 4.1). The total average streamflow from the gauge station at Ashaladja, according to analysis of historical records, is approximately $12.98 \text{ m}^3/\text{s}$, which translates into $409 \times 10^6 \text{ m}^3/\text{year}$. Therefore, the ratio of baseflow estimated by the model to total observed stream flow is approximately 49%. However, the gauge at Ashaladja does not capture the total outflow from the basin since the gauge is not located at the basin outlet. Therefore, the assumption is that the total discharge from the basin will be higher than that recorded at Ashaladja. As a result, the ratio may actually vary slightly from 49%. The ratio of baseflow to streamflow in this study falls well within ranges (30 – 60%) in the literature for arid and semi-arid regions (Hamel et al., 2013; Aboelnour et al., 2020), as rainfall in these areas are dictated by episodic events.

Table 4.4: Transient groundwater budget over the 2020 – 2023 period

Sources/Sinks	Flow In ($\times 10^6 \text{ m}^3/\text{year}$)	Flow Out ($\times 10^6 \text{ m}^3/\text{year}$)	Difference (m^3/year)	Difference (%)
Constant Head	0	-3.1		
Wells	0	-10.8		
River Leakage	55.4	-202.3		
Head Dep. Bounds	3.0	-0.058		
Recharge	157.8	0		
Total	216.2	-216.2	-168	-0.000077

4.3.5 Scenario analysis

The highly parameterised model was converted to a forward run by importing the optimal hydraulic parameter values estimated by the PEST model. The forward model was then used to

simulate various scenarios for the purposes of assessing the impacts of various developmental pathways. The scenarios run in this study represent the critical drivers and stresses envisioned to significantly impact groundwater resources in the basin. Given that climate models inherently yield diverse outcomes, and predictions of future abstractions are bedevilled with uncertainties, their incorporation extends the associated uncertainties in the scenarios run herein.

The first scenario involved maintaining groundwater recharge at the current rate and increasing abstraction at a rate commensurate with the population growth rate of 3.6% over twenty years from the baseline. Simulation of this scenario resulted in a steady increase in abstraction from 10.8×10^6 m³/year to 24.5×10^6 m³/year, representing an increase of about 127% from the baseline amount. The increase in groundwater abstraction by this rate over the 20 years constitutes ~ 16% of the baseline annual groundwater recharge in the basin. The increased abstraction over this period contributes to falling hydraulic heads in the basin and a consequential reduction in the contribution of groundwater to the rivers in the basin (Table 4.4). Simulation of this scenario suggests a reduced groundwater contribution to the stream network by 8% and a reduction in total stream discharge from the basin by 29% of the baseline conditions. This reduction has the potential to negatively impact groundwater-dependent ecosystems and wells tapping from shallow aquifers. The rate of reduction in the groundwater head in response to the enhanced abstractions was, however, shown by the model to have minimal effect on the distribution of the hydraulic head and flow pattern.

The second scenario coupled the first scenario of enhanced annual groundwater abstraction by 3.6% of the baseline rate, with projected changes in precipitation as predicted by two downscaled and bias-corrected climate models: HadGEM2-RCA4 (Collins et al., 2008) and MIROC5-RCA4 (Watanabe et al., 2010) under the RCP8.5 scenario. The two projections present the wettest

(MIROC5) and driest (HadGEM2-ES) future (2023-2043) precipitation projections for the basin out of a 26-climate model ensemble. The HadGEM2-ES model projects precipitation reduction in the southern half of the basin by up to 17% and an increase by up to 35% especially in the northern parts of the basin. The MIROC5 model, on the other hand, projects a much wetter precipitation regime which will increase between 24% and 63% from the baseline period.

Simulation of the relatively dry projection (HadGEM2-ES) revealed a declining trend in groundwater recharge over the period (Figure 4.7), leading to a small decrease in the overall groundwater recharge by 0.026% from the baseline to the future period. Groundwater abstraction within this period constitutes ~7% of the recharge, suggesting better groundwater resources relative to the first scenario. Average groundwater recharge in the HadGEM2-ES projection period decreased from a range of $14 - 263 \times 10^6 \text{ m}^3/\text{year}$ to $4 - 438 \times 10^6 \text{ m}^3/\text{year}$. Groundwater contribution to the stream network as baseflow in the first scenario with HadGEM2-ES projections (scenario two) generally suggests similar trends, reducing by 8% and 21% respectively from the baseline amounts. Simulation of the wetter future (MIROC5), on the other hand, suggests an increase in groundwater resources and gradual accumulation in groundwater recharge (Figure 4.7) in contrast to the drier climate model, and relatively large volumes of baseflow, with an increase of about 32% from the baseline period. The increase in groundwater flows in streams is a function of the appreciation in the water table depths across the basin.



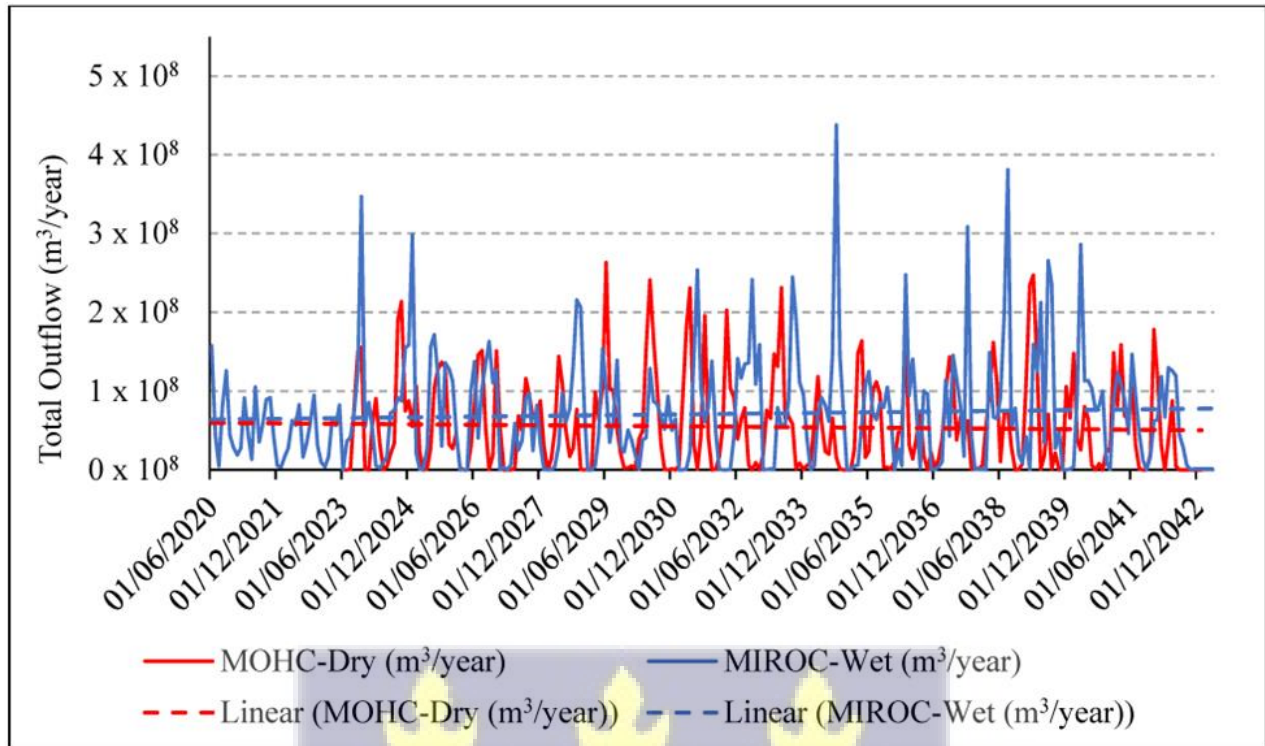


Figure 4.7: Groundwater recharge trend for the wet (MIROC5) and dry (HadGEM2-ES) precipitation projections

4.3.6 Conclusion

In this study, a new conceptual hydrogeology of the fractured bedrock system for the Densu River Basin in southwestern Ghana, consisting of two layers, was developed based on reviewed and new field data. The conceptual model was converted to a 3D numerical groundwater flow model and calibrated under steady state and transient conditions. The calibrated model was used to assess scenarios of abstraction and recharge stresses caused by population growth and projected climate change impacts on rainfall.

The results revealed hydraulic head ranges of less than one to 400 m, and reaching 630 m in high topographic areas, with the northern half of the basin presenting higher hydraulic heads. A

northeast–northwest groundwater flow pattern is observable in the north, which converges in the middle and flows southward, in consonance with the literature. On average, horizontal hydraulic conductivity ranges between 0 – 4 m/d, reaching 15 m/day, which occurs as patches in the basin, depicting the complex nature and occurrence of fracturing and permeability in the basin. The computed water balance for the transient period in the basin shows that the groundwater system experiences a net loss of 264 m³/year over the transient period, which may be the reason for the decline in water levels in the observation boreholes. The model also reveals the groundwater system discharges a net of approximately 202 x 10⁶ m³/year through the river network ending as runoff from the basin.

Scenario analysis revealed the groundwater system could sustain the cumulative effect of enhanced abstraction caused by population growth and the attendant water demand by 3.6 % per annum over twenty years, at the current recharge rate, without any significant impacts on the water levels and flow patterns. The increased abstraction over the 20 years constituted about 16% of the current groundwater recharge amount and also resulted in a reduction in groundwater contribution to the stream network by 8%, which could pose a threat to shallow aquifers and groundwater-dependent ecosystems.

Simulation of the second scenario; enhanced abstraction combined with climate change (reduced and enhanced groundwater recharge) revealed a slight decline in stream discharge, hydraulic head, and groundwater recharge for the second scenario in the basin, whereas the Wet condition scenario suggested accumulation of groundwater volumes and substantial groundwater contribution to the stream network in the basin.

CHAPTER FIVE

CONCLUSIONS AND RECOMMENDATIONS

5.1 Summary of main findings

This research thoroughly examined the multifaceted and complex nature of aquifer characterisation and 3D numerical groundwater flow modelling to assess the general hydrogeology of the Densu River Basin. A combination of field investigations, laboratory analyses, and advanced 3D numerical groundwater flow simulations provides deeper insights into groundwater recharge, general hydrogeological characteristics, hydrochemistry, and impacts of various water demands and recharge scenarios, aimed at providing a better understanding for improved water management in the basin.

Three methods for quantifying diffuse groundwater recharge, CMB, WTF, and BFF, revealed average values of 38 mm/year, 150 mm/year, and 80 mm/year, respectively, representing 3%, 15%, and 7%. The study revealed recharge estimates from the WTF and BFF techniques are highly comparable in the lower limits, whereas the CMB and WTF estimates compared well on the upper limits. As such, the overall recharge in the basin falls well within these limits and ranges from 27 - 338 mm/year, representing 4 – 28% of the average annual rainfall, with a catchment average value of ~ 15% of the average annual rainfall. High recharge in the basin occurs in the northern and high-elevation areas, whereas the south and low-elevation areas receive relatively small recharge amounts. Although the major rainy season peaks around May/June in the basin, the

highest groundwater recharge occurs in the peak of the minor rainy season in October, which is attributable to the 2.5-month lag time between rainfall and recharge.

Assessment of essential aquifer parameters, borehole logs, and hydrochemical data also revealed average thicknesses of 6 m and 32 m, respectively for the saprolite and saprock, which overlie the fractured bedrock. A cross-section through the basin shows the extreme north to have a higher weathered zone thickness, especially in rocks of the Birimian and Voltaian Supergroups, and thinnest in the central sections in the granites, with the bedrock outcropping variously. Several cases of slightly fractured to unfractured rocks which overlie the fractured bedrock in most parts of the basin suggest the presence of unconfined to semi-confined aquifers across the basin, with the main water-bearing zones stretching about 3 m thick. The recharge zones in the basins are largely characterised by weakly mineralised Na/Ca-HCO₃ water types, probably resulting from silicate mineral dissolution of amorphous silica, albite, anorthite, etc., which metamorphose into highly mineralised Na-Cl water types in the discharge zones as the basin discharges into the ocean. Mineral stability diagrams also revealed that the groundwater is stable in the kaolinite field, and probably at its intermediate stage of evolution in the hard rock terrain, where the clay mineral kaolinite provides a large surface area for significant ion exchange in the aquifer systems. Generally, the groundwater is physicochemically potable except in a few places where low pH and elevated Cl⁻, Na⁺, Fe, and F⁻ levels render the water unsuitable for drinking. The recharge and transition zones in the groundwater flow regime present the best water quality compared to the discharge zones.

Based on the recharge estimations and aquifer characterisation through the hydrogeochemical analysis described above, a new conceptual hydrogeology of the fractured bedrock system for the

basin consisting of two layers was developed. The conceptual model was converted to a 3D numerical groundwater flow model and calibrated under steady state and transient conditions. The results revealed hydraulic head ranges of less than one to 400 m, and reaching 630 m in high topographic areas, with the northern half of the basin presenting higher hydraulic heads. A northwest–northeast groundwater flow pattern is observable in the north, which converges in the middle and flows southward, in consonance with the literature. On average, horizontal hydraulic conductivity ranges between 0 – 4 m/d, reaching 15 m/day, which occurs as patches in the basin, depicting the complex nature and occurrence of fracturing and permeability in the basin.

The model-computed water balance shows the groundwater system experiences a net loss of 264 m³/year over the transient period, which may be the reason for the decline in water levels in the observation boreholes. The model also reveals that the groundwater system loses a net of approximately 202 x 10⁶ m³/year through the river network as discharge from the basin. Scenario analysis revealed the groundwater system could sustain the cumulative effect of enhanced abstraction caused by population growth and the attendant water demand by 3.6 % per annum over twenty years, at the current recharge rate, without any significant impacts on the water levels and flow patterns. The increased abstraction over the 20 years constituted about 16% of the current groundwater recharge amount and also resulted in a reduction in groundwater contribution to the stream network by 8% which could have negative implications for shallow aquifers and groundwater-dependent ecosystems.

Simulation of the second scenario; enhanced abstraction amidst reduced and enhanced groundwater recharge revealed a slight decline in stream discharge, hydraulic head, and groundwater recharge for the dry condition scenario in the basin, whereas the wet condition

scenario suggested a large accumulation of groundwater volumes and substantial groundwater contribution to the stream network in the basin. Hence, enhanced abstractions beyond the cumulative 3.6% per annum or at the same rate beyond 20 years under conditions of reduced recharge could significantly affect groundwater availability and levels.

5.2 Scientific contribution and study limitations

The approach of using multiple groundwater recharge estimation methods in this study demonstrates the importance of multiple recharge methods. The inherent weakness of the CMB, WTF and BFF methods is better understood, and the accuracy of estimates is improved by this approach. The lower limits of the CMB estimates in the basin could be disregarded because of the likely influence of chloride dissolution, seawater intrusion and sea spray; however, the BFF and WTF methods provide reliable lower limit estimates in the basin. Similarly, the upper limit estimates from the BFF, which may be considered as subdued recharge estimates, are put in proper context by the upper limit estimates from the CMB and WTF methods. These considerations put recharge estimation in the study area, especially a coastal basin, into proper perspective. Also, integrating hydrogeological and hydrochemical data with the recharge estimates in this study to create a conceptual model of the aquifer system provides a holistic understanding of the basin essential for accurate numerical modelling. Calibration of the model, using fixed pilot points at locations with known K values, proved effective in reducing the model uncertainty and on computing resources, as opposed to freeing all the pilot points. However, this assertion is specific to this study, and may be tested variously, especially where the geology differs, to ascertain the reliability of this process. The study provides a better understanding of the hydrogeological characteristics of the basin and the plausible consequences of various development pathways.

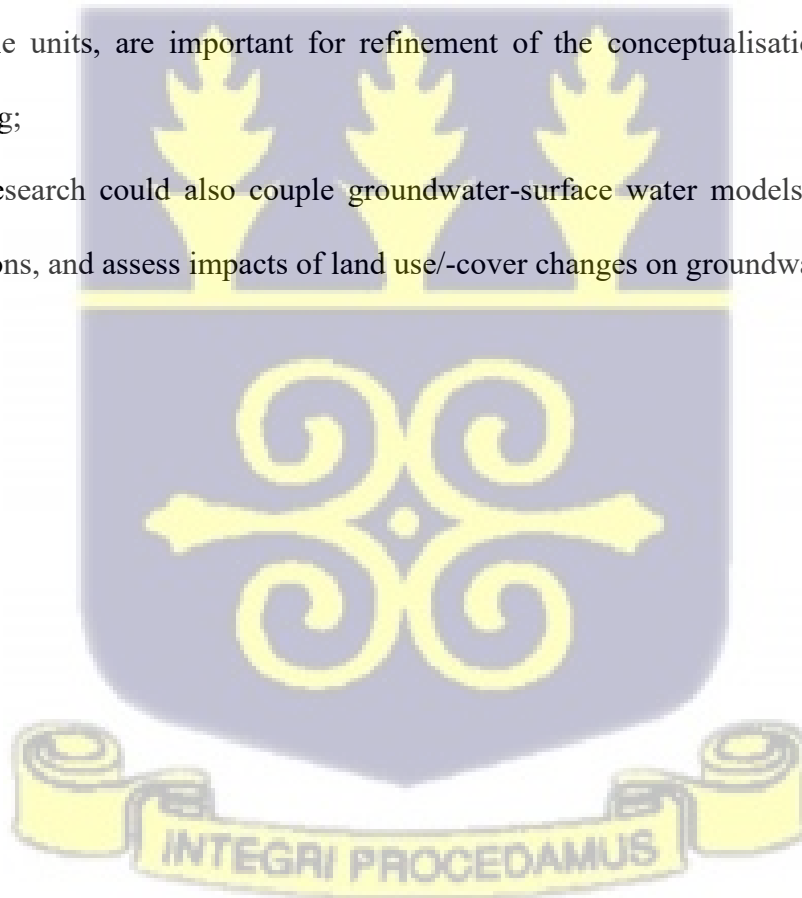
The limitations in this study include uncertainties associated with the spatial distribution of recharge and K , and proper conceptualisation of the lateral boundary conditions, which are key components of the model, since no independent data exist for validation purposes. Another major limitation was the limited number of 14 observation points, which were practically used in the calibration to interpolate hydraulic heads across the entire basin. Also, the impact of land use/-cover changes, which have a direct impact on groundwater recharge, was not considered, as groundwater models are constrained in that respect.

5.2 Recommendations

Following revelations from this research, the following recommendations must be considered for enhancing the understanding of the hydrogeology of the basin and for sustainable utilisation of the groundwater resources in the basin:

- ❖ Anthropogenic activities and disposal of municipal wastes in the areas identified as recharge zones in this study should be minimised to protect the quality of groundwater in the basin;
- ❖ Aligning large groundwater abstractions with the minor rainy season in October, a period of significant recharge, can improve water availability, lessen environmental stress, and promote sustainable resource management, provided local aquifer conditions could sustain it;
- ❖ Incorporation of numerical models into groundwater management tools with climate projections for better forecasting of groundwater availability and use by water resource managers;

- ❖ Enhanced documentation of groundwater abstractions in the basin for better understanding of the demand versus availability of the resource amidst other stresses;
- ❖ Depth-specific and continuous monitoring of groundwater levels for a proper understanding of the various aquifer systems and establishment of a quality monitoring program for real-time assessment for early detection of contamination events;
- ❖ Policy makers are advised to incorporate the findings of this research into the basin water management plans, balancing conservation and development.
- ❖ Further detailed investigations into the lithostratigraphy of the basin, especially the spatial variability in weathered zone thickness, aquifer geometry, and the lateral continuity of permeable units, are important for refinement of the conceptualisation and numerical modelling;
- ❖ Future research could also couple groundwater-surface water models to simulate their interactions, and assess impacts of land use/-cover changes on groundwater resources



REFERENCES

- Abanyie, S. K., Sunkari, E. D., Apea, O. B., Abagale, S., & Korboe, H. M. (2020). Assessment of the quality of water resources in the Upper East Region, Ghana: A review. *Sustainable Water Resources Management*, 6(4), 52. <https://doi.org/10.1007/s40899-020-00409-4>.
- Abbasnia, A., Radfard, M., Mahvi, A. H., Nabizadeh, R., Yousefi, M., Soleimani, H., & Alimohammadi, M. (2018). Groundwater quality assessment for irrigation purposes based on irrigation water quality index and its zoning with GIS in the villages of Chabahar, Sistan and Baluchistan, Iran. *Data in Brief*, 19, 623–631.
- Abbott, M. B., Bathurst, J. C., Cunge, J. A., O'Connell, P. E., & Rasmussen, J. (1986). An introduction to the European Hydrological System—Systeme Hydrologique Europeen, “SHE”, 1: History and philosophy of a physically-based, distributed modelling system. *Journal of Hydrology*, 87(1–2), 45–59.
- Aboelnour, M., Gitau, M. W., & Engel, B. A. (2020). A comparison of streamflow and baseflow responses to land-use change and the variation in climate parameters using SWAT. *Water*, 12(1), 191.
- Aboukarima, A. M., Al-Sulaiman, M. A., & El Marazky, M. S. (2018). Effect of sodium adsorption ratio and electric conductivity of the applied water on infiltration in a sandy-loam soil. *Water Sa*, 44(1), 105–110.
- Adhikari, R. K., Yilmaz, A. G., Mainali, B., Dyson, P., & Imteaz, M. A. (2022). Methods of Groundwater Recharge Estimation under Climate Change: A Review. *Sustainability*, 14(23), 15619.

- Adomako, D., Gibrilla, A., Akiti, T., Fianko, J. R., & Maloszewski, P. (2011a). Hydrogeochemical Evolution and Groundwater Flow in the Densu River Basin, Ghana. *Journal of Water Resource and Protection*, 03. <https://doi.org/10.4236/jwarp.2011.37065>.
- Adomako, D., Osae, S., Akiti, T. T., Faye, S., & Maloszewski, P. (2010). Geochemical and isotopic studies of groundwater conditions in the Densu River Basin of Ghana. *Environmental Earth Sciences*, 62(5), 1071–1084. <https://doi.org/10.1007/s12665-010-0595-2>.
- Adomako, D., Osae, S., Akiti, T. T., Faye, S., & Maloszewski, P. (2011b). Geochemical and isotopic studies of groundwater conditions in the Densu River Basin of Ghana. *Environmental Earth Sciences*, 62(5), 1071–1084. <https://doi.org/10.1007/s12665-010-0595-2>.
- Afrifa, G. Y., Chegbeleh, L. P., Sakyi, P. A., Yidana, S. M., Loh, Y. A. S., Ansah-Narh, T., & Manu, E. (2022). Quantifying nitrate pollution sources and natural background in an equatorial context: A case of the Densu Basin, Ghana. *Hydrological Sciences Journal*, 67(13), 1941–1953.
- Agodzo, S. K., Bessah, E., & Nyatuame, M. (2023). A review of the water resources of Ghana in a changing climate and anthropogenic stresses. *Frontiers in Water*, 4, 973825.
- Agyemang, V. O. (2025). Groundwater resources development for a sustainable water supply in developing countries: A case study of Ghana. *Cleaner Water*, 100104.
- Akisanmi, P. (2022). *Classification of Clay Minerals*. IntechOpen: London, UK.

- Akpataku, K. V., Rai, S. P., Gnazou, M. D.-T., Tampo, L., Bawa, L. M., Djaneye-Boundjou, G., & Faye, S. (2019). Hydrochemical and isotopic characterization of groundwater in the southeastern part of the Plateaux Region, Togo. *Hydrological Sciences Journal*, 64(8), 983–1000.
- Akurugu, B. A., Chegbeleh, L. P., & Yidana, S. M. (2020). Characterisation of groundwater flow and recharge in crystalline basement rocks in the Talensi district, Northern Ghana. *Journal of African Earth Sciences*, 161, 103665.
- Akurugu, B. A., Obuobie, E., Yidana, S. M., Stisen, S., Seidenfaden, I. K., & Chegbeleh, L. P. (2022). Groundwater resources assessment in the Densu Basin: A review. *Journal of Hydrology: Regional Studies*, 40, 101017. <https://doi.org/10.1016/j.ejrh.2022.101017>.
- Alfa, B. (2010). Distributed numerical modelling of hydrological/hydrogeological processes in the Densu Basin. University of Ghana.
- Alfa, B., Hasholt, B., Jørgensen, N., & Banoeng-Yakubo, B. (2011). Rainfall and Water Resources of a Coastal Basin of Ghana. *Journal of Hydrologic Engineering*, 16, 316–323. [https://doi.org/10.1061/\(ASCE\)HE.1943-5584.0000314](https://doi.org/10.1061/(ASCE)HE.1943-5584.0000314).
- Ali, M. H., Zaman, M. H., Biswas, P., Islam, M. A., & Karim, N. N. (2022). Estimating hydraulic conductivity, transmissibility and specific yield of aquifer in Barind Area, Bangladesh using pumping test. *European Journal of Environment and Earth Sciences*, 3(4), 90–96.

- Amer, R. (2021). Spatial Relationship between Irrigation Water Salinity, Waterlogging, and Cropland Degradation in the Arid and Semi-Arid Environments. *Remote Sensing*, 13(6), 1047.
- Amoako, J., Karikari, A. Y., Ansa-Asare, O. D., & Adu-Ofori, E. (2010). Water quality characteristics of Densu River basin in south-east Ghana. *Water Science and Technology*, 61(6), 1467–1477.
- Anderson, M. P., Woessner, W. W., & Hunt, R. J. (2015). *Applied groundwater modeling: Simulation of flow and advective transport (Second edition)*. Academic Press.
- Anduaem, T. G., Demeke, G. G., Ahmed, I., Dar, M. A., & Yibeltal, M. (2021). Groundwater recharge estimation using empirical methods from rainfall and streamflow records. *Journal of Hydrology: Regional Studies*, 37, 100917.
- APHA. (1995). *Standard methods for the examination of water and waste water*. American Journal of Public Health and the Nations FHealth, 56(3), 387–388.
- Appelo, C. A. J., & Postma, D. (2005). *Geochemistry, groundwater and pollution*. CRC press.
- Asare-Nuamah, P., & Botchway, E. (2019). Understanding climate variability and change: Analysis of temperature and rainfall across agroecological zones in Ghana. *Heliyon*, 5(10). [https://www.cell.com/heliyon/pdf/S2405-8440\(19\)36314-5.pdf](https://www.cell.com/heliyon/pdf/S2405-8440(19)36314-5.pdf).
- Atampugre, G., Nursey-Bray, M., & Adade, R. (2019). Using geospatial techniques to assess climate risks in savannah agroecological systems. *Remote Sensing Applications: Society and Environment*, 14, 100–107.

- Ayanlade, A., Oluwaranti, A., Ayanlade, O. S., Borderon, M., Sterly, H., Sakdapolrak, P., Jegede, M. O., Weldemariam, L. F., & Ayinde, A. F. (2022). Extreme climate events in sub-Saharan Africa: A call for improving agricultural technology transfer to enhance adaptive capacity. *Climate Services*, 27, 100311.
- Bam, E. K., Akiti, T. T., Osae, S., Ganyaglo, S. Y., Adomako, D., Gibrilla, A. A., Ahialey, E., & Ayanu, G. (2011). Major ions and trace elements partitioning in unsaturated zone profile of the Densu River Basin, Ghana and the implications for groundwater. *Afr J Environ Sci Technol*, 5(6), 427–436.
- Banoeng-Yakubu, B., Yidana, S. M., Ajayi, J. O., Loh, Y., & Aseidu, D. (2011). Hydrogeology and groundwater resources of Ghana: A review of the hydrogeology and hydrochemistry of Ghana. *Potable Water and Sanitation*, 142.
- Bayou, W. T., Wohnlich, S., Mohammed, M., & Ayenew, T. (2021). Application of hydrograph analysis techniques for estimating groundwater contribution in the Sor and Gebba streams of the Baro-Akobo river Basin, southwestern Ethiopia. *Water*, 13(15), 2006.
- Belhassan, K. (2022). *Water scarcity management in the Maghreb Region*.
- Blatt, H., Tracy, R., & Owens, B. (2006). *Petrology: Igneous, sedimentary, and metamorphic*. Macmillan.
- Bloomfield, J. P., Lewis, M. A., Newell, A. J., Loveless, S. E., & Stuart, M. E. (2020). Characterising variations in the salinity of deep groundwater systems: A case study from Great Britain (GB). *Journal of Hydrology: Regional Studies*, 28, 100684.

Brunner, P., & Simmons, C. T. (2012). HydroGeoSphere: A fully integrated, physically based hydrogeological model. *Ground Water*, 50(2), 170–176.

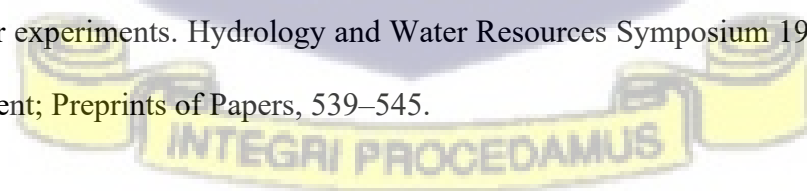
Burghof, S., Gabiri, G., Stumpp, C., Chesnaux, R., & Reichert, B. (2018). Development of a hydrogeological conceptual wetland model in the data-scarce north-eastern region of Kilombero Valley, Tanzania. *Hydrogeology Journal*, 26(1), 267–284.
<https://doi.org/10.1007/s10040-017-1649-2>

Canul-Macario, C., Salles, P., Hernández-Espriú, A., & Pacheco-Castro, R. (2021). Numerical modelling of the saline interface in coastal karstic aquifers within a conceptual model uncertainty framework. *Hydrogeology Journal*, 29(7), 2347–2362.
<https://doi.org/10.1007/s10040-021-02379-z>.

Carrard, N., Foster, T., & Willetts, J. (2019). Groundwater as a Source of Drinking Water in Southeast Asia and the Pacific: A Multi-Country Review of Current Reliance and Resource Concerns. *Water*, 11(8), Article 8. <https://doi.org/10.3390/w11081605>.

Chakraborty, M., Tejankar, A., Coppola, G., & Chakraborty, S. (2022). Assessment of groundwater quality using statistical methods: A case study. *Arabian Journal of Geosciences*, 15(12), 1136.

Chapman, T. G., & Maxwell, A. I. (1996). Baseflow separation-comparison of numerical methods with tracer experiments. *Hydrology and Water Resources Symposium 1996: Water and the Environment; Preprints of Papers*, 539–545.



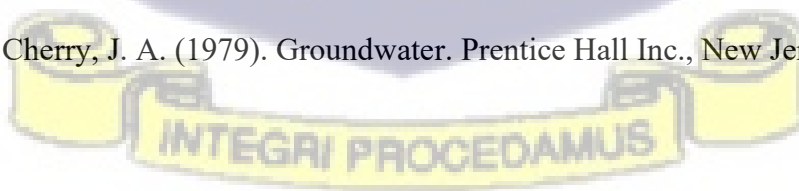
- Chegbeleh, L. P., Akurugu, B. A., & Yidana, S. M. (2020). Assessment of groundwater quality in the Talensi District, Northern Ghana. *The Scientific World Journal*, 2020.
- Chemingui, A., Sulis, M., & Paniconi, C. (2015). An assessment of recharge estimates from stream and well data and from a coupled surface-water/groundwater model for the des Anglais catchment, Quebec (Canada). *Hydrogeology Journal*, 23(8), 1731.
- Chen, J. S., Desai, D. A., Heyns, S. P., & Pietra, F. (2019). Literature review of numerical simulation and optimisation of the shot peening process. *Advances in Mechanical Engineering*, 11(3), 168781401881827. <https://doi.org/10.1177/1687814018818277>.
- Chen, S., & Gui, H. (2021). Calculating groundwater mixing ratios in multi-aquifers based on statistical methods: A case study. *Water Practice and Technology*, 16(2), 621–632.
- Chen, W.-P., & Lee, C.-H. (2003). Estimating ground-water recharge from streamflow records. *Environmental Geology*, 44, 257–265.
- Chen, X., Chen, Y. D., & Zhang, Z. (2007). A Numerical Modeling System of the Hydrological Cycle for Estimation of Water Fluxes in the Huaihe River Plain Region, China. *Journal of Hydrometeorology*, 8(4), 702–714. <https://doi.org/10.1175/JHM604.1>.
- Clarke, R., Lawrence, A., & Foster, S. (1996). *Groundwater: A threatened resource*. United Nations Environment Programme.
- Cloutier, V., Lefebvre, R., Therrien, R., & Savard, M. M. (2008). Multivariate statistical analysis of geochemical data as indicative of the hydrogeochemical evolution of groundwater in a sedimentary rock aquifer system. *Journal of Hydrology*, 353(3–4), 294–313.

- Collins, W. J., Bellouin, N., Doutriaux-Boucher, M., Gedney, N., Hinton, T., Jones, C. D., Liddicoat, S., Martin, G., O'Connor, F., & Rae, J. (2008). Evaluation of the HadGEM2 model (Vol. 74). Met Office Exeter, UK. https://www.inscc.utah.edu/~reichler/publications/papers/Collins_08_MetOffice_74.pdf
- Cook, P. G. (2003). A guide to regional groundwater flow in fractured rock aquifers. <https://ds.amu.edu.et/xmlui/bitstream/handle/123456789/8976/Guide%20to%20Regional%20Groundwater%20Flow%20in%20Fractured%20R.pdf?sequence=1&isAllowed=y>.
- Cooley, R. L. (1979). A method of estimating parameters and assessing reliability for models of steady state Groundwater flow: 2. Application of statistical analysis. *Water Resources Research*, 15(3), 603–617. <https://doi.org/10.1029/WR015i003p00603>.
- Cooper, H. H., & Jacob, C. E. (1946). A generalized graphical method for evaluating formation constants and summarizing well-field history. *Eos, Transactions American Geophysical Union*, 27(4), 526–534.
- Crosbie, R. S., & Rachakonda, P. K. (2021). Constraining probabilistic chloride mass-balance recharge estimates using baseflow and remotely sensed evapotranspiration: The Cambrian Limestone Aquifer in northern Australia. *Hydrogeology Journal*, 29(4), 1399–1419.
- Dapaah-Siakwan, S., & Gyau-Boakye, P. (2000). Hydrogeologic framework and borehole yields in Ghana. *Hydrogeology Journal*, 8(4), 405–416.
- Darko, P. K., Duah, A. A., & Dapaah-Siakwan, S. (2003). Groundwater Assessment: An Element of Integrated Water Resources Management – The Case of Densu River Basin. CSIR-Water Research Institute, WRI/CAR No. 54.

- Darko, P. K., & Krásny, J. (2007). Regional transmissivity distribution and groundwater potential in hard rock of Ghana. In *Groundwater in fractured rocks* (pp. 125–136). CRC Press. <https://www.taylorfrancis.com/chapters/edit/10.1201/9780203945650-13/regional-transmissivity-distribution-groundwater-potential-hard-rock-ghana-philip-darko-jir%CB%87%C3%AD-kr%C3%A1sny%C2%B4>.
- De Biase, M., Chidichimo, F., Maiolo, M., & Micallef, A. (2021). The impact of predicted climate change on groundwater resources in a mediterranean archipelago: A modelling study of the Maltese Islands. *Water*, 13(21), 3046.
- de Ruiter, L., Gunnæs, A. E., Dysthe, D. K., & Austrheim, H. (2021). Quartz dissolution associated with magnesium silicate hydrate cement precipitation. *Solid Earth*, 12(2), 389–404.
- De Vries, J., & Simmers, I. (2002). Groundwater recharge: An overview of process and challenges. *Hydrogeology Journal*, 10, 5–17. <https://doi.org/10.1007/s10040-001-0171-7>.
- Delin, G., Healy, R., Lorenz, D., & Nimmo, J. (2007). Comparison of local- to regional-scale estimates of ground-water recharge in Minnesota, USA. *Journal of Hydrology*, 334, 231–249. <https://doi.org/10.1016/j.jhydrol.2006.10.010>.
- Dibaj, M., Javadi, A. A., Akrami, M., Ke, K.-Y., Farmani, R., Tan, Y.-C., & Chen, A. S. (2020). Modelling seawater intrusion in the Pingtung coastal aquifer in Taiwan, under the influence of sea-level rise and changing abstraction regime. *Hydrogeology Journal*, 28(6), 2085–2103. <https://doi.org/10.1007/s10040-020-02172-4>.

- Diersch, H.-J. G. (2013). FEFLOW: Finite element modeling of flow, mass and heat transport in porous and fractured media. Springer Science & Business Media. https://books.google.com/books?hl=en&lr=&id=ZXXABAAAQBAJ&oi=fnd&pg=PR7&dq=FEFLOW&ots=w7mx6_erkg&sig=N7qJt52bVa9uyZQ-C2h5-CIZWPQ.
- Dinko, D. H., & Bahati, I. (2023). A Review of the Impact of Climate Change on Water Security and Livelihoods in Semiarid Africa: Cases From Kenya, Malawi, and Ghana. *Journal of Climate Resilience and Climate Justice*, 1, 107–118.
- Doherty, J. (2004). PEST model-independent parameter estimation user manual. Watermark Numerical Computing, Brisbane, Australia, 3338, 3349.
- Duah, A. A., Akurugu, B. A., Darko, P. K., Manu, E., & Mainoo, P. A. (2021). Groundwater recharge and potential exploitation in the Densu basin, Southwestern Ghana. *Journal of African Earth Sciences*, 183, 104332.
- Duodu, A. (2009). Geological Map of Ghana 1:1 000 000. Geological Survey Department, Accra, Ghana. (Bundesanstalt für Geowissenschaften und Rohstoffe (BGR), Hanover, Germany).
- Eckhardt, K. (2005). How to construct recursive digital filters for baseflow separation. *Hydrological Processes: An International Journal*, 19(2), 507–515.
- El Alfy, M. (2014). Numerical groundwater modelling as an effective tool for management of water resources in arid areas. *Hydrological Sciences Journal*, 59(6), 1259–1274. <https://doi.org/10.1080/02626667.2013.836278>.

- Elsayed, S., Hussein, H., Moghanm, F. S., Khedher, K. M., Eid, E. M., & Gad, M. (2020). Application of irrigation water quality indices and multivariate statistical techniques for surface water quality assessments in the Northern Nile Delta, Egypt. *Water*, 12(12), 3300.
- Epting, J., Michel, A., Affolter, A., & Huggenberger, P. (2021). Climate change effects on groundwater recharge and temperatures in Swiss alluvial aquifers. *Journal of Hydrology X*, 11, 100071.
- Evantri, D., Purwanto, M. Y. J., Pandjaitan, N., & Waspodo, R. S. B. (2023). The Dynamic Model of Water Balance in A Sub-Basin. *Jurnal Teknik Pertanian Lampung (Journal of Agricultural Engineering)*, 12(1), Article 1. <https://doi.org/10.23960/jtep-l.v12i1.236-245>.
- FAO. (2019). Groundwater for sustainable development: A framework for action. <http://www.fao.org/documents/card/en/c/ca5904en>.
- Fienen, M., Hunt, R., Krabbenhoft, D., & Clemo, T. (2009). Obtaining parsimonious hydraulic conductivity fields using head and transport observations: A Bayesian geostatistical parameter estimation approach. *Water Resources Research*, 45(8), 2008WR007431. <https://doi.org/10.1029/2008WR007431>.
- Foster, S., Eichholz, M., Nlend, B., & Gathu, J. (2020). Securing the critical role of groundwater for the resilient water-supply of urban Africa. *Water Policy*, 22(1), 121–132.
- Freeze, R. A., & Cherry, J. A. (1979). *Groundwater*. Prentice Hall Inc., New Jersey.



Geneviève, L., Romain, C., & Marie-Amélie, B. (2020). Water-table fluctuation method for assessing aquifer recharge: Application to Canadian aquifers and comparison with other methods. *Hydrogeology Journal*, 28(2), 521–533.

Ghana Statistical Service. (2021). Ghana 2021 population and housing census; general report— Volume 3A. Population of regions and districts. https://statsghana.gov.gh/gssmain/fileUpload/pressrelease/2021%20PHC%20General%20Report%20Vol%203A_Population%20of%20Regions%20and%20Districts_181121.pdf.

Gibrilla, A., Shiloh, O., Tetteh T, A., Dickson, A., Samuel Y, G., Edward PK, B., & Alhassan, H. (2010). Hydrogeochemical and groundwater quality studies in the northern part of the Densu River Basin of Ghana. *Journal of Water Resource and Protection*, 2010.

Graphic, D. (2001). Ghana Newspaper, September 14. Farming along Densu Banned. A Report by Boahene Asamoah and Caesar Abagali, 32.

Guggenmos, M. R., Daughney, C. J., Jackson, B. M., & Morgenstern, U. (2011). Regional-scale identification of groundwater-surface water interaction using hydrochemistry and multivariate statistical methods, Wairarapa Valley, New Zealand. *Hydrology and Earth System Sciences*, 15(11), 3383–3398.

Guttman, J., & Zuckerman, H. (1995). Flow model in the eastern basin of the Judea and Samaria hills. Tel-Aviv: Tahal Consulting Engineers Ltd, 1(95), 66.



- Gyasi-Agyei, Y., Obuobie, E., Yu, B., Addi, M., & Yahaya, B. (2023). Optimal selection of daily satellite precipitation product based on structural similarity index at 1 km resolution for the Pra catchment, Ghana. *Scientific Reports*, 13(1), 16702.
- Gyimah, R. A. A., Gyamfi, C., Anornu, G. K., Karikari, A. Y., & Tsyawo, F. W. (2021). Multivariate statistical analysis of water quality of the Densu River, Ghana. *International Journal of River Basin Management*, 19(2), 189–199. <https://doi.org/10.1080/15715124.2020.1803337>.
- Hagan, G. B., & Darko, E. (2020). Stochastic analysis of the groundwater velocity field and implications for contaminant transport within the Ga East and Adentan municipalities, Ghana. *Journal of African Earth Sciences*, 170, 103929.
- Hamel, P., Daly, E., & Fletcher, T. D. (2013). Source-control stormwater management for mitigating the impacts of urbanisation on baseflow: A review. *Journal of Hydrology*, 485, 201–211. <https://doi.org/10.1016/j.jhydrol.2013.01.001>.
- Hao, A., Zhang, Y., Zhang, E., Li, Z., Yu, J., Huang, W., Yang, J., & Wang, Y. (2018). Groundwater resources and related environmental issues in China. *Hydrogeology Journal*, 26(5), 1325–1337.
- Harbaugh, A. W., Banta, E. R., Hill, M. C., & McDonald, M. G. (2000). Modflow-2000, the u. S. Geological survey modular ground-water model-user guide to modularization concepts and the ground-water flow process. https://inside.mines.edu/~epoeter/583CSM/DOC3_MODFLOW2000_ModConcepts_GWF_lowProcess_ofr00-92.pdf.

- Healy, R. W., & Cook, P. G. (2002). Using groundwater levels to estimate recharge. *Hydrogeology Journal*, 10(1), 91–109. <https://doi.org/10.1007/s10040-001-0178-0>.
- Healy, R. W., & Scanlon, B. R. (2010). *Estimating Groundwater Recharge*. Cambridge University Press, 257.
- Hem, J. D. (1985). *Study and interpretation of the chemical characteristics of natural water* (Vol. 2254). Department of the Interior, US Geological Survey.
- Heřmanská, M., Voigt, M. J., Marieni, C., Declercq, J., & Oelkers, E. H. (2022). A comprehensive and internally consistent mineral dissolution rate database: Part I: Primary silicate minerals and glasses. *Chemical Geology*, 597, 120807.
- Holland, S. M. (2006). Cluster analysis. <http://stratigrafia.org/software/pdf/clusterTutorial.pdf>.
- Hoogesteger, J. (2022). Regulating agricultural groundwater use in arid and semi-arid regions of the Global South: Challenges and socio-environmental impacts. *Current Opinion in Environmental Science & Health*, 27, 100341.
- Howard, G., Calow, R., Macdonald, A., & Bartram, J. (2016). Climate change and water and sanitation: Likely impacts and emerging trends for action. *Annual Review of Environment and Resources*, 41, 253–276.
- Huet, M., Chesnaux, R., Boucher, M.-A., & Poirier, C. (2016). Comparing various approaches for assessing groundwater recharge at a regional scale in the Canadian Shield. *Hydrological Sciences Journal*, 61(12), 2267–2283.

IPCC. (2022). Summary for Policymakers [H.-O. Pörtner, D.C. Roberts, E.S. Poloczanska, K. Mintenbeck, M. Tignor, A. Alegría, M. Craig, S. Langsdorf, S. Löschke, V. Möller, A. Okem (Eds.)]. In: Climate Change 2022: Impacts, Adaptation, and Vulnerability. Contribution of Working Group II to the Sixth Assessment Report of the Intergovernmental Panel on Climate Change. 10.1017/9781009325844.001.

Islam, M., Van Camp, M., Hossain, D., Sarker, M. M. R., Bhuiyan, M. A. Q., Karim, M. M., & Walraevens, K. (2022). Hydrogeochemical processes and groundwater quality of over-exploited Dupi Tila aquifer in Dhaka city, Bangladesh. *Environmental Science and Pollution Research*, 29(49), 74458–74479.

Issahaku, A., Champion, B. B., & Edziyie, R. (2016). Rainfall and temperature changes and variability in the Upper East Region of Ghana. *Earth and Space Science*, 3(8), 284–294. <https://doi.org/10.1002/2016EA000161>.

Jie, Z., van Heyden, J., Bendel, D., & Barthel, R. (2011). Combination of soil-water balance models and water-table fluctuation methods for evaluation and improvement of groundwater recharge calculations. *Hydrogeology Journal*, 19(8), 1487.

Johnson, A. I. (1967). Specific yield: Compilation of specific yields for various materials. US Government Printing Office. https://books.google.com/books?hl=en&lr=&id=OBehL77jirEC&oi=fnd&pg=PA1&dq=Specific+Yield+Compilation+of+Specific+Yields+for+Various+Materials&ots=RKgJkOcVmC&sig=wMMec8GmyDS-w2T_SC8TTFbYzmk.

- Jovein, E. B., Motlagh, A. G., & Hosseini, S. M. (2023). Estimation of the groundwater recharge coefficient by minimizing the sum total error of a regional water balance. *Environmental Earth Sciences*, 82(13), 323. <https://doi.org/10.1007/s12665-023-11008-9>.
- Kang, G., Luo, L., Pokhrel, Y., Lusch, D., & Phanikumar, M. S. (2021). Quantifying the spatiotemporal dynamics of recharge in a composite Great Lakes watershed using a high-resolution hydrology model and multi-source data. https://scholar.google.com/scholar?hl=en&as_sdt=0%2C5&q=Quantifying+the+spatiotemporal+dynamics+of+recharge+in+a+composite+Great+Lakes+watershed+using+a+high-resolution+hydrology+model+and+multi-source+data&btnG=.
- Karikari, A. Y., & Ansa-Asare, O. D. (2006). Physico-chemical and microbial water quality assessment of Densu River of Ghana. *West African Journal of Applied Ecology*, 10(1).
- Kesse, G. O. (1985). The mineral and rock resources of Ghana.
- Kissel, M., & Schmalz, B. (2020). Comparison of baseflow separation methods in the german low mountain range. *Water*, 12(6), 1740.
- Kortatsi, B. K. (1994). Groundwater utilization in Ghana. *Future Groundwater Resources at Risk; Proceedings of the Helsinki Conference, June 1994*. https://www.google.com/url?sa=t&rct=j&q=&esrc=s&source=web&cd=&ved=2ahUKEwj4ltr547ftAhUL6RoKHVwwAvwQFjAAegQIAhAC&url=http%3A%2F%2Fhydrologie.org%2Fredbooks%2Fa222%2Fiahs_222_0149.pdf&usq=AOvVaw30FHY1OBZ_xL_4NtNB_NISL.

- Kortatsi, B. K., Tay, C. K., Anornu, G., Hayford, E., & Dartey, G. A. (2008). Hydrogeochemical evaluation of groundwater in the lower Offin basin, Ghana. *Environmental Geology*, 53(8), 1651–1662. <https://doi.org/10.1007/s00254-007-0772-0>.
- Kotb, A., Mosaad, S., & Kehew, A. E. (2021). Geophysical and hydrogeological applications for groundwater evaluation, east El-Minia area, upper Egypt. *Journal of African Earth Sciences*, 184, 104384.
- Kumar, C. P. (2012). Climate change and its impact on groundwater resources. *International Journal of Engineering and Science*, 1(5), 43–60.
- Kumarasamy, P., Dahms, H.-U., Jeon, H.-J., Rajendran, A., & Arthur James, R. (2014). Irrigation water quality assessment—An example from the Tamiraparani river, Southern India. *Arabian Journal of Geosciences*, 7, 5209–5220.
- Kusangaya, S., Warburton, M. L., Van Garderen, E. A., & Jewitt, G. P. (2014). Impacts of climate change on water resources in southern Africa: A review. *Physics and Chemistry of the Earth, Parts a/b/c*, 67, 47–54.
- Lafare, A. E. A., Peach, D. W., & Hughes, A. G. (2021). Use of point scale models to improve conceptual understanding in complex aquifers: An example from a sandstone aquifer in the Eden valley, Cumbria, UK. *Hydrological Processes*, 35(5), e14143. <https://doi.org/10.1002/hyp.14143>.



- Lamarca-Irisarri, D., Van Driessche, A. E., Jordan, G., Cappelli, C., & Huertas, F. J. (2019). The role of pH, temperature, and NH_4^+ during mica weathering. *ACS Earth and Space Chemistry*, 3(11), 2613–2622.
- Langevin, C. D., Thorne Jr, D. T., Dausman, A. M., Sukop, M. C., & Guo, W. (2008). SEAWAT version 4: A computer program for simulation of multi-species solute and heat transport. Geological Survey (US). <https://pubs.er.usgs.gov/publication/tm6A22>.
- Lanini, S., Caballero, Y., & Le Cointe, P. (2020). ESPERE version 2 User's Guide.
- Larbi, I., Hountondji, F. C., Annor, T., Agyare, W. A., Mwangi Gathenya, J., & Amuzu, J. (2018). Spatio-temporal trend analysis of rainfall and temperature extremes in the Veua Catchment, Ghana. *Climate*, 6(4), 87.
- Lazaratou, C. V., Vayenas, D. V., & Papoulis, D. (2020). The role of clays, clay minerals and clay-based materials for nitrate removal from water systems: A review. *Applied Clay Science*, 185, 105377.
- Lee, D.-H., Kim, N.-W., & Chung, I.-M. (2010). Comparison of Groundwater Recharge between HELP Model and SWAT Model. *Journal of Korea Water Resources Association*, 43(4), 383–391.
- Lee, K. K., & Risley, J. C. (2002). Estimates of ground-water recharge, base flow, and stream reach gains and losses in the Willamette River Basin, Oregon. US Department of the Interior, US Geological Survey. <https://books.google.com/books?hl=en&lr=&id=7IaTOOXByysC&oi=fnd&pg=PA1&dq=>

[Estimates+of+Ground-](#)

[Water+Recharge,+Base+Flow,+and+Stream+Reach+Gains+and+Losses+in+the+Willamette+River+Basin,+Oregon&ots=jFjuS6Hyji&sig=Ebe4dlkgYP2lg5dHhPUJInddkbA.](#)

Lerner, D. N., Issar, A., & Simmers, I. (1990). Groundwater recharge: A guide to understanding and estimating natural recharge.

Li, Y., Wu, P., Xiao-Qin, H., Zhang, B., Zhao-Xiang, X., Yang, L., Li, J., Lu-Chen, W., Yu-Fang, S., & Xu-Chen, M. (2021). Groundwater sources, flow patterns, and hydrochemistry of the Central Yinchuan Plain, China. *Hydrogeology Journal*, 29(2), 591–606.

Liang, Z., Chen, J., Jiang, T., Li, K., Gao, L., Wang, Z., Li, S., & Xie, Z. (2018). Identification of the dominant hydrogeochemical processes and characterization of potential contaminants in groundwater in Qingyuan, China, by multivariate statistical analysis. *RSC Advances*, 8(58), 33243–33255.

Liu, W., Qin, D., Yang, Y., & Guo, G. (2023). Enrichment of Manganese at Low Background Level Groundwater Systems: A Study of Groundwater from Quaternary Porous Aquifers in Changping Region, Beijing, China. *Water*, 15(8), 1537.

Loh, Y. S. A., Akurugu, B. A., Manu, E., & Aliou, A.-S. (2019). Assessment of groundwater quality and the main controls on its hydrochemistry in some Voltaian and basement aquifers, northern Ghana. *Groundwater for Sustainable Development*, 10, 100296. <https://doi.org/10.1016/j.gsd.2019.100296>.

- Loh, Y. S. A., Yidana, S. M., Banoeng-Yakubo, B., Sakyi, P. A., Addai, M. O., & Asiedu, D. K. (2016). Determination of the mineral stability field of evolving groundwater in the Lake Bosumtwi impact crater and surrounding areas. *Journal of African Earth Sciences*, 121, 286–300.
- Lutterodt, G., Van de Vossenberg, J., Hoiting, Y., Kamara, A. K., Oduro-Kwarteng, S., & Foppen, J. W. A. (2018). Microbial groundwater quality status of hand-dug wells and boreholes in the Dodowa area of Ghana. *International Journal of Environmental Research and Public Health*, 15(4), 730.
- Lutz, A., Thomas, J. M., & Keita, M. (2010). Effects of population growth and climate variability on sustainable groundwater in Mali, West Africa. *Sustainability*, 3(1), 21–34.
- Lyne, V., & Hollick, M. (1979). Stochastic time-variable rainfall-runoff modelling. *Institute of Engineers Australia National Conference*, 79(10), 89–93.
https://www.academia.edu/download/39814987/Stochastic_Time-Variable_Rainfall-Runoff20151108-28652-1m3nhhta.pdf.
- MacDonald, A. M., Lark, R. M., Taylor, R. G., Abiye, T., Fallas, H. C., Favreau, G., Goni, I. B., Kebede, S., Scanlon, B., & Sorensen, J. P. (2021). Mapping groundwater recharge in Africa from ground observations and implications for water security. *Environmental Research Letters*, 16(3), 034012.
- Malík, P., Marián, C., Jaromír, Š., Radovan, Č., & Bajtoš, P. (2021). Recharge, delayed groundwater-level rise and specific yield in the Triassic karst aquifer of the Kopa Mountain, in the Western Carpathians, Slovakia. *Hydrogeology Journal*, 29(1), 499–518.

Mandel, S., & Shiftan, Z. L. (1981). Groundwater Resources: Investigation and Development. Elsevier Science.

Mantey, S., Tagoe, N. D., & Aduah, M. S. (2011). Detecting areas of vegetation change in the Densu River Basin, Ghana. WIT Press, Southampton, UK.

Manu, E., De Lucia, M., & Kühn, M. (2023). Hydrochemical Characterization of Surface Water and Groundwater in the Crystalline Basement Aquifer System in the Pra Basin (Ghana). *Water*, 15(7), 1325.

Margat, J., & Van der Gun, J. (2013). Groundwater around the world: A geographic synopsis. Crc Press.

<https://books.google.com/books?hl=en&lr=&id=2qFWeXvPGVEC&oi=fnd&pg=PP1&dq=Groundwater+accounts+for+97-+99%25+of+all+liquid+fresh+water+on+earth+&ots=AwBfFSubfc&sig=h65RiqFyiJmBlqyZB-vidBLyU0>

Martín-Loeches, M., Pavón-García, J., Molina-Navarro, E., Martínez-Santos, P., Almeida, C., Reyes-López, J., Cienfuegos-Hevia, I., & Sastre-Merlín, A. (2020). Hydrogeochemistry of granitic mountain zones and the influence of adjacent sedimentary basins at their tectonic borders: The case of the Spanish Central System batholith. *Hydrogeology Journal*, 28(7).

Maxwell, R. M., Kollet, S. J., Smith, S. G., Woodward, C. S., Falgout, R. D., Ferguson, I. M., Baldwin, C., Bosl, W. J., Hornung, R., & Ashby, S. (2009). ParFlow user's manual. International Ground Water Modeling Center Report GWMI, 1(2009), 129.

- Mazvimavi, K., Nyathi, P., & Murendo, C. (2011). Conservation Agriculture practices and challenges in Zimbabwe. <http://oar.icrisat.org/id/eprint/2844>.
- McDonald, M. G., & Harbaugh, A. W. (2003). The history of MODFLOW. *Ground Water*, 41(2), 280.
- Mensah, O. F., Alo, C., & Yidana, S. M. (2014). Evaluation of Groundwater Recharge Estimates in a Partially Metamorphosed Sedimentary Basin in a Tropical Environment: Application of Natural Tracers [Research Article]. *The Scientific World Journal*. <https://doi.org/10.1155/2014/419508>.
- Moharir, K., Pande, C., & Patil, S. (2017). Inverse modelling of aquifer parameters in basaltic rock with the help of pumping test method using MODFLOW software. *Geoscience Frontiers*, 8(6), 1385–1395.
- Moriasi, D. N., Gitau, M. W., Pai, N., & Daggupati, P. (2015). Hydrologic and Water Quality Models: Performance Measures and Evaluation Criteria. *Transactions of the ASABE*, 58(6), 1763–1785. <https://doi.org/10.13031/trans.58.10715>.
- Mullaney, J. R., Lorenz, D. L., & Arntson, A. D. (2009). Chloride in groundwater and surface water in areas underlain by the glacial aquifer system, northern United States (Vol. 2009). US Geological Survey Reston, VA. <https://pubs.usgs.gov/sir/2009/5086/>.
- Nimmo, J. R., Horowitz, C., & Mitchell, L. (2015). Discrete-Storm Water-Table Fluctuation Method to Estimate Episodic Recharge. *Groundwater*, 53(2), 282–292. <https://doi.org/10.1111/gwat.12177>.

- Nkhonjera, G. K. (2017). Understanding the impact of climate change on the dwindling water resources of South Africa, focusing mainly on Olifants River basin: A review. *Environmental Science & Policy*, 71, 19–29.
- Nyakundi, R., Nyadawa, M., & Mwangi, J. (2022). Effect of recharge and abstraction on groundwater levels. *Civil Engineering Journal*, 8(5), 910–925.
- Obiri-Nyarko, F., Asugre, S. J., Asare, S. V., Duah, A. A., Karikari, A. Y., Kwiatkowska-Malina, J., & Malina, G. (2022). Hydrogeochemical Studies to Assess the Suitability of Groundwater for Drinking and Irrigation Purposes: The Upper East Region of Ghana Case Study. *Agriculture*, 12(12), 1973.
- Obuobie, E., Diekkrüger, B., Agyekum, W., & Agodzo, S. (2012). Groundwater level monitoring and recharge estimation in the White Volta River basin of Ghana. *Journal of African Earth Sciences*, 71–72, 80–86. <https://doi.org/10.1016/j.jafrearsci.2012.06.005>.
- Oliver, M. A., & Webster, R. (2015). *Basic Steps in Geostatistics: The Variogram and Kriging*. Springer International Publishing. <https://doi.org/10.1007/978-3-319-15865-5>.
- Ophori, D. U., & Tóth, J. (1989). Patterns of Ground-Water Chemistry, Ross Creek Basin, Alberta, Canada. *Groundwater*, 27(1), 20–26. <https://doi.org/10.1111/j.1745-6584.1989.tb00003.x>
- Oti, J. O. (2019). *Modelling the Impacts of Climate Change on Water Resources in Ghana: A Case study of the Densu River Basin [Master's Thesis, PAUWES]*. <http://repository.pauwes-cop.net/handle/1/329>.

- Panday, S., & Huyakorn, P. S. (2008). MODFLOW SURFACT: A state-of-the-art use of vadose zone flow and transport equations and numerical techniques for environmental evaluations. *Vadose Zone Journal*, 7(2), 610–631.
- Parkhurst, D. L., & Appelo, C. A. J. (2013). Description of input and examples for PHREEQC version 3—A computer program for speciation, batch-reaction, one-dimensional transport, and inverse geochemical calculations. *US Geological Survey Techniques and Methods*, 6(A43), 497.
- Pivić, R., Maksimović, J., Dinić, Z., Jaramaz, D., Majstorović, H., Vidojević, D., & Stanojković-Sebić, A. (2022). Hydrochemical Assessment of Water Used for Agricultural Soil Irrigation in the Water Area of the Three Morava Rivers in the Republic of Serbia. *Agronomy*, 12(5), 1177.
- Priestley, S. C., Shand, P., Love, A. J., Crossey, L. J., Karlstrom, K. E., Keppel, M. N., Wohling, D. L., & Rousseau-Guetin, P. (2019). Hydrochemical variations of groundwater and spring discharge of the western Great Artesian Basin.
- Pruess, K., & Battistelli, A. (2002). TMVOC, a numerical simulator for three-phase non-isothermal flows of multicomponent hydrocarbon mixtures in saturated-unsaturated heterogeneous media. <https://escholarship.org/content/qt73m7d7c4/qt73m7d7c4.pdf>.
- Pulido-Velazquez, D., Romero, J., Collados-Lara, A.-J., Alcalá, F. J., Fernández-Chacón, F., & Baena-Ruiz, L. (2020). Using the turnover time index to identify potential strategic groundwater resources to manage droughts within continental Spain. *Water*, 12(11), 3281.

- Qablawi, B. (2016). A comparison of four methods to estimate groundwater recharge for Northeastern South Dakota. South Dakota State University.
- Ramesh, K., & Elango, L. (2012). Groundwater quality and its suitability for domestic and agricultural use in Tondiar river basin, Tamil Nadu, India. *Environmental Monitoring and Assessment*, 184(6), 3887–3899.
- Sadeak, S., Al Amin, M., Chowdhury, T., Mia, M. B., Alam, M. J., Ahmed, K. M., & Khan, M. R. (2023). Comparison of the groundwater recharge estimations of the highly exploited aquifers in Bangladesh and their sustainability. *Groundwater for Sustainable Development*, 20, 100896.
- Sanford, Ward E., Plummer, L. N., McAda, Douglas P., Bexfield, Laura M., & Anderholm, Scott K. (2004). Hydrochemical tracers in the middle Rio Grande Basin, USA: 2. Calibration of a groundwater-flow model. *Hydrogeology Journal*, 12(4). <https://doi.org/10.1007/s10040-004-0326-4>.
- Scanlon, B., Healy, R., & Cook, P. (2002). Choosing Appropriate Techniques for Quantifying Groundwater Recharge. *Hydrogeology Journal*, 10, 18–39. <https://doi.org/10.1007/s10040-001-0176-2>.
- Schoeller, H. (1965). Qualitative evaluation of groundwater resources. *Methods and Techniques of Groundwater Investigations and Development*. UNESCO, 5483.
- Sedenkor, D. E., Sridhar, M. K. C., Lawson, E. T., & Ikporukpo, C. O. (2019). Spatial Variation of Water Quality in the Densu River Basin, Nsawam-Adoagyiri Municipality, Ghana.

- Seidenfaden, I. K., Mansour, M., Bessiere, H., Pulido-Velazquez, D., Højberg, A., Samolov, K. A., Baena-Ruiz, L., Bishop, H., Dessi, B., & Hinsby, K. (2023). Evaluating recharge estimates based on groundwater head from different lumped models in Europe. *Journal of Hydrology: Regional Studies*, 47, 101399.
- Shapoori, V., Peterson, T. J., Western, A. W., & Costelloe, J. F. (2015). Estimating aquifer properties using groundwater hydrograph modelling. *Hydrological Processes*, 29(26), 5424–5437. <https://doi.org/10.1002/hyp.10583>.
- Sikdar, P. K., Banerjee, S., & Chakraborty, S. (2022). Understanding the Past-Present-Future Hydrogeologic System Through Numerical Groundwater Modeling of South Bengal Basin, India. *Frontiers in Water*, 3, 801299.
- Simmonds, S. (2009). The Nugget Effect: In describing the variability of an [PhD Thesis, Rhodes University]. https://www.researchgate.net/profile/Sarah-Jane-Gill/publication/316878381_The_nugget_effect/links/5eba56a04585152169c84cb7/The-nugget-effect.pdf.
- Šimůnek, J., Van Genuchten, M. T., & Šejna, M. (2016). Recent developments and applications of the HYDRUS computer software packages. *Vadose Zone Journal*, 15(7). <https://pubs.geoscienceworld.org/msa/vzj/article/15/7/vzj2016.04.0033/246468>.
- Singh, A., Panda, S. N., Uzokwe, V. N., & Krause, P. (2019). An assessment of groundwater recharge estimation techniques for sustainable resource management. *Groundwater for Sustainable Development*, 9, 100218.

- Sinha, B. P. C., & Sharma, S. K. (1988). Natural ground water recharge estimation methodologies in India. In *Estimation of natural groundwater recharge* (pp. 301–311). Springer.
- Somaratne, N., & Smettem, K. R. J. (2014). Theory of the generalized chloride mass balance method for recharge estimation in groundwater basins characterised by point and diffuse recharge. *Hydrology and Earth System Sciences Discussions*, 11(1), 307–332.
- Sundaray, S. K., Nayak, B. B., & Bhatta, D. (2009). Environmental studies on river water quality with reference to suitability for agricultural purposes: Mahanadi river estuarine system, India—a case study. *Environmental Monitoring and Assessment*, 155, 227–243.
- Swain, S., Taloor, A. K., Dhal, L., Sahoo, S., & Al-Ansari, N. (2022). Impact of climate change on groundwater hydrology: A comprehensive review and current status of the Indian hydrogeology. *Applied Water Science*, 12(6), 120. <https://doi.org/10.1007/s13201-022-01652-0>.
- Sylla, M. B., Nikiema, P. M., Gibba, P., Kebe, I., & Klutse, N. A. B. (2016). Climate Change over West Africa: Recent Trends and Future Projections. In J. A. Yaro & J. Hesselberg (Eds.), *Adaptation to Climate Change and Variability in Rural West Africa* (pp. 25–40). Springer International Publishing. https://doi.org/10.1007/978-3-319-31499-0_3.
- Tadesse, N., Bairu, A., & Bheemalingeswara, K. (2011). Suitability of groundwater quality for irrigation with reference to hand dug wells, Hantebet Catchment, Tigray, Northern Ethiopia. *Momona Ethiopian Journal of Science*, 3(2).

- Tay, C. K. (2021). Hydrogeochemical framework of groundwater within the Asutifi-North District of the Brong-Ahafo Region, Ghana. *Applied Water Science*, 11(4), 72.
- Tay, C., & Kortatsi, B. (2008). Groundwater quality studies: A case study of the Densu Basin, Ghana. *West African Journal of Applied Ecology*, 12(1).
- Tesoriero, A. J., Spruill, T. B., & Eimers, J. L. (2004). Geochemistry of shallow ground water in coastal plain environments in the southeastern United States: Implications for aquifer susceptibility. *Applied Geochemistry*, 19(9), 1471–1482.
- Tiedeman, C. R., Goode, D. J., & Hsieh, P. A. (1997). Numerical simulation of ground-water flow through glacial deposits and crystalline bedrock in the Mirror Lake area, Grafton County, New Hampshire. US Government Printing Office.
- Tularam, G. A., & Ilahee, M. (2008). Exponential smoothing method of base flow separation and its impact on continuous loss estimates. *American Journal of Environmental Sciences*, 4(2), 136.
- USSL (United States Salinity Laboratory), 1954. Diagnosis and Improvement of Saline and Alkaline Soils. USDA Agric handbook, Washington DC. No. 60.
- Varol, S., & Davraz, A. (2015). Evaluation of the groundwater quality with WQI (Water Quality Index) and multivariate analysis: A case study of the Tefenni plain (Burdur/Turkey). *Environmental Earth Sciences*, 73, 1725–1744.
- Veeraswamy, D., John, J. E., Chidamparam, P., Boopathi, G., Subramanian, A., Ettiyagounder, P., Santhosh, A., Srinivasulu, A., Lal, A., & Naidu, R. (2023). A Critical Review of Climate

Change Impacts on Groundwater Resources: A Focus on Current Status, Future Possibilities, and Role of Simulation Models. <https://www.preprints.org/manuscript/202312.1248>.

Velis, M., Conti, K. I., & Biermann, F. (2017). Groundwater and human development: Synergies and trade-offs within the context of the sustainable development goals. *Sustainability Science*, 12(6), 1007–1017. <https://doi.org/10.1007/s11625-017-0490-9>.

Voss, C. I., & Provost, A. M. (2002). SUTRA: A model for 2D or 3D saturated-unsaturated, variable-density ground-water flow with solute or energy transport. US Geological Survey. <https://pubs.er.usgs.gov/publication/wri024231>.

Vyshpolsky, F., Qadir, M., Karimov, A., Mukhamedjanov, K., Bekbaev, U., Paroda, R., Aw-Hassan, A., & Karajeh, F. (2008). Enhancing the productivity of high-magnesium soil and water resources in Central Asia through the application of phosphogypsum. *Land Degradation & Development*, 19(1), 45–56.

Wada, Y., & Bierkens, M. F. (2014). Sustainability of global water use: Past reconstruction and future projections. *Environmental Research Letters*, 9(10), 104003.

Wakejo, W. K., Meshesha, B. T., Habtu, N. G., & Mekonnen, Y. G. (2022). Anthropogenic nitrate contamination of water resources in Ethiopia: An overview. *Water Supply*, 22(11), 8157–8172.

Walker, D., Parkin, G., Schmitter, P., Gowing, J., Tilahun, S. A., Haile, A. T., & Yimam, A. Y. (2019). Insights From a Multi-Method Recharge Estimation Comparison Study. *Groundwater*, 57(2), 245–258. <https://doi.org/10.1111/gwat.12801>.

Watanabe, M., Suzuki, T., O'ishi, R., Komuro, Y., Watanabe, S., Emori, S., Takemura, T., Chikira, M., Ogura, T., & Sekiguchi, M. (2010). Improved climate simulation by MIROC5: Mean states, variability, and climate sensitivity. *Journal of Climate*, 23(23), 6312–6335.

Water Resources Commission. (2007). Integrated Water Resources Management Plan: Densu River Basin.

<https://www.google.com/url?sa=t&rct=j&q=&esrc=s&source=web&cd=&ved=2ahUKEwjUs76Dh-bsAhVbSBUIHfebDdUQFjAAegQIAhAC&url=http%3A%2F%2Fwww.wrc-gh.org%2Fdmtdocument%2F16&usg=AOvVaw1wWtXp9K5uGAG1n7Bj6BVV>.

WHO. (2017). Guidelines for drinking-water quality: First addendum to the fourth edition.

Wilcox, L. (1955). Classification and use of irrigation waters. US Department of Agriculture.

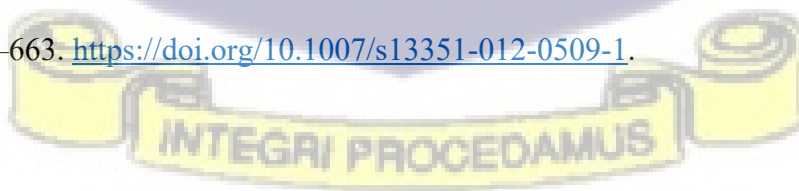
Xiao, S., Fang, Y., Chen, J., Zou, Z., Gao, Y., Xu, P., Jiao, X., & Ren, M. (2023). Assessing the Hydrochemistry, Groundwater Drinking Quality, and Possible Hazard to Human Health in Shizuishan Area, Northwest China. *Water*, 15(6), 1082.

Yang, L., Qi, Y., Zheng, C., Andrews, C. B., Yue, S., Lin, S., Li, Y., Wang, C., Xu, Y., & Li, H. (2018). A modified water-table fluctuation method to characterize regional groundwater discharge. *Water*, 10(4), 503.

Yankey, R. K., Akiti, T. T., Osae, S., Fianko, J. R., Duncan, A. E., Amartey, E. O., Essuman, D. K., & Agyemang, O. (2011). The hydrochemical characteristics of groundwater in the Tarkwa mining area, Ghana. <https://ir.ucc.edu.gh/xmlui/handle/123456789/5734>.

- Yeh, H.-F., Lee, C.-H., Chen, J.-F., & Chen, W.-P. (2007). Estimation of groundwater recharge using water balance model. *Water Resources*, 34, 153–162.
- Yidana, S. M., Alfa, B., Banoeng-Yakubo, B., & Obeng Addai, M. (2014). Simulation of groundwater flow in a crystalline rock aquifer system in Southern Ghana—an evaluation of the effects of increased groundwater abstraction on the aquifers using a transient groundwater flow model. *Hydrological Processes*, 28(3), 1084–1094.
- Yidana, S. M., Banoeng-Yakubo, B., & Sakyi, P. A. (2012). Identifying key processes in the hydrochemistry of a basin through the combined use of factor and regression models. *Journal of Earth System Science*, 121(2), 491–507.
- Yidana, S. M., Bawoyobie, P., Sakyi, P., & Fynn, O. F. (2018). Evolutionary analysis of groundwater flow: Application of multivariate statistical analysis to hydrochemical data in the Densu Basin, Ghana. *Journal of African Earth Sciences*, 138, 167–176.
- Yidana, S. M., Dzikunoo, E. A., Aliou, A.-S., Adams, R. M., Chagbeleh, L. P., & Anani, C. (2020). The geological and hydrogeological framework of the Panabako, Kodjari, and Bimbilla formations of the Voltaian supergroup—Revelations from groundwater hydrochemical data. *Applied Geochemistry*, 115, 104533.
- Yidana, S. M., Essel, S. K., Addai, M. O., & Fynn, O. F. (2015). A preliminary analysis of the hydrogeological conditions and groundwater flow in some parts of a crystalline aquifer system: Afigya Sekyere South District, Ghana. *Journal of African Earth Sciences*, 104, 132–139.

- Yidana, S. M., & Ophori, D. (2008). Groundwater resources management in the Afram Plains area, Ghana. *KSCE Journal of Civil Engineering*, 12(5), 349.
- Yiran, G. A., & Stringer, L. C. (2016). Spatio-temporal analyses of impacts of multiple climatic hazards in a savannah ecosystem of Ghana. *Climate Risk Management*, 14, 11–26.
- Younger, P. L., Boyce, A. J., & Waring, A. J. (2015). Chloride waters of Great Britain revisited: From subsea formation waters to onshore geothermal fluids. *Proceedings of the Geologists' Association*, 126(4–5), 453–465.
- Zaman, M., Shahid, S. A., Heng, L., Zaman, M., Shahid, S. A., & Heng, L. (2018). Irrigation water quality. *Guideline for Salinity Assessment, Mitigation and Adaptation Using Nuclear and Related Techniques*, 113–131.
- Zamani, M. G., Moridi, A., & Yazdi, J. (2022). Groundwater management in arid and semi-arid regions. *Arabian Journal of Geosciences*, 15(4), 362.
- Zhang, Y., Zhou, X., Liu, H., Kuo, H., Mingxiao, Y., & Mengru, T. (2020). Characterization of a saline hot spring depositing travertine in the red beds in the Simao Basin of China. *Hydrogeology Journal*, 28(4), 1431–1447.
- Zheng, Z., Zhang, W., Xu, J., Zhao, L., Chen, J., & Yan, Z. (2012). Numerical simulation and evaluation of a new hydrological model coupled with GRAPES. *Acta Meteorologica Sinica*, 26(5), 653–663. <https://doi.org/10.1007/s13351-012-0509-1>.



Zomlot, Z., Verbeiren, B., Huysmans, M., & Batelaan, O. (2015). Spatial distribution of groundwater recharge and base flow: Assessment of controlling factors. *Journal of Hydrology: Regional Studies*, 4, 349–368. <https://doi.org/10.1016/j.ejrh.2015.07.005>.

Zougmore, R., Jalloh, A., & Tioro, A. (2014). Climate-smart soil water and nutrient management options in semiarid West Africa: A review of evidence and analysis of stone bunds and zaï techniques. *Agriculture & Food Security*, 3(1), 16. <https://doi.org/10.1186/2048-7010-3-16>.

